ABSTRACT

Rigorous TE Solution to the Staircase Model of the Dielectric Wedge Antenna

by
Wan-Yu Chen

The rigorous TE solution to the staircase model of the dielectric wedge antenna is presented. The fundamental, even TE surface wave mode of the dielectric slab waveguide is taken to excite a dielectric wedge which is formed by symmetrically tapering the slab. The method of solution is based on Marcuse's step-transition method. Radiation patterns of power gain are presented which show increased maximum power gains and narrower main lobe beamwidths for longer wedges. For higher dielectric constant material, the main lobe beamwidth is increased. In all cases examined, negligible sidelobes were obtained.

RIGOROUS TE SOLUTION TO THE STAIRCASE MODEL OF THE DIELECTRIC WEDGE ANTENNA

by
Wan-Yu Chen

A Thesis
Submitted to the Faculty of
New Jersey Institute of Technology
in Partial Fulfillment of the Requirements for the Degree of
Master of Science in Electrical Engineering

Department of Electrical and Computer Engineering

October 1993

Blank Page

BIOGRAPHICAL SKETCH

Author: Wan-Yu Chen

Degree: Master of Science in Electrical Engineering

Date: October 1993

Undergraduate and Graduate Education:

- Master of Science in Electrical Engineering,
  New Jersey Institute of Technology, Newark, NJ, 1993

- Bachelor of Electrical Engineering,
  Chung-Yuan Christian University, Chung-Li, Taiwan, R.O.C., 1990

Major: Electrical Engineering

BIOGRAPHICAL SKETCH

Author: Wan-Yu Chen

Degree: Master of Science in Electrical Engineering

Date: October 1993

Date of Birth: November 25, 1968

Place of Birth: Kaohsiung, Taiwan, R.O.C.

Undergraduate and Graduate Education:

- Master of Science in Electrical Engineering,
  New Jersey Institute of Technology, Newark, NJ, 1993

- Bachelor of Electrical Engineering,
  Chung-Yuan Christian University, Chung-Li, Taiwan, R.O.C., 1990

Major: Electrical Engineering

This thesis is dedicated to

My Father, Mother, Brother and Sisters

ACKNOWLEDGMENT

The author wishes to express her sincere gratitude to her supervisor, Professor Gerald Whitman, for his insight, guidance, and assistance throughout this research. A special thanks is due to Professor Gary Wu for his friendship and helpful suggestions. Gratitude is also extended to Professors Edip Niver and Gary Wu for serving as members of the thesis committee.

The author appreciates the advice about the VAX/VMS system that received from Mr. Henry Frystak, System Administrator VAX/VMS Usenet Newsmanager, NJIT Computing Services Department.

Deep thanks to my sister, Wan-Ling Chen, and my brother-in-law, Ming-Wan Young, for their concern and help during the past two years.

And finally, thanks to my friend, Shee-Tuck Kwan, for use of his computer system and for his moral support during the last few months.

TABLE OF CONTENTS

Chapter **Page**

LIST OF TABLES

Table **Page**

LIST OF FIGURES

Figure **Page**

CHAPTER 1

INTRODUCTION

Current interest in tapered dielectric radiators stems from their compatibility with dielectric waveguides and the availability of both lowloss silicon and solid state energy sources, which permit integration for use in millimeter wave and integrated optical devices [1 - 3]. Millimeter wave devices usually involve open structures in which the electromagnetic field is not confined to a finite region of space. Hence, energy leakage occurs. For a structure to be a waveguide, the leakage has to be minimized. If the structure is an antenna then efficient coupling to the radiation field must be effected. By tapering a dielectric guide along it axis, a guided surface wave field gets transformed into a radiation field which is characterized by maximum intensity in the forward direction. It has been shown that tapering a dielectric guide, as opposed to suddenly truncating it, improves the radiation characteristics (increased directivity and lower side lobe levels) over a wider frequency band [4 - 6].

Tapered dielectric antennas have been studied for some time; see [2] for a comprehensive list of references. Rigorous theoretical approaches to analyze these antennas, such as, the coupled mode theory or the full wave method [7 - 9] are available. However, they are mathematically very complex and usually require an iterative procedure just to obtain a solution to lowest order. In particular, the field of the two dimensional dielectric wedge antenna fed by a guide of the same material has eluded being completely determined [2]. The method of analysis presented here yields the rigorous TE field solution for this integrated structure assuming a staircase model of the dielectric wedge antenna.

A single surface wave mode is assumed to be guided by a dielectric slab waveguide which evolves continuously into a dielectric wedge. The dielectric wedge is modeled by using the staircase approximation. The field scattered by each step discontinuity is then rigorously formulated and solved numerically. The method of solution is based on the step-transition method introduced by Marcuse [10, 11], who applied it to step-tapered transitions between waveguides of different, but uniform cross-sections.

Many methods have been developed to study taper transitions between dielectric guides or fibers. Several approaches, including the couple mode theory, the step-transition method and the propagating-beam methods are reviewed in [12], which also introduces the so called "exact numerical method" that we have chosen to use. This method is based on Marcuse's step-transition method, but applies orthogonality relations to obtain a sparse, diagonally dominant matrix that allows for repeatable, efficient and accurate numerical solution of the linear system of equations which is obtained at each step discontinuity. It showed be noted, however, that the "exact numerical method' as presented in [12] was done *incorrectly*. The correct formulation is developed in Chapter 2. The numerical method used is described in Chapter 3 and numerical results are presented in Chapter 4. Because the "corrected exact numerical method" in Chapter 2 depends on the accuracy that is obtained at a single step discontinuity, comparisons are made in Chapter 4 with the published results of Rozzi and others [13 - 15] for the single step discontinuity problem. Finally, in Chapter 4, the radiation patterns of power gain for the integrated slab waveguide/wedge radiator are presented for various wedge lengths and for different dielectric materials.

CHAPTER 2

FORMULATION

The physical geometry under consideration is a lossless, semi-infinite, dielectric slab waveguide of thickness $2D_1$ which, beginning at z = 0, is tapered to a point at z = L. A model for this tapered dielectric is depicted in Figure 1, wherein the smooth tapered portion is replaced by short slab waveguide segments of equal length Δz and uniform cross-sectional areas of progressively smaller widths $2D_i$, i = 2, ..., M-1, with $D_M = 0$, for z > L. In Figure 1, only four uniform slab waveguides are shown and the tapered section is modeled by three slab waveguides of successfully smaller widths D_2, D_3, andD_4 such that $D_1 > D_2 > D_3 > D_4 > D_5 = 0$. The regions of space where the electromagnetic field is to be found number 5; the semi-infinite slab waveguide occupies the region z < 0 (region i = 1), the taper is segmented into three regions (i = 2, 3, and 4), while the semi-infinite free space region is identified as region M = 5. Each region i, i = 1, 2, ..., 5, is further separated into 3 sub-regions identified by I_i, II_i, III_i, where II_i is occupied by the dielectric and sub-regions I_i and III_i are free space above and below the dielectric, respectively. The last region in Figure 1 is such that II_5 does not exist since the dielectric is taken to truncate at z = L with a finite width $2D_4$.

A fundamental, even TE surface wave mode of an infinite uniform dielectric slab waveguide is assumed to be incident in the +z direction from z = $-\infty$. This mode, normalized to unity incident power, does not experience cutoff and can propagate along very thin slab waveguides. Because of this excitation and the staircase approximation for the wedge geometry, it is assumed that the field is TE everywhere. Hence, the field components in each region are E_{yi}, H_{xi} and H_{zi}. Since the geometry and excitation of the structure in Figure 1 are independent of the y-coordinate, all field quantities are independent of the y-coordinate. Hence, the time harmonic, source-free Maxwell field equations for the TE field with respect to the z-axis in each region (i) take the form :

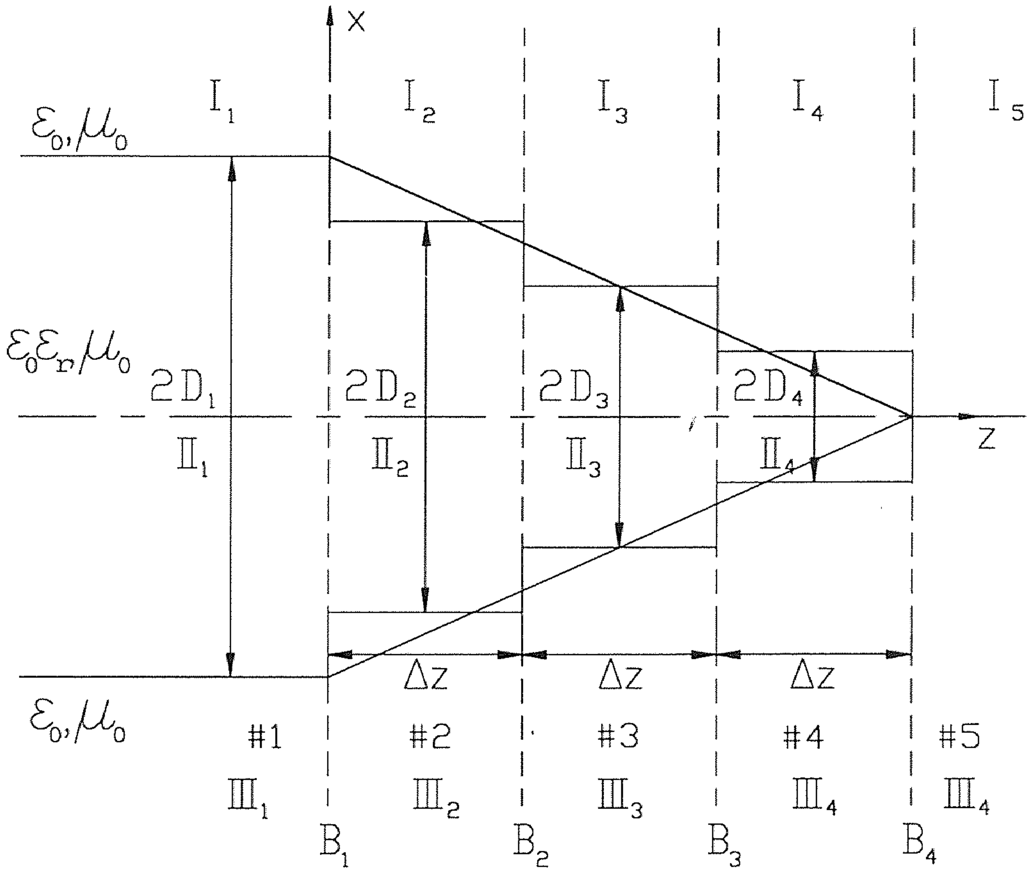

Figure 1 Staircase approximation.

$$\eta_0 H_{xi} = \frac{1}{jk_0}\frac{\partial E_{yi}}{\partial z}\ , \qquad \eta_0 H_{zi} = -\frac{1}{jk_0}\frac{\partial E_{yi}}{\partial x}, \tag{2.1a}$$

$$\eta_0[\frac{\partial H_{xi}}{\partial z} - \frac{\partial H_{zi}}{\partial x}] = jk_0[\frac{k_i(x)}{k_0}]^{1/2} E_{yi}\ , \tag{2.1b}$$

where

$$k_i(x) = \begin{cases} k_0 & |x| > D_i \\ k & |x| < D_i\ , \end{cases} \tag{2.1c}$$

$$k = k_0 \varepsilon_r^{\ 1/2} = \omega\,(\mu_0 \varepsilon_0 \varepsilon_r)^{1/2}, \qquad \eta_0 = (\mu_0/\varepsilon_0)^{1/2}. \tag{2.1d}$$

The quantity ω is the angular frequency, (μ_0, ε_0) the permeability and permittivity of free space and ε_r is the dielectric constant. The above fields assume a time-dependence of $\exp(j\omega t)$ which is suppressed.

Substitution of (2.1a) into (2.1b) yields the reduced wave equation

$$[\frac{\partial^2}{\partial x^2} + \frac{\partial^2}{\partial z^2} + k_i^2(x)]E_{yi} = 0, \qquad (2.2)$$

where $k_i^2(x)$ is given in (2.1c). Once E_{yi} is determined from (2.2), the other components H_{xi} and H_{zi} follow from (2.1a).

Before discussing the consequences of the step discontinuities, it is first necessary to present the complete orthonormal set of modes which are supported by an infinite, lossless, dielectric slab waveguide of arbitrary thickness 2D. Since excitation and slab geometry are symmetric about the z-axis, only even surface and even radiation modes are included in the complete set. Hence, an arbitrary, even TE field in each region (i) of Figure 1 can be expressed in terms of these modes, with D replaced by D_i and with parameters identified by the subscript "i".

The slab modes are found by solving Maxwell's source-free field equations subject to the appropriate boundary conditions. The boundary conditions are the continuity of the tangential electric and magnetic fields at interfaces located at x = ±D. Analytic expressions for these modes are well known [11] and will only be summarized in the discussion to follow.

2.1 Even TE Modes of the Dielectric Slab Waveguide of Thickness 2D

Note that the subscript "i" which appears in (2.1) and (2.2) has been dropped for convenience since only one waveguide of thickness 2D is being considered here.

Let

$$E_y = \mathrm{v}(z)\Phi(x). \tag{2.3}$$

Substitution of (2.3) into (2.2) yields

$$\frac{d^2\mathrm{v}}{dz^2} + \beta^2\mathrm{v} = 0, \tag{2.4a}$$

$$\frac{d^2\Phi}{dx^2} + k_x^2\Phi = 0, \tag{2.4b}$$

with

$$k_x^2 = k^2(x) - \beta^2, \tag{2.4c}$$

where $k(x)$ is defined in (2.1c) which means that the parameter k_x is also different in the regions $|x| > D$ and $|x| < D$.

Solving (2.4a) gives

$$\mathrm{v}(z) = Ae^{-j\beta z} + Be^{j\beta z} \tag{2.5}$$

with unknown complex constants A and B. These constants will be determined later by applying the boundary conditions of continuity of tangential electric and magnetic fields at the step discontinuities.

Solutions to (2.4b) must satisfy the boundary conditions of continuity of the tangential electric and magnetic fields across the interfaces at $x = \pm D$. These boundary conditions yield continuity at $x = \pm D$ of β, $\Phi(x)$ and $d\Phi / dx$. The continuity of the propagation constant β is a statement of Snell's law of refraction and dictates that β is a constant for all x. Depending on the allowable value of β, the one dimensional reduced wave equation (2.4b), subject to the afore mentioned boundary conditions, yield different modal solutions.

2.1.1 Even Surface Wave Modes

For β real in the range $k_0 \le |\beta| \le k$, solutions to the reduced wave equation (2.4b) which satisfy the boundary conditions are standing waves in the slab cross section and evanescent fields in the surrounding air regions. The associated potential solutions are [11]

$$\Phi(x) = \begin{cases} C_n \cos(k_{xn} D) e^{-\alpha_{xn}(|x|-D)} & D \le |x| < \infty \\ C_n \cos(k_{xn} x) & -D \le x \le D, \end{cases} \tag{2.6}$$

with

$$C_n = [\frac{\alpha_{xn}}{1+\alpha_{xn} D}]^{1/2}, \tag{2.6a}$$

$$k_{xn} = [k^2 - \beta_n^2]^{1/2} \quad , \tag{2.6b}$$

$$\alpha_{xn} = [\beta_n^2 - k_0^2]^{1/2} \quad , \tag{2.6c}$$

and the dispersion relation (eigenvalue equation) is

$$k_{xn} \tan(k_{xn} D) = \alpha_{xn}. \tag{2.7}$$

The dispersion relation specifies allowable, discrete, real values $\beta = \beta_n$, n = 0, 1, 2,..., that identify even surface wave modes. The potential functions $\Phi_n(x)$ are orthogonal and satisfy the relation

$$\int_{-\infty}^{\infty} \Phi_m(x)\Phi_n(x)dx = \delta_{mn} , \tag{2.8}$$

where δ_{mn} is the Kronecker delta function.

2.1.2 Even Radiation Modes

The complete set of modes of the dielectric slab waveguide consists of a finite, discrete spectrum of surface wave modes plus an infinite, continuous spectrum of propagating and evanescent radiation modes. Propagating radiation modes correspond to β real in the range $0 \le |\beta| \le k_0$, while evanescent radiation modes occur when $\beta = -j|\beta|$ for $0 < |\beta| < \infty$. Radiation modes consist of standing waves both inside and outside the slab. Such waves satisfy Maxwell's equations and boundary conditions on the slab surfaces at $x = \pm D$. Radiation modes can be thought of as being excited by a source at $z = -\infty$ which extends over the range $D < |x| < \infty$ [11].

In contrast to surface wave modes, the satisfaction of boundary conditions do not yield for the radiation modes a dispersion equation for β. Thus, all values of β in the ranges specified above are allowed and each corresponds to a radiation mode. The radiation modes are derivable from the wave equation (2.4b), subject to the continuity conditions at $x = \pm D$. The even radiation potential solutions are given by [11]

$$\Phi(x,u) = \begin{cases} C(u)[\cos(vD)\cos(u(|x|-D)) - \frac{v}{u}\sin(vD)\sin(u(|x|-D))] & D \le |x| < \infty \\ C(u)\cos(vx) & -D \le x \le D, \end{cases} \tag{2.9}$$

with

$$C(u) = \{\frac{\pi}{2}[\cos^2(vD) + (\frac{v}{u})^2 \sin^2(vD)]\}^{-1/2}, \tag{2.9a}$$

$$u = (k_0^2 - \beta^2)^{1/2}, \tag{2.9b}$$

$$v = (k^2 - \beta^2)^{1/2} = (k^2 - k_0^2 + u^2)^{1/2}. \tag{2.9c}$$

Since $u \ge 0$ for radiation modes, (2.9b) substantiates that β is real when $0 \le u \le k_0$, while $\beta = -j|\beta|$ when $k_0 \le u < \infty$; see (2.12c).

The potential functions $\Phi(x,u)$ are orthonormal and satisfy the relation

$$\int_0^\infty \Phi(x,u)\Phi(x,u')dx = \delta(u-u'), \tag{2.10}$$

where $\delta(u-u')$ is the Dirac delta function. In addition, the surface wave modes and the radiation modes are mutually orthogonal, i.e.,

$$\int_{-\infty}^\infty \Phi_n(x)\Phi(x,u)dx = 2\int_0^\infty \Phi_n(x)\Phi(x,u)dx = 0. \tag{2.11}$$

2.2 Arbitrary, Even TE Field of a Slab Waveguide

Returning to the geometry of Figure 1, the electric field in each region (i) is represented by the expansion [11]

$$E_{yi} = \sum_{n=0}^{N} \mathrm{v}_{in}(z)\Phi_{in}(x) + \int_0^\infty \mathrm{v}_i(z,u)\Phi_i(x,u)du. \tag{2.12}$$

From (2.5),

$$\mathrm{v}_{in}(z) = A_{in} e^{-j\beta_{in} z} + B_{in} e^{j\beta_{in} z}, \tag{2.12a}$$

$$\mathrm{v}_i(z,u) = A_i(u) e^{-j\beta_i(u) z} + B_i(u) e^{j\beta_i(u) z}, \tag{2.12b}$$

and from (2.9b),

$$\beta_i(u) = \begin{cases} (k_0^2 - u^2)^{1/2} & k_0^2 > u^2 \\ 0 & k_0^2 = u^2 \\ -j(u^2 - k_0^2)^{1/2} & k_0^2 < u^2, \end{cases} \tag{2.12c}$$

and β_{in} for D_i are determined from (2.6b), (2.6c) and (2.7), the eigenvalue equation. The summation over the integer n in (2.12) identifies all the propagating even surface wave modes and the integral over u represents the continuous spectrum of even radiation modes.

Substituting (2.12) into (2.1a) gives

$$\eta_0 H_{xi} = \sum_{n=0}^{N} i_{in}(z)\Phi_{in}(x) + \int_0^{\infty} i_i(z,u)\Phi_i(x,u)du, \tag{2.13a}$$

$$\eta_0 H_{zi} = \frac{1}{-jk_0}\left[\sum_{n=0}^{N} \mathrm{v}_{in}(z)\frac{d\Phi_{in}(x)}{dx} + \frac{\partial}{\partial x}\int_0^{\infty} \mathrm{v}_i(z,u)\Phi_i(x,u)du\right], \tag{2.13b}$$

where

$$i_{in}(z) = \frac{1}{jk_0}\frac{d\mathrm{v}_{in}(z)}{dz} = -\frac{\beta_{in}}{k_0}[A_{in} e^{-j\beta_{in} z} - B_{in} e^{j\beta_{in} z}], \tag{2.13c}$$

$$i_i(z,u) = \frac{1}{jk_0}\frac{\partial \mathrm{v}_i(z,u)}{\partial z} = -\frac{\beta_i(u)}{k_0}[A_i(u) e^{-j\beta_i(u) z} - B_i(u) e^{j\beta_i(u) z}]. \tag{2.13d}$$

Recall that the field components E_{yi}, H_{xi} and H_{zi}, as represented by (2.12) and (2.13), exist in each region (i), i = 1,...5, of Figure 1. To find the unknown expansion coefficients in each region (i), the boundary conditions of the continuity of tangential electric field and tangential magnetic field at the step discontinuities B_i, i = 1,...4, must be imposed.

To find the rigorous field solution, however, it is convenient to find partial fields first and then to construct the rigorous field solution as a superposition of the partial fields. A partial field is a field that is established due to a single step discontinuity, *i.e.*, the effect of subsequent steps discontinuities are ignored. This construction will now be clarified with reference to Figure 2.

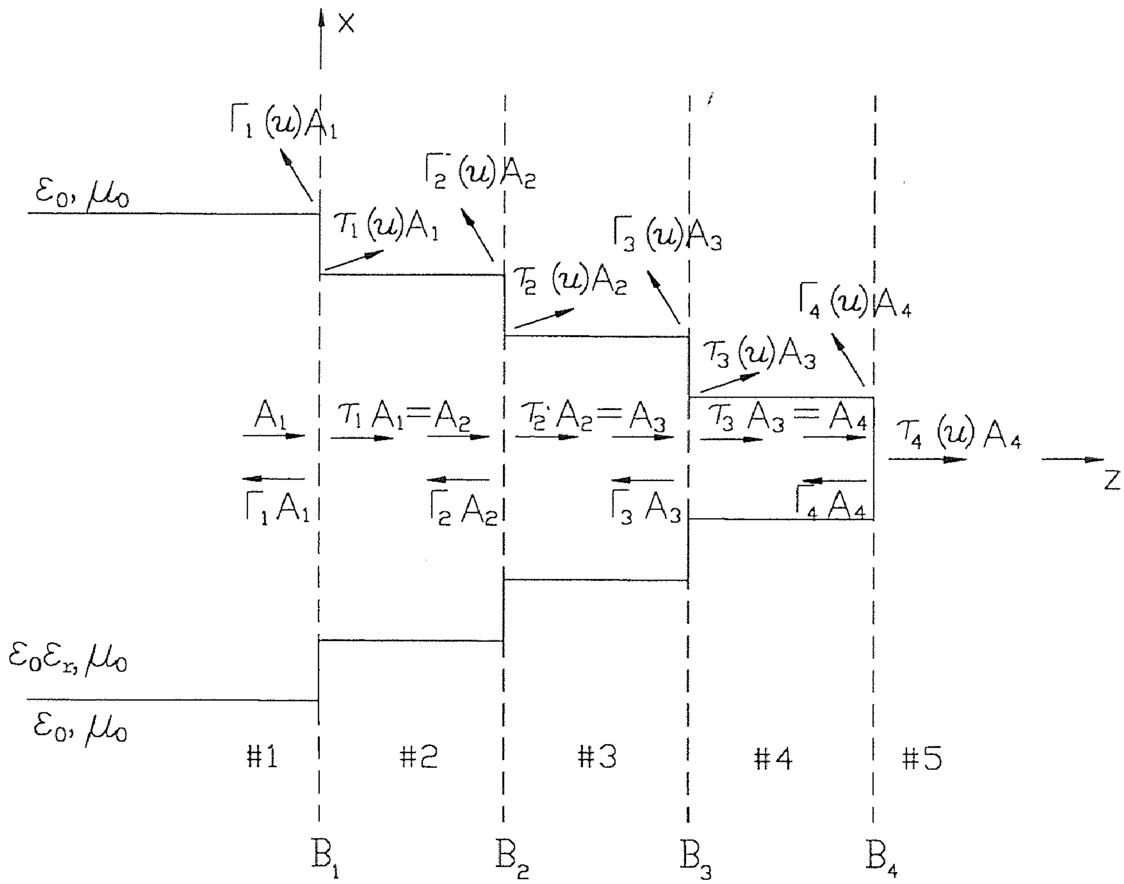

Figure 2 First forward partial field wave constituents at each step discontinuity.

2.3 Partial Fields

Initially, an incident even TE surface wave mode (labeled A_1 in Figure 2) is guided by a slab waveguide of thickness $2D_1$ in region 1 ($z < 0$). When this incident wave strikes the step discontinuity at $z = 0$ (boundary plane B_1), transmitted ($A_2 = \tau_1 A_1$) and reflected

$(B_1 = \Gamma_1 A_1)$ surface waves as well as forward $(A_2(u) = \tau_1(u)A_1)$ and backward $(B_1(u) = \Gamma_1(u)A_1)$ radiation modes get excited. Assume that only the n = 0 surface wave mode is non-zero, and ignore for the moment in region 2 both the backward going surface wave $(B_2 = \Gamma_2 A_2)$ and backward going radiation modes $(B_2(u) = \Gamma_2(u)A_2)$ which are established because of the step discontinuities to the right at B_i, i = 2,...,4. Under these conditions, the unknown parameters $(\Gamma_1, \Gamma_1(u))$ are reflection coefficients and $(\tau_1, \tau_1(u))$ are transmission coefficients for the single step discontinuity at z = 0. The partial fields in region 1 (z < 0) take the forms

$$\begin{aligned} E_{y1}^{f1} &= \mathrm{v}_1(z)\Phi_1(x) + \int_0^\infty \mathrm{v}_1(z,u)\Phi_1(x,u)du \\ &= A_1\{[e^{-j\beta_1 z} + \Gamma_1 e^{j\beta_1 z}]\Phi_1(x) + \int_0^\infty \Gamma_1(u)e^{j\beta_1(u)z}\Phi_1(x,u)du\}, \end{aligned} \tag{2.14a}$$

$$\eta_0 H_{x1}^{f1} = -\frac{A_1}{k_0}\{\beta_1[e^{-j\beta_1 z} - \Gamma_1 e^{j\beta_1 z}]\Phi_1(x) - \int_0^\infty \beta_1(u)\Gamma_1(u)e^{j\beta_1(u)z}\Phi_1(x,u)du\}, \tag{2.14b}$$

$$\eta_0 H_{z1}^{f1} = \frac{jA_1}{k_0}\{[e^{-j\beta_1 z} + \Gamma_1 e^{j\beta_1 z}]\frac{d\Phi_1(x)}{dx} + \frac{\partial}{\partial x}\int_0^\infty \Gamma_1(u)e^{j\beta_1(u)z}\Phi_1(x,u)du\}, \tag{2.14c}$$

where normalization to unity power of the incident even TE_0 surface wave mode gives

$$|A_1| = (\frac{2\eta_0 k_0}{\beta_1})^{1/2} . \tag{2.14d}$$

The partial fields in region 2 (0 < z < Δz) are given by

$$\begin{aligned} E_{y2}^{f1} &= \mathrm{v}_2(z)\Phi_2(x) + \int_0^\infty \mathrm{v}_2(z,u)\Phi_2(x,u)du \\ &= A_1\{[\tau_1 e^{-j\beta_2 z}\Phi_2(x) + \int_0^\infty \tau_1(u)e^{-j\beta_2(u)z}\Phi_2(x,u)du\}, \end{aligned} \tag{2.15a}$$

$$\eta_0 H_{x2}^{f1} = -\frac{A_1}{k_0}[\beta_2\tau_1 e^{-j\beta_2 z}\Phi_2(x) + \int_0^\infty \beta_2(u)\tau_1(u)e^{-j\beta_2(u)z}\Phi_2(x,u)du], \tag{2.15b}$$

$$\eta_0 H_{z2}^{f1} = \frac{jA_1}{k_0}[\tau_1 e^{-j\beta_2 z}\frac{d\Phi_2(x)}{dx} + \frac{\partial}{\partial x}\int_0^\infty \tau_1(u)e^{-j\beta_2(u)z}\Phi_2(x,u)du]. \tag{2.15c}$$

The subscripts "1" and "2" define the regions where the partial fields exist, whereas the superscript "$f1$" identifies the first forward partial field contributions to the rigorous field solution. The use of the term "forward" signifies that the step discontinuities to the right are considered sequentially. To be discussed later, a "backward" partial field contribution arises by considering wave progression back from the tip toward the step discontinuities to the left sequentially.

2.3.1 Reflection and Transmission Coefficients at a Step Discontinuity

The unknown reflection and transmission coefficients at each step discontinuity are found following the procedure discussed in [12]. However, significant differences in the formulation are introduced. Firstly, the parameters $\tau(u=0)$, $\Gamma(u=0)$, $\tau(u=k_0)$ and $\Gamma(u=k_0)$ are not assumed to be zero as had been done in [12]. Secondly, in the numerical evaluation of the infinite integral, truncation is taken to include evanescent radiation modes. Thirdly, as will be seen shortly, certain double integrals are evaluated correctly, whereas in [12] these integrals were evaluated incorrectly. Finally, normalized parameters are introduced; [12] did not include comparison of results with other published data because their formulation was not properly normalized.

We chose the method in [12] to solve the problem of scattering at a single step discontinuity because the system of linear equations obtained involves a numerically efficient matrix that is sparse and diagonally dominant and because a similar system of equations is obtained at each subsequent step discontinuity.

Before implementing the method, we define the following normalized parameters:

$$\bar{k}_0 = k_0 D_1, \quad \bar{k}_1 = k_1 D_1, \quad \bar{k}_{xn} = k_{xn} D_1, \quad \bar{\alpha}_{xn} = \alpha_{xn} D_1, \quad \bar{\beta}_n = \beta_n D_1,$$

$$\bar{u}_i = u_i D_1, \quad \bar{v}_i = v_i D_1, \quad \bar{\beta}_n(\bar{u}_i) = \beta_n(u_i) D_1,$$

$$\bar{x} = \frac{x}{D_1}, \quad \bar{z} = \frac{z}{D_1}, \quad \bar{\rho} = \frac{\rho}{D_1}, \quad \bar{R}_i = \frac{D_i}{D_1},$$

$$\bar{\Gamma}_i = \Gamma_i, \quad \bar{\tau}_i = \tau_i, \quad \bar{\Gamma}_i(\bar{u}) = \frac{\Gamma_i(u)}{\sqrt{D_1}}, \quad \bar{\tau}_i(\bar{u}) = \frac{\tau_i(u)}{\sqrt{D_1}},$$

$$\overline{E}_{yi}(\overline{x},\overline{z}) = \sqrt{D_1}E_{yi}(x,z),\ \overline{H}_{yi}(\overline{x},\overline{z}) = \sqrt{D_1}H_{yi}(x,z),\ \overline{H}_{zi}(\overline{x},\overline{z}) = \sqrt{D_1}H_{zi}(x,z)$$

$$i = 1, 2, \ldots \qquad (2.16)$$

Introducing the normalized parameters (2.16) into (2.14) and (2.15), substituting into the continuity boundary conditions

$$\overline{E}_{y1}(\overline{x},\overline{z}=0) = \overline{E}_{y2}(\overline{x},\overline{z}=0),\ \ \overline{H}_{x1}(\overline{x},\overline{z}=0) = \overline{H}_{x2}(\overline{x},\overline{z}=0) \qquad (2.17)$$

gives

$$(1+\overline{\Gamma}_1)\overline{\Phi}_1(\overline{x}) + \int_0^\infty \overline{\Gamma}_1(\overline{u})\overline{\Phi}_1(\overline{x},\overline{u})d\overline{u} = \overline{\tau}_1\overline{\Phi}_2(\overline{x}) + \int_0^\infty \overline{\tau}_1(\overline{u})\overline{\Phi}_2(\overline{x},\overline{u})d\overline{u}, \qquad (2.18a)$$

$$\overline{\beta}_1(1-\overline{\Gamma}_1)\overline{\Phi}_1(\overline{x}) - \int_0^\infty \overline{\beta}_1(\overline{u})\overline{\Gamma}_1(\overline{u})\overline{\Phi}_1(\overline{x},\overline{u})d\overline{u} = \overline{\beta}_2\overline{\tau}_1\overline{\Phi}_2(\overline{x}) + \int_0^\infty \overline{\beta}_2(\overline{u})\overline{\tau}_1(\overline{u})\overline{\Phi}_2(\overline{x},\overline{u})d\overline{u}, \qquad (2.18b)$$

where $(\overline{\beta}_1, \overline{\beta}_1(\overline{u}))$ and $(\overline{\beta}_2, \overline{\beta}_2(\overline{u}))$ are normalized propagation constants in regions i = 1 and i = 2, respectively; $\overline{\beta}_1$ and $\overline{\beta}_2$ are determined from the eigenvalue equation (2.7) for D_1 and D_2, respectively, while $\overline{\beta}_1(\overline{u})$, $\overline{\beta}_2(\overline{u})$ are both given by (2.12c); both (2.7) and (2.12c) are reformulated using normalized parameters. In addition,

$$\overline{\Phi}_i(\overline{x}) = \sqrt{D_1}\Phi_i(x), \qquad \overline{\Phi}_i(\overline{x},\overline{u}) = \Phi_i(x,u), \qquad (2.18c)$$

with

$$\overline{C}_i = \sqrt{D_1}C_i, \qquad \overline{C}_i(\overline{u}) = C_i(u); \qquad (2.18d)$$

see (2.6), where $\Phi_n(x)$ is rewritten as $\Phi_i(x)$, the integer n = 0 being suppressed and the integer "i" introduced to identify uniform waveguide regions; see also (2.9), where $\Phi(x,u)$ is given and $\Phi_i(x,u)$ is obtained by replacing D with D_i.

Multiplying (2.18a) by $\overline{\Phi}_1(\overline{x})$ and (2.18b) by $\overline{\Phi}_2(\overline{x})$, integrating over $\overline{x}$ from - ∞ to + ∞, interchanging the order of the integrations over $\overline{u}$ and $\overline{x}$, and using the normalized versions of the orthogonality relations (2.8) and (2.11) yield, respectively, the computationally more efficient relationships

$$1+\overline{\Gamma}_1 = \overline{\tau}_1\overline{I}_{12} + \int_0^\infty \overline{\tau}_1(\overline{u})\overline{I}_{12}(\overline{u})d\overline{u}, \qquad (2.19a)$$

$$\overline{\beta}_1(1-\overline{\Gamma}_1)\overline{I}_{12} = \overline{\tau}_1\overline{\beta}_2 + \int_0^\infty \overline{\beta}_1(\overline{u})\overline{\Gamma}_1(\overline{u})\overline{I}_{21}(\overline{u})d\overline{u}, \qquad (2.19b)$$

where

$$\overline{I}_{12} = \int_{-\infty}^{\infty} \overline{\Phi}_1(\overline{x})\overline{\Phi}_2(\overline{x})d\overline{x}, \tag{2.19c}$$

$$\overline{I}_{\substack{12\\21}}(\overline{u}_j) = \int_{-\infty}^{\infty} \overline{\Phi}_{\substack{1\\2}}(\overline{x})\overline{\Phi}_{\substack{2\\1}}(\overline{x},\overline{u}_j)d\overline{x}. \tag{2.19d}$$

To solve (2.19), the integrals over $\overline{x}$ are first evaluated explicitly. Next, the remaining integrals are truncated at $\overline{u} = \overline{u}_N = 2\overline{k}_0$ and discretized. The value of $\overline{u}_N = 2\overline{k}_0$ insures that both propagating and evanescent radiation modes are included . Following the procedure used in [12], Simpson's one - third rule approximation is used. For example, the integral in (2.19a) is approximated as:

$$\begin{aligned}\int_0^{\infty} \overline{\tau}_1(\overline{u})\overline{I}_{12}(\overline{u})d\overline{u} &\equiv \int_0^{\infty} \overline{f}_1(\overline{u})d\overline{u} \approx \int_0^{\overline{u}_N} \overline{f}_1(\overline{u})d\overline{u} \\ &\approx \frac{\Delta\overline{u}}{3}[\overline{f}_1(\overline{u}_0) + 4\sum_{\substack{m=1\\ \text{odd}}}^{N-1}\overline{f}_1(\overline{u}_m) + 2\sum_{\substack{m=2\\ \text{even}}}^{N-2}\overline{f}_1(\overline{u}_m) + \overline{f}_1(\overline{u}_N)],\end{aligned} \tag{2.20a}$$

where

$$\overline{f}(\overline{u}_m) = \overline{\tau}_1(\overline{u}_m)\overline{I}_{12}(\overline{u}_m),$$

$$\Delta\overline{u} = \frac{\overline{u}_N}{N}, \quad \overline{u}_m = m\Delta\overline{u}, \; m = 0, 1, 2, \ldots, N \qquad (N = \text{even}). \tag{2.20b}$$

Similarly, the integral over $\overline{u}$ in (2.19b) is evaluated approximately:

$$\begin{aligned}\int_0^{\infty} \overline{\beta}_1(\overline{u})\overline{\Gamma}_1(\overline{u})\overline{I}_{21}(\overline{u})d\overline{u} &\equiv \int_0^{\infty} \overline{g}_1(\overline{u})d\overline{u} \approx \int_0^{\overline{u}_N} \overline{g}_1(\overline{u})d\overline{u} \\ &\approx \frac{\Delta\overline{u}}{3}[\overline{g}_1(\overline{u}_0) + 4\sum_{\substack{m=1\\ \text{odd}}}^{N-1}\overline{g}_1(\overline{u}_m) + 2\sum_{\substack{m=2\\ \text{even}}}^{N-2}\overline{g}_1(\overline{u}_m) + \overline{g}_1(\overline{u}_N)],\end{aligned} \tag{2.21a}$$

where

$$\overline{g}_1(\overline{u}_m) = \overline{\beta}_1(\overline{u}_m)\overline{\Gamma}_1(\overline{u}_m)\overline{I}_{21}(\overline{u}_m). \tag{2.21b}$$

It is now necessary to determine 2N+4 unknowns, namely, $\overline{\Gamma}_1$, $\overline{\tau}_1$, $\overline{\Gamma}_1(\overline{u}_m)$, $\overline{\tau}_1(\overline{u}_m)$, $m = 0, 1, 2, \ldots, N$. However, we have only two equations, (2.19a) and (2.19b) with (2.20) and (2.21). To obtain additional equations, multiply (2.18a) by $\overline{\Phi}_1(\overline{x},\overline{u}_j)$ and (2.18b) by

$\overline{\Phi}_2(\overline{x},\overline{u}_j)$, integrate the resulting equations over $\overline{x}$ from - ∞ to + ∞ and evaluated the resultant double integral as shown in Appendix A to obtain:

$$2\overline{\Gamma}_1(\overline{u}_j) = \overline{\tau}_1 \overline{I}_{21}(\overline{u}_j) + \left(\int_0^{\overline{u}_j-\delta} + \int_{\overline{u}_j+\delta}^{\infty}\right)\overline{\tau}_1(\overline{u})\overline{I}_{21}(\overline{u},\overline{u}_j)d\overline{u} + \overline{\tau}_1(\overline{u}_j)\overline{T}_{12}(\overline{u}_j), \tag{2.22a}$$

$$\begin{aligned}\overline{\beta}_1(1-\overline{\Gamma}_1)\overline{I}_{12}(\overline{u}_j) = 2\overline{\beta}_2(\overline{u}_j)\overline{\tau}_1(\overline{u}_j) + \left(\int_0^{\overline{u}_j-\delta} + \int_{\overline{u}_j+\delta}^{\infty}\right)\overline{\beta}_1(\overline{u})\overline{\Gamma}_1(\overline{u})\overline{I}_{12}(\overline{u},\overline{u}_j)d\overline{u} \\ + \overline{\beta}_1(\overline{u}_j)\overline{\Gamma}_1(\overline{u}_j)\overline{T}_{12}(\overline{u}_j)\end{aligned}, \tag{2.22b}$$

$$j = 0, 1, 2, \ldots, N,$$

where

$$\begin{aligned}\overline{T}_{12}(\overline{u}_j) = \pi\overline{C}_1(\overline{u}_j)\overline{C}_2(\overline{u}_j)\{\cos(\overline{u}_j(1-\overline{R}_{21}))[\cos\overline{v}_j\cos(\overline{v}_j\overline{R}_{21}) \\ +(\frac{\overline{v}_j}{\overline{u}_j})^2\sin\overline{v}_j\sin(\overline{v}_j\overline{R}_{21})] + \frac{\overline{v}_j}{\overline{u}_j}\sin(\overline{u}_j(1-\overline{R}_{21}))\sin(\overline{v}_j(1-\overline{R}_{21}))\},\end{aligned} \tag{2.22c}$$

$$\overline{I}_{\substack{12\\21}}(\overline{u},\overline{u}_j) = \int_{-\infty}^{\infty}\overline{\Phi}_{\substack{1\\2}}(\overline{x},\overline{u})\overline{\Phi}_{\substack{2\\1}}(\overline{x},\overline{u}_j)d\overline{x}\ , \qquad \overline{I}_{\substack{12\\21}}(\overline{u}_j) = \overline{I}_{\substack{12\\21}}(\overline{u})\Big|_{\overline{u}=\overline{u}_j}, \tag{2.22d}$$

and $0 < \delta << 1$. As before, the integrals over $\overline{u}$ in (2.22) are truncated at $\overline{u} = \overline{u}_N = 2\overline{k}_0$ and discretized using Simpson's one - third approximation to give

$$\begin{aligned}\left(\int_0^{\overline{u}_j-\delta} + \int_{\overline{u}_j+\delta}^{\infty}\right)\overline{\tau}_1(\overline{u})\overline{I}_{21}(\overline{u},\overline{u}_j)d\overline{u} \equiv \left(\int_0^{\overline{u}_j-\delta} + \int_{\overline{u}_j+\delta}^{\infty}\right)\overline{h}_1(\overline{u},\overline{u}_j)d\overline{u} \\ \approx \frac{\Delta\overline{u}}{3}[\overline{h}_1(\overline{u}_0,\overline{u}_j) + 4\sum_{\substack{m=1\\ \text{odd}}}^{N-1}\overline{h}_1(\overline{u}_m,\overline{u}_j) + 2\sum_{\substack{m=2\\ \text{even}}}^{N-2}\overline{h}_1(\overline{u}_m,\overline{u}_j) + \overline{h}_1(\overline{u}_N,\overline{u}_j)]\end{aligned} \tag{2.23a}$$

and

$$\begin{aligned}\left(\int_0^{\overline{u}_j-\delta} + \int_{\overline{u}_j+\delta}^{\infty}\right)\overline{\beta}_1(\overline{u})\overline{\Gamma}_1(\overline{u})\overline{I}_{12}(\overline{u},\overline{u}_j)d\overline{u} \equiv \left(\int_0^{\overline{u}_j-\delta} + \int_{\overline{u}_j+\delta}^{\infty}\right)\overline{e}_1(\overline{u},\overline{u}_j)d\overline{u} \\ \approx \frac{\Delta\overline{u}}{3}[\overline{e}_1(\overline{u}_0,\overline{u}_j) + 4\sum_{\substack{m=1\\ \text{odd}}}^{N-1}\overline{e}_1(\overline{u}_m,\overline{u}_j) + 2\sum_{\substack{m=2\\ \text{even}}}^{N-1}\overline{e}_1(\overline{u}_m,\overline{u}_j) + \overline{e}_1(\overline{u}_N,\overline{u}_j)],\end{aligned} \tag{2.23b}$$

where the infinite limit is truncated at $\overline{u}_N$ and

$$\overline{h}_1(\overline{u}_m,\overline{u}_j) = \overline{\tau}_1(\overline{u}_m)\overline{I}_{21}(\overline{u}_m,\overline{u}_j), \qquad \overline{u}_m \neq \overline{u}_j, \tag{2.23c}$$

$$\overline{e}_1(\overline{u}_m,\overline{u}_j) = \overline{\beta}_1(\overline{u}_m)\overline{\Gamma}_1(\overline{u}_m)\overline{I}_{12}(\overline{u}_m,\overline{u}_j), \qquad \overline{u}_m \neq \overline{u}_j, \tag{2.23d}$$

and $\overline{I}_{12}(\bar{u}_m,\bar{u}_j)$ and $\overline{I}_{21}(\bar{u}_m,\bar{u}_j)$are given by (2.21d) with $\bar{u}$ replaced by $\bar{u}_m$. Thus, the system of linear equations (2.19a), (2.19b) and (2.22a), (2.22b) together with (2.20), (2.21) and (2.23) permit the determination of the 2N+4 unknowns, namely, $\overline{\Gamma}_1, \overline{\tau}_1, \overline{\Gamma}_1(\bar{u}_m)$, and $\overline{\tau}_1(\bar{u}_m)$, m = 1, 2, ..., N.

From (2.9) it follow that $\bar{A}(\bar{u}=\bar{u}_0=0)=0$; hence, (2.19d) give $\overline{I}_{12}(\bar{u}_0)=0$ and $\overline{I}_{21}(\bar{u}_0)=0$. Thus from (2.20b), $\bar{f}_1(\bar{u}_0)=\overline{\tau}_1(\bar{u}_0)\overline{I}_{12}(\bar{u}_0)$ = 0 and from (2.21b), $\bar{g}_1(\bar{u}_0)=$ $\overline{\beta}_1(\bar{u}_0)\overline{\Gamma}_1(\bar{u}_0)\overline{I}_{21}(\bar{u}_0)=0$. Also, from the normalized form of (2.12c), it follows that $\overline{\beta}_1(\bar{u}_m=\bar{k}_0)=0$; therefore, (2.21b) gives $\bar{g}_1(\bar{u}_m=\bar{k}_0)=\overline{\beta}_1(\bar{u}_m=\bar{k}_0)\overline{\Gamma}_1(\bar{u}_m=\bar{k}_0)$ $\overline{I}_{21}(\bar{u}_m=\bar{k}_0)$ = 0. Hence, only 2N+1 unknowns can be found at B_1 since $\bar{f}_1(\bar{u}_0), \bar{g}_1(\bar{u}_0)$ and $\bar{g}_1(\bar{u}_m=\bar{k}_0)$ are zero. This means that we use (2.19) and (2.22) to find $\overline{\Gamma}_1$, $\overline{\tau}_1$, $\overline{\Gamma}_1(\bar{u}_m)$and $\overline{\tau}_1(\bar{u}_m)$, m = 1, 2, ..., N, with the exception of $\overline{\Gamma}_1(\bar{u}_m=\bar{k}_0)$ and that $\overline{\tau}_1(\bar{u}_0=0)$, $\overline{\Gamma}_1(\bar{u}_0=0)$ and $\overline{\Gamma}_1(\bar{u}_m=\bar{k}_0)$ cannot be determined.

The procedure is repeated at each step discontinuity. The difference in the formulation, at B_2 in Figure 2 for example, is that the non-zero wave constituents assumed to strike the discontinuity at $\bar{z}=\Delta\bar{z}$ include now both a single guided surface wave mode, represented by $\bar{A}_2$, plus the forward traveling radiation modes, represented by $\bar{A}_2(\bar{u})$ $(\bar{A}_2(\bar{u})=\overline{\tau}_1(\bar{u})\bar{A}_1,\ \ 0\le\bar{u}<\infty)$. As before, both the reflected surface wave mode $(\overline{B_2}=\overline{\Gamma}_2\bar{A}_2)$ and the reflected radiation modes $(\overline{B_2}(\bar{u})=\overline{\Gamma}_2(\bar{u})\bar{A}_2,\ 0\le\bar{u}<\infty)$ in region 3 are neglected. Thus, the normalized transverse field components in region 2 are now:

$$\begin{aligned}\overline{E}_{y2}^{f1} &= \bar{A}_2\{[e^{-j\overline{\beta}_2\bar{z}}+\overline{\Gamma}_2e^{j\overline{\beta}_2\bar{z}}]\overline{\Phi}_2(\bar{x})+\int_0^\infty\overline{\Gamma}_2(\bar{u})e^{j\overline{\beta}_2(\bar{u})\bar{z}}\overline{\Phi}_2(\bar{x},\bar{u})d\bar{u}\} \\ &+\bar{A}_1\int_0^\infty\overline{\tau}_1(\bar{u})e^{-j\overline{\beta}_2(\bar{u})\bar{z}}\overline{\Phi}_2(\bar{x},\bar{u})d\bar{u},\end{aligned} \tag{2.24a}$$

$$\begin{aligned}\eta_0\overline{H}_{x2}^{f1} &= -\frac{\bar{A}_2}{\bar{k}_0}\{\overline{\beta}_2[e^{-j\overline{\beta}_2\bar{z}}-\overline{\Gamma}_2e^{j\overline{\beta}_2\bar{z}}]\overline{\Phi}_2(\bar{x})-\int_0^\infty\overline{\beta}_2(\bar{u})\overline{\Gamma}_2(\bar{u})e^{j\overline{\beta}_2(\bar{u})\bar{z}}\overline{\Phi}_2(\bar{x},\bar{u})d\bar{u}\} \\ &-\frac{\bar{A}_1}{\bar{k}_0}\int_0^\infty\overline{\beta}_2(\bar{u})\overline{\tau}_1(\bar{u})e^{-j\overline{\beta}_2(\bar{u})\bar{z}}\overline{\Phi}_2(\bar{x},\bar{u})d\bar{u},\end{aligned} \tag{2.24b}$$

and the transverse field components in region 3 (neglecting reflected waves from steps to the right) are :

$$E_{y3}^{f1} = \bar{A}_2\{[\bar{\tau}_2 e^{-j\bar{\beta}_3\bar{z}}\overline{\Phi}_3(\bar{x}) + \int_0^{\infty}\bar{\tau}_2(\bar{u})e^{-j\bar{\beta}_3(\bar{u})\bar{z}}\overline{\Phi}_3(\bar{x},\bar{u})d\bar{u}\}, \tag{2.25a}$$

$$\eta_0\bar{H}_{x3}^{f1} = -\frac{\bar{A}_2}{\bar{k}_0}[\bar{\beta}_3\bar{\tau}_2 e^{-j\bar{\beta}_3\bar{z}}\overline{\Phi}_3(\bar{x}) + \int_0^{\infty}\bar{\beta}_3(\bar{u})\bar{\tau}_2(\bar{u})e^{-j\bar{\beta}_3(\bar{u})\bar{z}}\overline{\Phi}_3(\bar{x},\bar{u})d\bar{u}]. \tag{2.25b}$$

Applying the boundary conditions of the continuity of E_y and H_x at $\bar{z} = \Delta\bar{z}$, noting that $\bar{A}_2 = \bar{\tau}_1\bar{A}_1$, truncating the integrals over $\bar{u}$ at $\bar{u} = \bar{u}_N = 2\bar{k}_0$, discretizing the remaining integral over finite limits of integration from $\bar{u} = 0$ to $\bar{u} = \bar{u}_N$ and using the orthogonality relations in a similar fashion as was done previously at B_1 yield the following system of 2N+1 linear equations for the 2N+1 unknowns $\bar{\Gamma}_2$, $\bar{\tau}_2$, $\bar{\Gamma}_2(\bar{u}_m)$ and $\bar{\tau}_2(\bar{u}_m)$, m = 1, 2, ..., N, not including $\bar{\Gamma}_2(\bar{u}_m = \bar{k}_0)$:

$$\begin{aligned} &e^{-j\bar{\beta}_2\Delta\bar{z}} + \bar{\Gamma}_2 e^{j\bar{\beta}_2\Delta\bar{z}} \\ &= \bar{\tau}_2 e^{-j\bar{\beta}_3\Delta\bar{z}}\overline{I_{23}} + \int_0^{\infty}\bar{\tau}_2(\bar{u})e^{-j\bar{\beta}_3(\bar{u})\Delta\bar{z}}\overline{I_{23}}(\bar{u})d\bar{u}, \end{aligned} \tag{2.26a}$$

$$\begin{aligned} &\bar{\tau}_1\bar{\beta}_2(e^{-j\bar{\beta}_2\Delta\bar{z}} - \bar{\Gamma}_2 e^{j\bar{\beta}_2\Delta\bar{z}})\overline{I_{23}} + \int_0^{\infty}[\bar{\tau}_1(\bar{u})e^{-j\bar{\beta}_2(\bar{u})\Delta\bar{z}} - \bar{\tau}_1\bar{\Gamma}_2(\bar{u})e^{j\bar{\beta}_2(\bar{u})\Delta\bar{z}}]\bar{\beta}_2(\bar{u})\overline{I_{32}}(\bar{u})d\bar{u} \\ &= \bar{\tau}_1\bar{\tau}_2\bar{\beta}_3 e^{-j\bar{\beta}_3\Delta\bar{z}}, \end{aligned} \tag{2.26b}$$

$$\begin{aligned} &2[\bar{\tau}_1(\bar{u}_j)e^{-j\bar{\beta}_2(\bar{u}_j)\Delta\bar{z}} + \bar{\tau}_1\bar{\Gamma}_2(\bar{u}_j)e^{j\bar{\beta}_2(\bar{u}_j)\Delta\bar{z}}] \\ &= \bar{\tau}_1\bar{\tau}_2 e^{-j\bar{\beta}_3(\bar{u}_j)\Delta\bar{z}}\overline{I_{32}}(\bar{u}_j) + (\int_0^{\bar{u}_j-\delta} + \int_{\bar{u}_j+\delta}^{\infty})\bar{\tau}_1\bar{\tau}_2(\bar{u})e^{-j\bar{\beta}_3(\bar{u})\Delta\bar{z}}\overline{I_{32}}(\bar{u},\bar{u}_j)d\bar{u} \\ &+ \bar{\tau}_1\bar{\tau}_2(\bar{u}_j)e^{-j\bar{\beta}_3(\bar{u}_j)\Delta\bar{z}}\overline{T_{23}}(\bar{u}_j), \end{aligned} \tag{2.26c}$$

$$\bar{\tau}_1\bar{\beta}_2(e^{-j\bar{\beta}_2\Delta\bar{z}}-\bar{\Gamma}_2e^{j\bar{\beta}_2\Delta\bar{z}})\bar{I}_{23}(\bar{u}_j)$$
$$+(\int_0^{\bar{u}_j-\delta}+\int_{\bar{u}_j+\delta}^{\infty})[\bar{\tau}_1(\bar{u})e^{-j\bar{\beta}_2(\bar{u})\Delta\bar{z}}-\bar{\tau}_1\bar{\Gamma}_2(\bar{u})e^{j\bar{\beta}_2(\bar{u})\Delta\bar{z}}]\bar{\beta}_2(\bar{u})\bar{I}_{23}(\bar{u},\bar{u}_j)d\bar{u}$$
$$+[\bar{\tau}_1(\bar{u}_j)e^{-j\bar{\beta}_2(\bar{u}_j)\Delta\bar{z}}-\bar{\tau}_1\bar{\Gamma}_2(\bar{u}_j)e^{j\bar{\beta}_2(\bar{u}_j)\Delta\bar{z}}]\bar{\beta}_2(\bar{u}_j)\bar{T}_{23}(\bar{u}_j)$$
$$=2\bar{\tau}_1\bar{\tau}_2(\bar{u}_j)\bar{\beta}_3(\bar{u}_j)e^{-j\bar{\beta}_3(\bar{u}_j)\Delta\bar{z}}, \qquad j=1,2,\ldots,N \tag{2.26d}$$

where

$$\bar{T}_{23}(\bar{u}_j)=\pi\bar{C}_2(\bar{u}_j)\bar{C}_3(\bar{u}_j)\{\cos(\bar{u}_j(\bar{R}_{21}-\bar{R}_{31}))[\cos(\bar{v}_j\bar{R}_{21})\cos(\bar{v}_jR_{31})$$
$$+(\frac{\bar{v}_j}{\bar{u}_j})^2\sin(\bar{v}_j\bar{R}_{21})\sin(\bar{v}_jR_{31})]+\frac{\bar{v}_j}{\bar{u}_j}\sin(\bar{u}_j(\bar{R}_{21}-\bar{R}_{31}))\sin(\bar{v}_j(\bar{R}_{21}-\bar{R}_{31}))\}, \tag{2.26e}$$

and

$$\bar{I}_{23}=\int_{-\infty}^{\infty}\bar{\Phi}_2(\bar{x})\bar{\Phi}_3(\bar{x})d\bar{x}, \tag{2.26f}$$

$$\bar{I}_{23}(\bar{u}_j)=\int_{-\infty}^{\infty}\bar{\Phi}_2(\bar{x})\bar{\Phi}_3(\bar{x},\bar{u}_j)d\bar{x}, \tag{2.26f}$$

$$\bar{I}_{32}(\bar{u}_j)=\int_{-\infty}^{\infty}\bar{\Phi}_3(\bar{x})\bar{\Phi}_2(\bar{x},\bar{u}_j)d\bar{x}, \tag{2.26f}$$

$$\bar{I}_{32}(\bar{u},\bar{u}_j)=\int_{-\infty}^{\infty}\bar{\Phi}_3(\bar{x},\bar{u})\bar{\Phi}_2(\bar{x},\bar{u}_j)d\bar{x}\ , \tag{2.26f}$$

with $0<\delta<<1$.

The remaining two step discontinuities at B_3 and B_4 in Figure 2 yield similar linear systems of equations so that the partial fields in regions 3, 4 and 5 can also be found. The overlaps integral encountered in (2.19) and (2.26) are evaluated in Appendix B.

2.4 Rigorous Field Solution

In Section 2.3 , the first forward partial fields in regions 1 and 2 were found explicitly by applying boundary conditions at B_1 and B_2, respectively. The scatter processes involved were approximate in that certain reflected fields were ignored. It was pointed out that the process was repeated and boundary conditions were applied at B_3 and B_4 in a similar fashion to obtain the remaining first forward partial fields in regions 3, 4 and 5. In all cases, the backward surface and radiation modes were taken to be zero to the right of B_i, i = 1, ..., 4, when the forward partial fields

$$\overline{E}_{yi}^{f1}, \overline{H}_{xi}^{f1} \text{ and } \overline{H}_{zi}^{f1} \qquad i = 1, 2, \ldots, 5, \tag{2.27}$$

were determined; the subscript "i" identifies the region where the field is located and the superscript "$f1$" identifies each constituent as being the "first forward" partial field contribution to the rigorous field solution.

To obtain a more accurate description of the total field, the waves which progress to the left (in the backward direction) that were ignored in the above formulation must be considered. This is accomplished by considering both of the backward surface wave mode and the backward radiation modes scattered by the abrupt termination at B_4 to be scattered by the step discontinuity at B_3. Now, however, by considering wave progression to the left and applying boundary conditions at each step discontinuity B_3, B_2, and B_1(in this order), the "first backward" partial field components are obtained; these are designated

$$\overline{E}_{yi}^{b1}, \overline{H}_{xi}^{b1} \text{ and } \overline{H}_{zi}^{b1}, \qquad i = 1, 2, 3, 4.$$

See Figure 3 for a schematic of the wave constituent in each region "i" as the wave field progress in the forward direction (Figure 3(a)), then progresses in the backward direction (Figure 3(b)) and progresses once again in the forward direction for a second time (Figure 3(c)). This processes can be repeated as often as needed to approximate the total field to the desired order of accuracy. Using only the wave processes depicted in Figure 3,*i.e.*, the first and second forward progressions(identified by the superscripts $f1$ and $f2$, respectively) and the first backward progression(identified by the superscripts $b1$), the total fields constituents in each region (i) can be formally approximated as follows:

In region 1:

$$E_{y1}^{Total} \cong E_{y1}^{f1} + E_{y1}^{b1}, \qquad H_{x1}^{Total} \cong H_{x1}^{f1} + H_{x1}^{b1}, \qquad H_{z1}^{Total} \cong H_{z1}^{f1} + H_{z1}^{b1}.$$

In region 2, 3, 4:

$$E_{yi}^{Total} \cong E_{yi}^{f1} + E_{yi}^{b1} + E_{yi}^{f2},\ H_{xi}^{Total} \cong H_{xi}^{f1} + H_{xi}^{b1} + H_{xi}^{f2},\ H_{zi}^{Total} \cong H_{zi}^{f1} + H_{zi}^{b1} + H_{zi}^{f2},$$
$$i = 2, 3, 4.$$

In region 5:

$$E_{y5}^{Total} \cong E_{y5}^{f1} + E_{y5}^{f2}, \qquad H_{x5}^{Total} \cong H_{x5}^{f1} + H_{x5}^{f2}, \qquad H_{z5}^{Total} \cong H_{z5}^{f1} + H_{z5}^{f2}. \qquad (2.29)$$

The accuracy of the total field will depend on how many forward and backward partial fields are included in the final results.

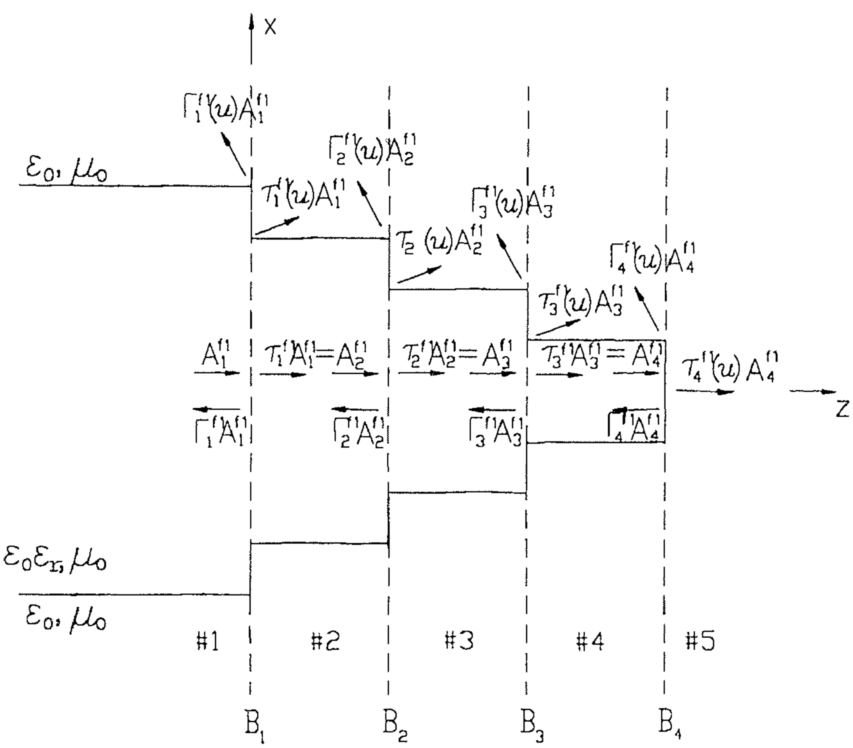

(a)

Figure 3 Partial field wave constituents at each step discontinuity (a) first forward (b) first backward (c) second forward.

Figure 3 (Continued)

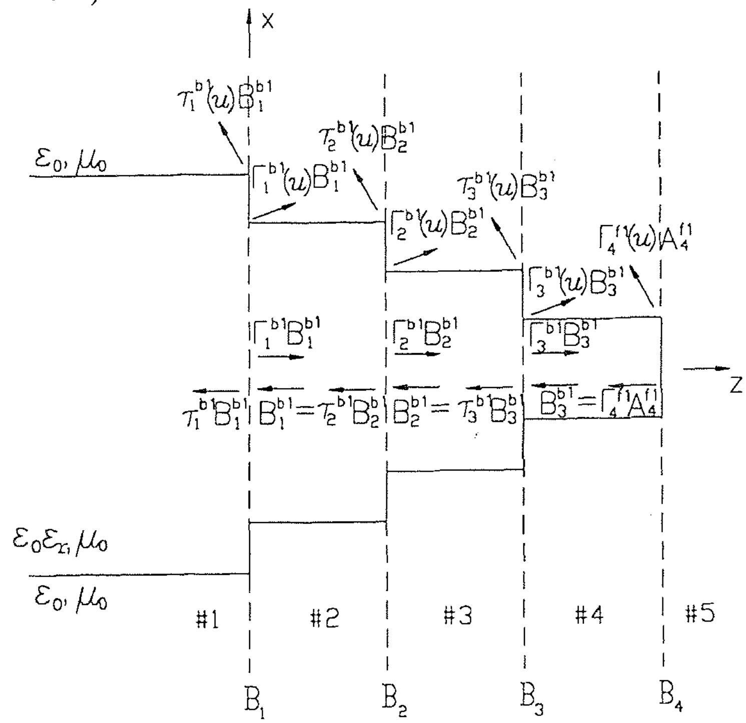

(b)

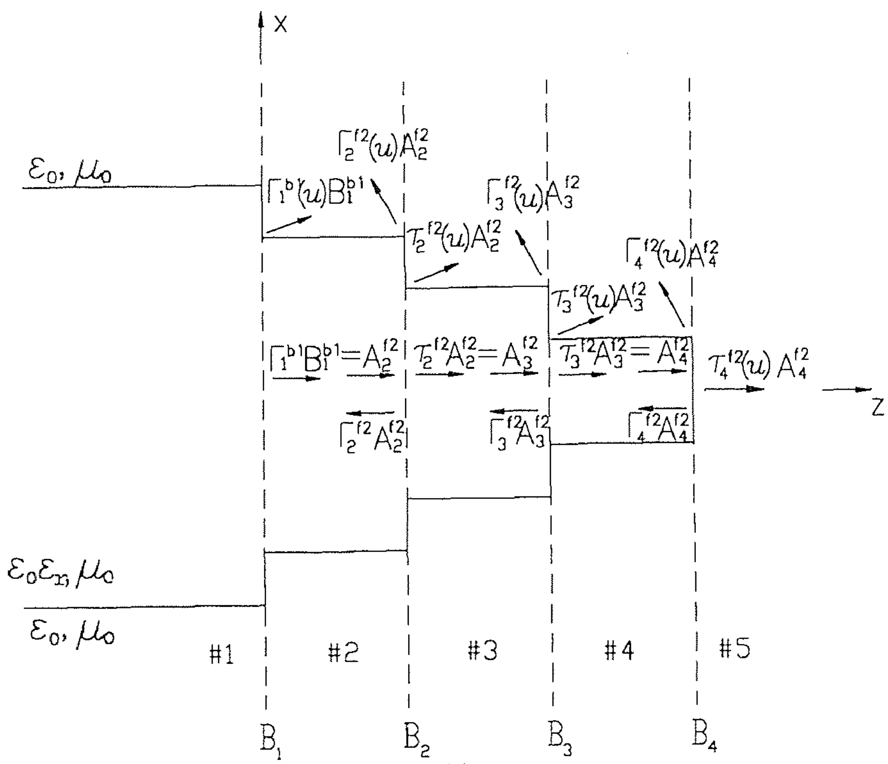

(c)

CHAPTER 3

NUMERICAL METHOD

The computer program essentially solves the linear system of equation in matrix form which is obtained at each step discontinuity. At the first step discontinuity, for example, the matrix equation is obtained from (2.19) and (2.22) with (2.20), (2.21) and (2.23); at the second step it is obtained from (2.26). Note that only first forward partial fields were considered in the derivation of these equations. The programs were written in ANSI 77 FORTRAN and executed on VAX/VMS system. LOTUS-123 was used to construct tables and figures. The program for solving the single step discontinuity is listed in Appendix E whereas the complete program is listed in Appendix F.

In the program (Appendix E or Appendix F), the subroutine named DISPER uses bi-section method [16] to solve the dispersion equation. The bi-section method was chosen because data was obtained in a few cases for dielectric materials of nearly equal refractive indices, which caused the Newton-Raphson method [16] not to converge.

The program is separated into five parts. The first part is the initial parameters setup. The parameters are

N: The number used to determine the size of $\Delta\bar{u}$; see (2.20b),

C: The size of the matrix (C = 2N+1),

NO: The integer one or two which multiples $\bar{u}_N$,

KD: The normalized slab width k_0D_1,

ER: The dielectric constant of the tapered slab,

NS: The dielectric constant of the material external to the tapered slab which usually is air, so that NS = 1.

In order for the main program to treat more than one step, the following parameters are also specified:

STEP: The number of step discontinuities,

KL: The normalized wedge length $k_0 L$,

ITER: The number of forward and backward progressions.

The second part of the main program calculates expressions and overlap integrals for the matrices. In the program, the FIND_UN subroutine finds the parameters $\bar{u}_i, \bar{v}(\bar{u}_i)$ and $\bar{\beta}_i(\bar{u}_i)$ for a radiation mode; GUIDED, GDRAD, and RADRAD are the subroutines for solving the overlap integrals. The third part of the program constructs the matrix equations. The subroutine named FORWARD is used when the wave transmits in the forward direction. The subroutine named BACKWARD is used when the wave transmits in the backward direction. The fourth part of the program solves the matrix equation using Gaussian Elimination decomposition. This is done in the COEF subroutine. The last part of the program calculates the guided and radiated powers by using the formulas in Appendix C, and calculates the radiation pattern of power gain which is solved by the subroutines PATTERNT and PATTERNR to determine the forward ($0 < \theta < \pi/2$) and backward ($\pi/2 < \theta < \pi$) radiation patterns of power gain, respectively, by using the formulas in Appendix D. LOTUS-123 is used to plot the radiation patterns of power gain .

For the computer system used (VAX/VMS), it takes one minute to calculate a 242×242 matrix; four minutes to calculate a 402×402 matrix(the times mentioned here are all CPU time and for the single step solution). The CPU charged time for multiple steps is obtained by multiplying the number of steps with the single step CPU charged time.

CHAPTER 4

NUMERICAL RESULTS

Recall that the dielectric wedge is approximated by a sequence of short slab segments of progressively smaller widths. Hence, a more accurate determination of the field scattered by the wedge geometry is obtained via the method presented in Chapter 2 by increasing the number of segments used. In theory, the method developed yields a rigorous solution provided the field solution at a single step discontinuity is accurately determined. To ascertain this accuracy, comparisons were made with the published data for scattering from a single step discontinuity.

Tables 1 - 4 compare data with that of P. G. Suchoski, Jr. and V. Ramaswamy [12]. Table 1 describes scattering at a step discontinuity which is modest, but not small since $D_2/D_1 = 0.6$, and for dielectric media with indices of refraction that are numerically close, which is of interest in the design of integrated optical devices. In Table 1 observe that, as far as conservation of power is concerned, the corrections made to [12] which are implemented here yield a significant redistribution of power, although conservation of power is well satisfied in both cases. Note that the power contained in the reflected surface wave mode(P_{ref}^{G}) is over twice as large, the power carried by the transmitted radiation mode(P_{trans}^{RAD}) is about 10% smaller and the power in the reflected radiation modes(P_{ref}^{RAD}) is approximately two orders of magnitude smaller than that of [12]. See Appendix C for the various power expressions. To facilitate comparison, truncation was taken at $u_N = k_0 D_1$ as was done in [12]. Data is also presented in Table 2 for truncation at both $u_N = k_0 D_1$ and $u_N = 2k_0 D_1$; note that N is twice as large for the latter to insure that the same number of propagating radiation modes are considered. Observe in Table 2 that the power in each mode remains nearly invariant even when evanescent waves are considered. This shows that our expressions possess good convergence properties.

Table 1 Comparison of result with P. G. Suchoski, Jr. and V. Ramaswamy at a modest step discontinuity. The refractive index of the two dielectric slabs is n_1 = 1.54, that of the surrounding medium is n_2 = 1.52, free space wavelength λ_0 = 0.6328μm, D_1 = 0.5μm, D_2 = 0.3μm for (a) P. G. Suchoski, Jr. and V. Ramaswamy; (b) the present method; (c) percentage difference between the present method and Suchoski, Jr. / Ramaswamy.

N =	P^G_{trans}	P^G_{ref}	P^{RAD}_{trans}	P^{RAD}_{ref}	P^{TOTAL}
50	0.99161766	0.0000011	0.00739380	0.00097930	0.99999190
70	0.99161685	0.0000011	0.00739540	0.00098020	0.99999360
100	0.99161620	0.0000011	0.00739630	0.00098080	0.99999440
120	0.99161626	0.0000011	0.00739670	0.00098120	0.99999530
150	0.99161630	0.0000011	0.00739690	0.00098130	0.99999560

(a)

N =	P^G_{trans}	P^G_{ref}	P^{RAD}_{trans}	P^{RAD}_{ref}	P^{TOTAL}
50	0.99339604	0.00000239	0.00658774	0.00001153	0.99999770
70	0.99339542	0.00000239	0.00658849	0.00001202	0.99999832
100	0.99339464	0.00000239	0.00658915	0.00001249	0.99999868
120	0.99339429	0.00000239	0.00658943	0.00001272	0.99999883
150	0.99339390	0.00000239	0.00658974	0.00001297	0.99999899

(b)

N =	P^G_{trans}	P^G_{ref}	P^{RAD}_{trans}	P^{RAD}_{ref}	P^{TOTAL}
50	0.179%	117.273%	10.902%	98.823%	0.001%
70	0.179%	117.273%	10.911%	98.774%	0.000%
100	0.179%	117.273%	10.913%	98.727%	0.000%
120	0.179%	117.273%	10.914%	98.704%	0.000%
150	0.179%	117.273%	10.912%	98.678%	0.000%

(c)

Table 2 Use different truncation maximum for the single step discontinuity problem with index of refraction n_1 = 1.54 for the slabs and n_2 = 1.52 for the surrounding medium, λ_0 = 0.6328μm, D_1 = 0.5μm, D_2 = 0.3μm for (a) $u_N = k_0 D_1$ (b) $u_N = 2k_0 D_1$.

N =	P^G_{trans}	P^G_{ref}	P^{RAD}_{trans}	P^{RAD}_{ref}	P^{TOTAL}
50	0.99339604	0.00000239	0.00658774	0.00001153	0.99999770
70	0.99339542	0.00000239	0.00658849	0.00001202	0.99999832
100	0.99339464	0.00000239	0.00658915	0.00001249	0.99999868
120	0.99339429	0.00000239	0.00658943	0.00001272	0.99999883
150	0.99339390	0.00000239	0.00658974	0.00001297	0.99999899

(a)

Table 2 (continued)

N =	P^{G}_{trans}	P^{G}_{ref}	P^{RAD}_{trans}	P^{RAD}_{ref}	P^{TOTAL}
100	0.99339482	0.00000241	0.00658781	0.00001174	0.99999678
140	0.99339438	0.00000241	0.00658860	0.00001225	0.99999764
200	0.99339372	0.00000242	0.00658930	0.00001275	0.99999819
240	0.99339342	0.00000242	0.00658960	0.00001298	0.99999841
300	0.99339306	0.00000242	0.00658992	0.00001325	0.99999865

(b)

For the same dielectric media, Tables 3 and 4 show conservation of power at a step discontinuity that is large since $D_2/D_1 = 0.2$. In this case, the results show a significant redistribution of power for all wave constituents, even though conservation of power is again satisfied. Hence, justification of results based solely on conservation of power can be misleading as was illustrated in Table 1.

Table 3 Comparison of result with P. G. Suchoski, Jr. and V. Ramaswamy at a large step discontinuity. The refractive index of the two dielectric slabs is $n_1 = 1.54$, that of the surrounding medium is $n_2 = 1.52$, free space wavelength $\lambda_0 = 0.6328\mu m$, $D_1 = 0.5\mu m$, $D_2 = 0.1\mu m$ for (a) P.G. Suchoski, Jr. and V. Ramaswamy; (b) the present method; (c) percentage difference between the present method and Suchoski, Jr. / Ramaswamy.

N =	P^{G}_{trans}	P^{G}_{ref}	P^{RAD}_{trans}	P^{RAD}_{ref}	P^{TOTAL}
50	0.73635	0.000081	0.24162	0.02596	1.00401
70	0.73728	0.000093	0.24199	0.02385	1.00321
100	0.73742	0.000099	0.24262	0.02243	1.00257
120	0.73743	0.000102	0.24300	0.02139	1.00192
150	0.73744	0.000103	0.24310	0.01949	1.00013

(a)

N =	P^{G}_{trans}	P^{G}_{ref}	P^{RAD}_{trans}	P^{RAD}_{ref}	P^{TOTAL}
50	0.79408	0.000015	0.20508	0.00014	0.99931
70	0.79526	0.000014	0.20472	0.00007	1.00007
100	0.79535	0.000014	0.20470	0.00004	1.00011
120	0.79533	0.000014	0.20471	0.00003	1.00009
150	0.79530	0.000014	0.20472	0.00003	1.00007

(b)

Table 3 (continued)

N =	P^G_{trans}	P^G_{ref}	P^{RAD}_{trans}	P^{RAD}_{ref}	P^{TOTAL}
50	7.840%	80.901%	15.125%	99.467%	0.468%
70	7.864%	84.989%	15.399%	99.703%	0.313%
100	7.856%	85.828%	15.629%	99.817%	0.246%
120	7.852%	86.176%	15.756%	99.844%	0.183%
150	7.847%	86.262%	15.786%	99.862%	0.006%

(c)

Table 4 Use different truncation maximum for the single step discontinuity problem with index of refraction n_1 = 1.54 for the slabs and n_2 = 1.52 for the surrounding medium, λ_0 = 0.6328μm, D_1 = 0.5μm, D_2 = 0.1μm for (a) $u_N = k_0 D_1$ (b) $u_N = 2k_0 D_1$.

N =	P^G_{trans}	P^G_{ref}	P^{RAD}_{trans}	P^{RAD}_{ref}	P^{TOTAL}
50	0.79407806	0.00001547	0.20507549	0.00013831	0.99930732
70	0.79525757	0.00001396	0.20472562	0.00007085	1.00006800
100	0.79535123	0.00001403	0.20469998	0.00004110	1.00010634
120	0.79532966	0.00001410	0.20471231	0.00003332	1.00008938
150	0.79530572	0.00001415	0.20472383	0.00002694	1.00007064

(a)

N =	P^G_{trans}	P^G_{ref}	P^{RAD}_{trans}	P^{RAD}_{ref}	P^{TOTAL}
100	0.79407805	0.00001549	0.20507542	0.00013831	0.99930726
140	0.79525756	0.00001398	0.20472556	0.00007085	1.00006796
200	0.79535123	0.00001406	0.20469993	0.00004110	1.00010631
240	0.79532965	0.00001412	0.20471226	0.00003332	1.00008936
300	0.79530572	0.00001418	0.20472379	0.00002694	1.00007062

(b)

Table 5 compares results with K. Hirayama and M. Koshiba [15]. They used a combination of the finite-element and boundary-element methods. Observing that discrepancies appear only in P^G_{ref}, the power in the reflected surface wave mode, and that conservation of power are satisfied better in our case for the larger discontinuity of D_2/D_1 = 0.2. Again, there is very good agreement for the distribution of power among the modes which indicates that evanescent modes need not be considered when only power conservation is being verified.

Table 5 Comparison of results with K. Hirayama and M. Koshiba for $\varepsilon_R = 5$, $u_N = 2k_0D_1$, $n_2 = 1$ and N = 400.

D_2/D_1=0.04	P^G_{trans}	P^G_{ref}	P^{RAD}	P^{TOTAL}
Hirayama/Koshiba	0.36200	0.01000	0.6278	0.9998
Present method	0.35692	0.01255	0.6305	1.0010
Percentage Difference	-1.403%	25.500%	0.430%	0.120%

(a)

D_2/D_1=0.2	P^G_{trans}	P^G_{ref}	P^{RAD}	P^{TOTAL}
Hirayama/Koshiba	0.88660	0.04160	0.07150	0.9996
Present method	0.87877	0.04973	0.07149	0.9998
Percentage Difference	-0.872%	19.543%	-0.014%	0.020%

(b)

Many papers in the literature have treated the problem of scattering from a single step discontinuity [13 - 15, 17 - 27]. Several of these papers compare their results with T. E. Rozzi who used a rigorous variational approach [13]; this is done here in Figure 4 and Figure 5. In Figure 4, the radiated power($P^{RAD}_{trans}+P^{RAD}_{ref}$) (normalized to the incident power that is carried by the fundamental TE mode incident either from the left (z < 0) or from the right (z > 0)) is plotted versus D_2/D_1; the larger slab cross-section ($2D_1$) is taken to the left, which differs from Rozzi [13] who placed the narrower slab on the left. In our formulation, incident power is taken to be unity. The magnitude of the reflection and transmission coefficients looking to the right ($|\overline{\Gamma}^f|, |\overline{\tau}^f|$) and to the left ($|\overline{\Gamma}^b|, |\overline{\tau}^b|$) are also plotted in Figure 4. As is evident, excellent agreement is obtained between our result and that of Rozzi.

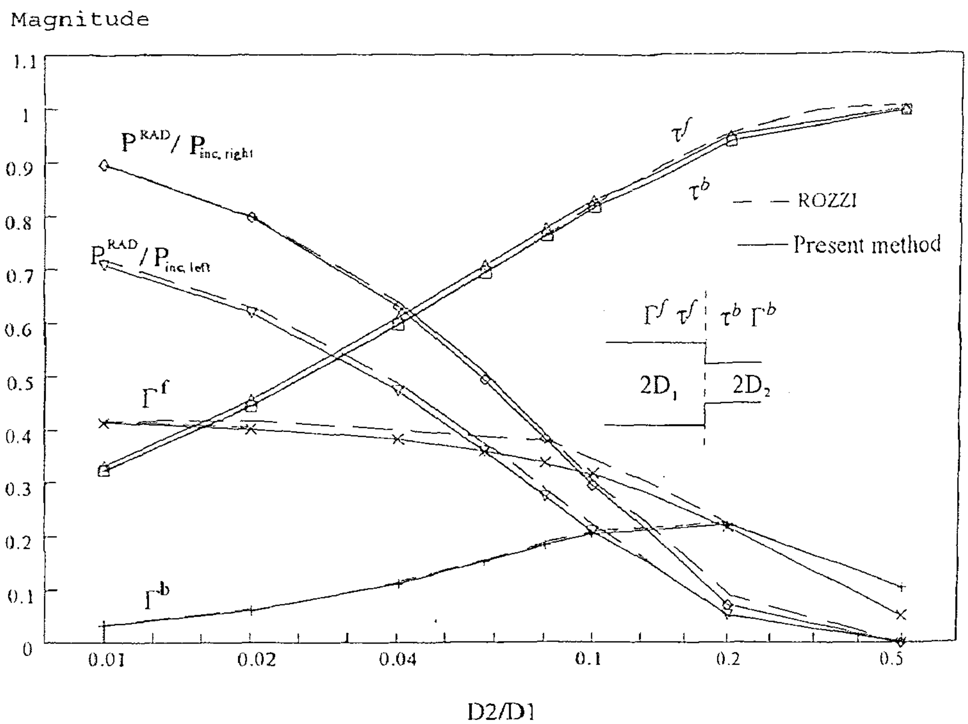

Figure 4 The normalized radiated powers and the amplitudes of the reflection and transmission coefficients of a step discontinuity between two slab waveguides versus relative step height for $k_0D_1 = 1$, $\varepsilon_r = 5$, $u_N = 2k_0D_1$ and N = 400.

Figure 5 is a plot of the radiation pattern of power gain due to a step discontinuity, where the power gain $G(\theta)$ is normalized to the incident power; see Appendix D for the derivation of the expression for power gain in the two regions z < 0 and z > L, where L is the wedge length. Results in Figure 5 show good agreement between the three methods plotted; see [26]. Note that a discontinuity appears in the region nearθ = 90°; this was to be expected because different field expressions and hence different integrals were asymptotically evaluated in the two regions z > L, 0 < θ < 90° and z < 0, 90° < θ < 180°.

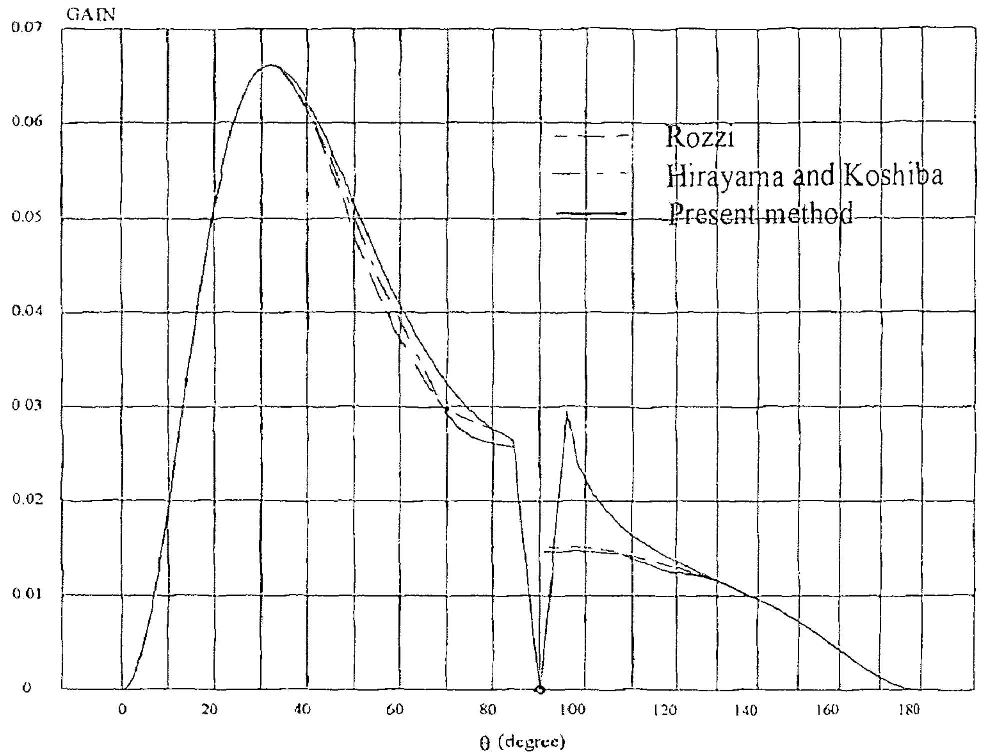

Figure 5 Radiation pattern of power gain for single step discontinuity for $k_0 D_1 = 1$, $\varepsilon_r = 5$, $u_N = 2k_0 D_1$ and N = 400.

In Figure 6 - 9, the radiation patterns of power gain of different dielectric wedges are presented. The material chosen is silicon (ε_r= 12) and lucite (ε_r= 2.56). In Figure 6, the wedge parameters are $\varepsilon_r = 2.56$, $L/\lambda_0 = 0.25$, $D_1/\lambda_0 = 1/(2\pi)$, $u_N = k_0 D_1$ and N = 150. For this relatively short wedge (quarter-wavelength), the radiation pattern of power gain is obtained for three different numbers of steps, namely, 32, 64 and 128, and only the first forward partial field contribution to the total field needed to be calculated and is plotted in the forward direction (0° < θ < 90°), but the first forward and first backward partial wave constituents are needed in the backward direction (90° <θ < 180°). Figure 6(a) shows the pattern in the range from θ = 0° to θ = 90°, while Figure 6(b) gives the backscatter pattern over the range from θ = 90° to θ = 180°. Values of the gain function are not valid near θ = 0° and θ = 180° because the first-order stationary phase method is not valid when a stationary phase point is near an endpoint. Figure 6(a) shows that in determining the forward radiation pattern of power gain, only 32 steps are needed for convergence. In Figure 6(b), the gain decreases when the number of steps increased, except at the point near θ = 90° where it increases.

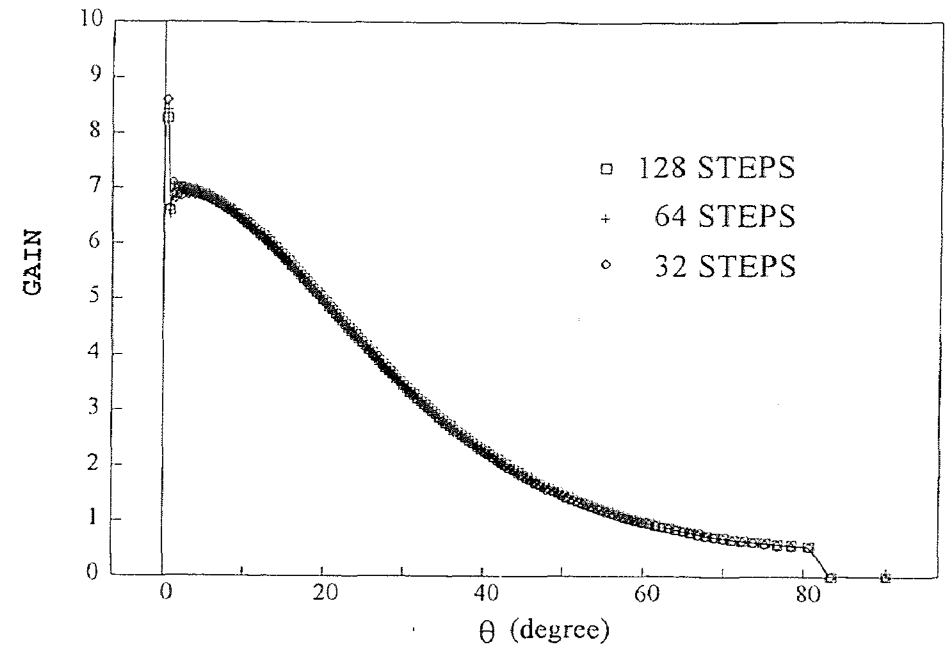

(a)

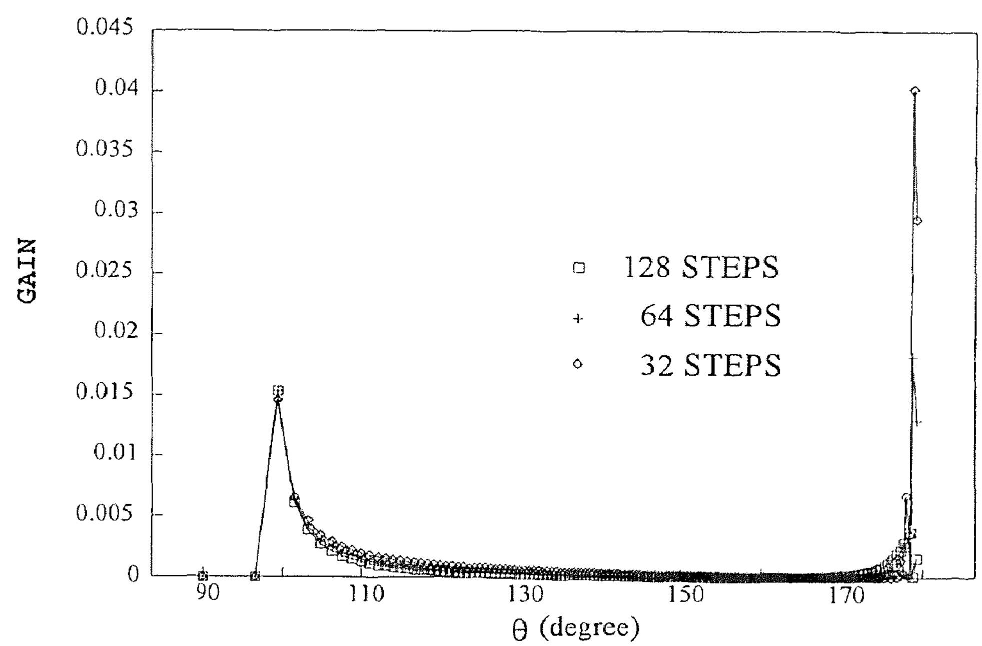

(b)

Figure 6 Radiation pattern of power gain of the slab/wedge for $\varepsilon_r = 2.56$, $L/\lambda_0 = 0.25$, $D_1/\lambda_0 = 1/(2\pi)$ $u_N = k_0 D_1$ and N = 150 for (a) z > L, 0° < θ < 90°; (b) z > 0, 90° < θ < 180°; (c) 0° < θ < 180° in dB scale.

Figure 6 (Continued)

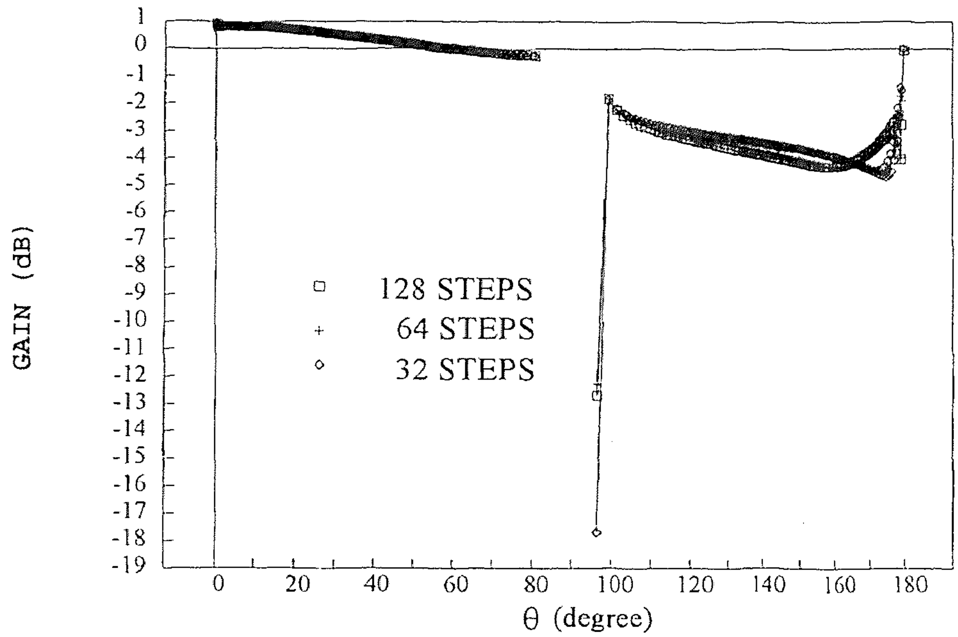

(c)

For comparison ε_r is now taken to be 12 while the slab/wedge geometry remains identical to the one used in Figure 6. As before, the radiation pattern of power gain is obtained for three different numbers of steps, namely, 32, 64 and 128. Again, only the first forward partial field is need for the forward radiation pattern of power gain ($0° < \theta < 90°$), but both the first forward and first backward partial fields are needed for the backward radiation pattern of power gain. Figure 7(a) shows the pattern in the range from $\theta = 0°$ to $\theta = 90°$, while Figure 7(b) gives the backscatter pattern over the range from $\theta = 90°$ to $\theta = 180°$. Again, the values of the gain function are not valid near $\theta = 0°$ and $\theta = 180°$. A comparison with Figure 6 shows that numerical results become worse for the quarter wavelength wedge when $\varepsilon_r = 12$. This occurs because the difference between the dielectric constants of the wedge and the surrounding medium (air) is large, which affects the accuracy of the numerical solution.

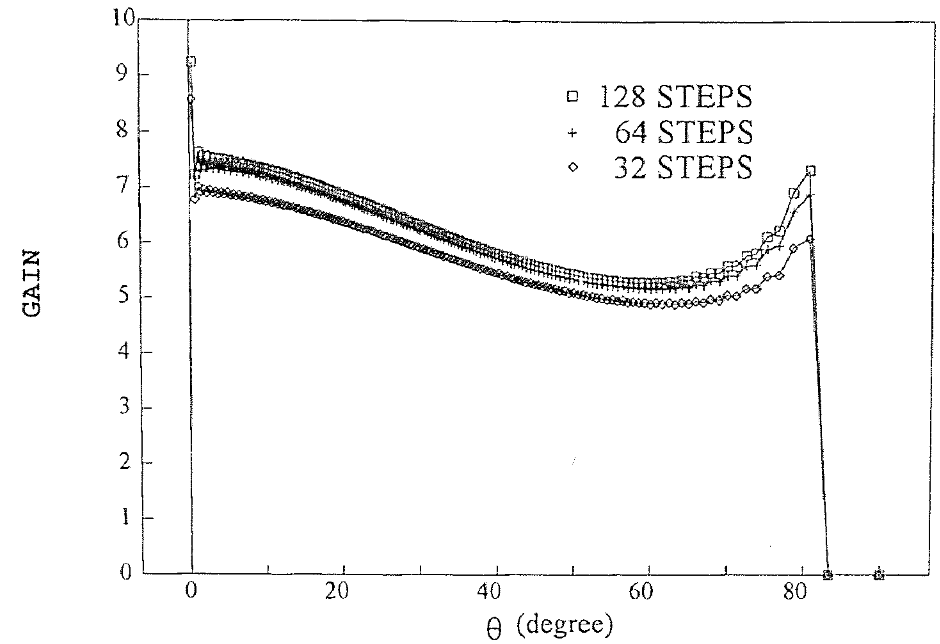

(a)

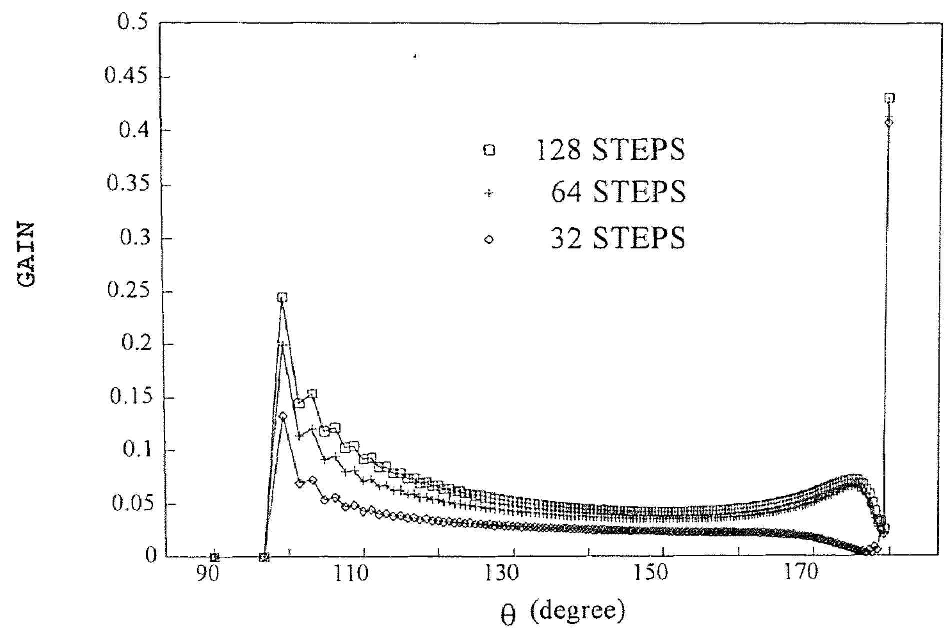

(b)

Figure 7 Radiation pattern of power gain of the slab/wedge for $\varepsilon_r = 12$, $L/\lambda_0 = 0.25$, $D_1/\lambda_0 = 1/(2\pi)$, $u_N = k_0 D_1$ and N = 150 for (a) z > L, 0° < θ < 90°; (b) z > 0, 90° < θ < 180°; (c) 0° < θ < 180° in dB scale.

Figure 7 (Continued)

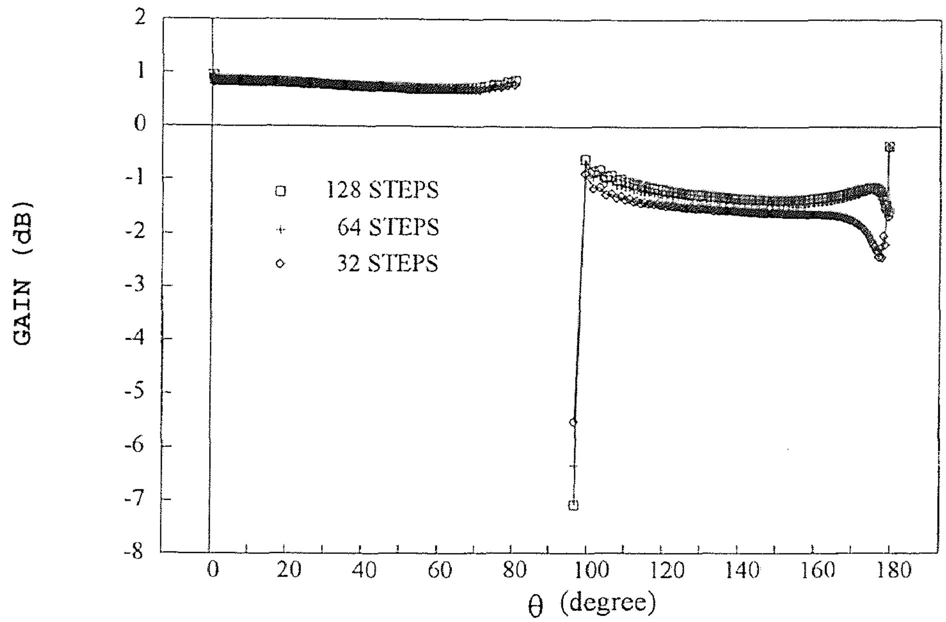

(c)

A comparison of the radiation pattern of power gain for the five wavelength long wedge for the two materials (ε_r = 2.56 and 12) are presented in Figures 8 and 9, respectively. In Figure 8, $\varepsilon_r = 2.56$, $L/\lambda_0 = 5$, $D_1/\lambda_0 = 1/(2\pi)$, $u_N = k_0 D_1$ and N = 150. Figure 8(a) shows the pattern in the range from θ = 0° to θ = 90°, while Figure 8(b) gives the backscatter pattern over the range from θ = 90° to θ = 180°. A comparison to Figure 6 shows that for ε_r = 2.56 the longer taper produces more gain, a narrower beamwidth, again minimal side lobes and appears to connect smoothly across the θ = 90° plane, as it should.

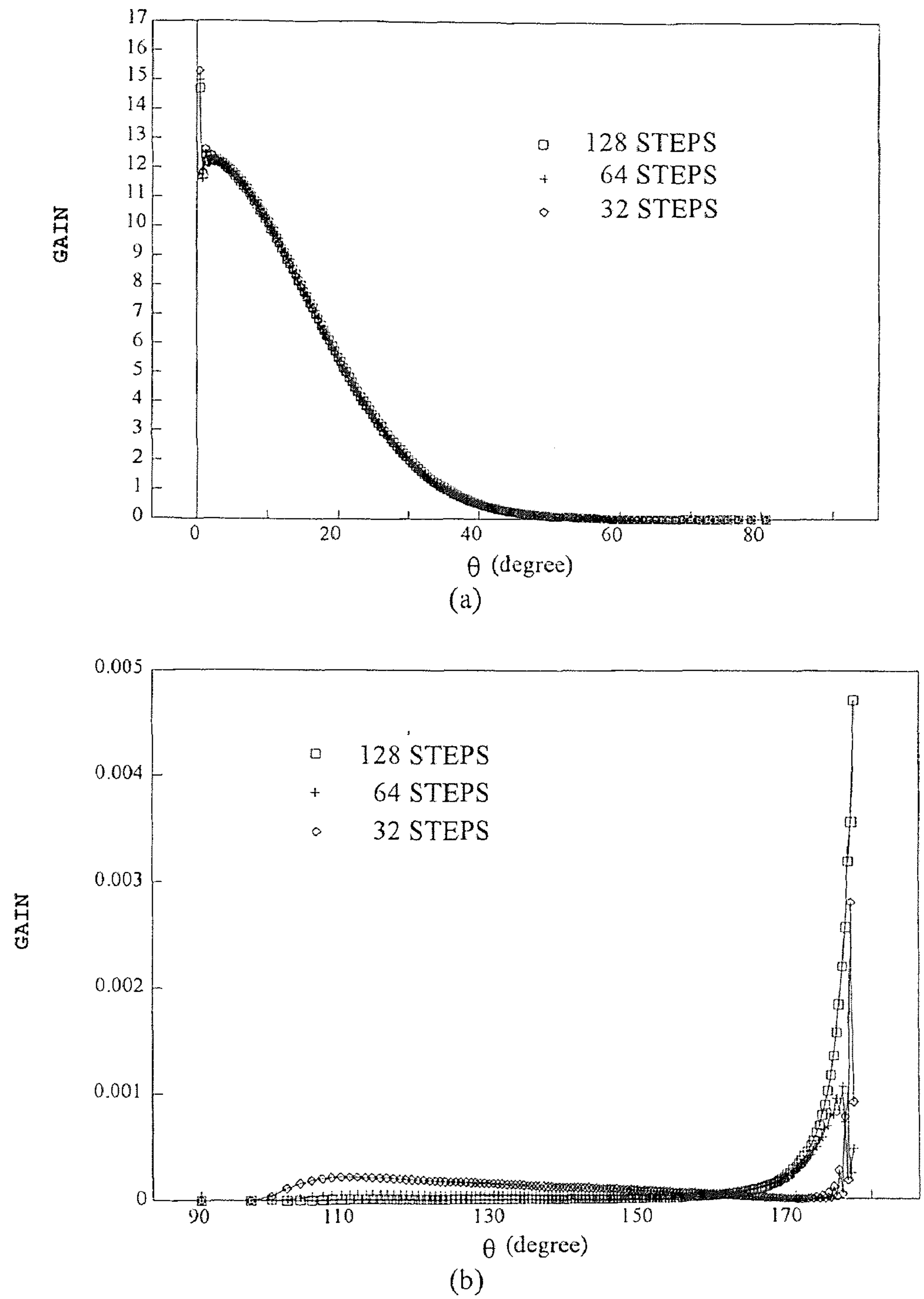

Figure 8 Radiation pattern of power gain of the slab/wedge for $\varepsilon_r = 2.56$, $L/\lambda_0 = 5$, $D_1/\lambda_0 = 1/(2\pi)$, $u_N = k_0 D_1$ and N = 150 for (a) z > L, 0° < θ < 90°; (b) z > 0, 90° < θ < 180°; (c) 0° < θ < 180° in dB scale.

Figure 8 (Continued)

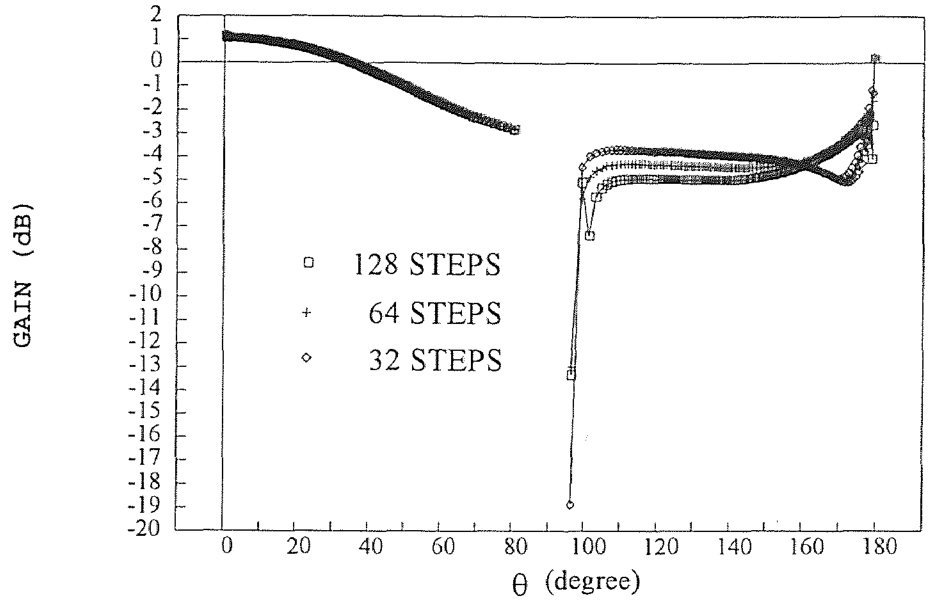

(c)

On comparing Figure 9 to Figure 7, it is apperent that the radiation patterns of power gain are smoother for the five wavelength wedge than for the quarter wavelength wedge and that the higher dielectric is not as deleterious as was the case in Figure 7.

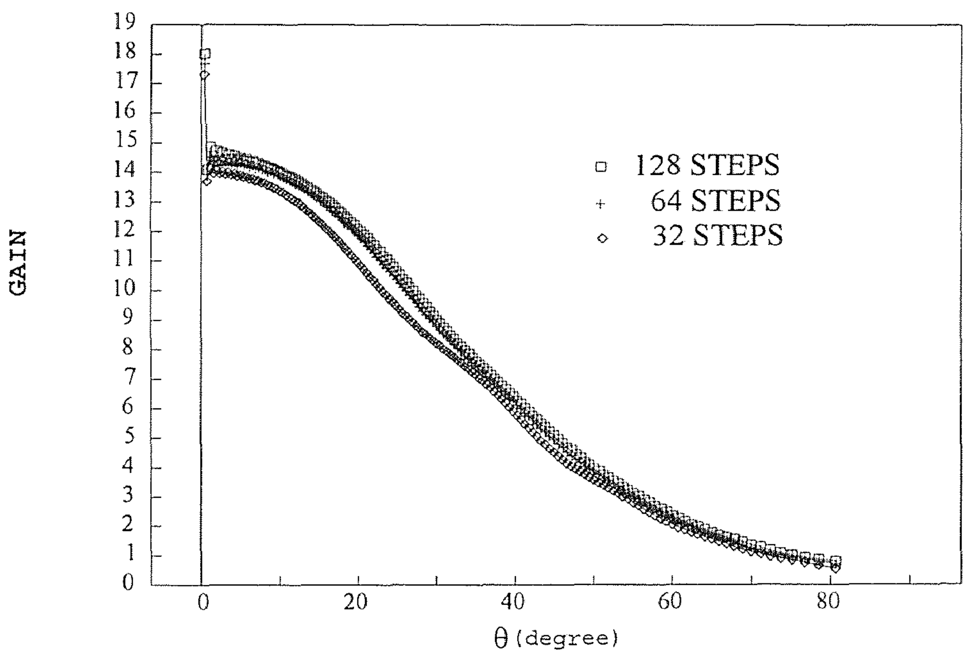

(a)

Figure 9 Radiation pattern of power gain of the slab/wedge for $\varepsilon_r = 12$, $L/\lambda_0 = 5$, $D_1/\lambda_0 = 1/(2\pi)$, $u_N = k_0 D_1$ and N = 150 for (a) z > L, 0° < θ < 90°; (b) z > 0, 90° < θ < 180°; (c) 0° < θ < 180° in dB scale.

Figure 9 (Continued)

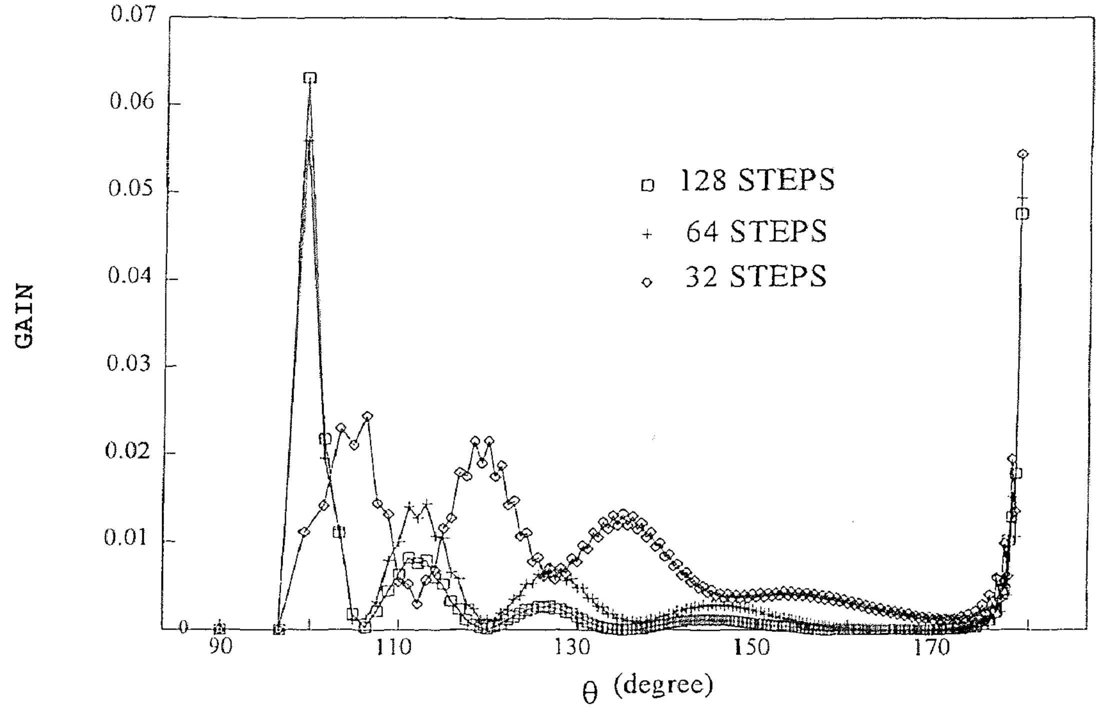

(b)

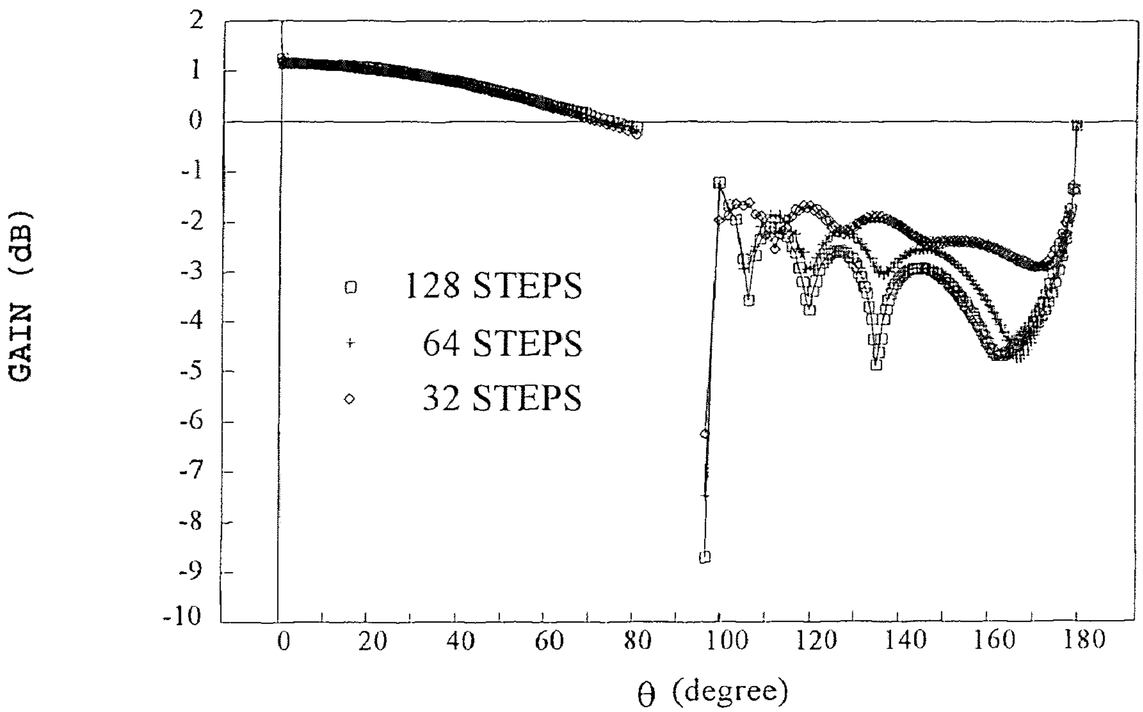

(c)

Figures 10, 11 and 12 yield a more comprehensive examination of the relationship between the length of the wedge and the value of its dielectric constant. For ε_r = 2.56, Figure 10 shows that a larger length wedge increases the maximum gain of the antenna, narrows the beamwidth and lowers the side lobe levels (although, these remain inconsequential for all the lengths considered). Figure 11 shows that a larger ε_r causes the maximum gain to increase, but also created a wider main lobe beam and produces a greater discontinuity to occur in the vicinity of the θ = 90° plane. Only for the L = $10\lambda_0$ case do the forward and backscatter patterns tend to join smoothly across the θ = 90° plane.

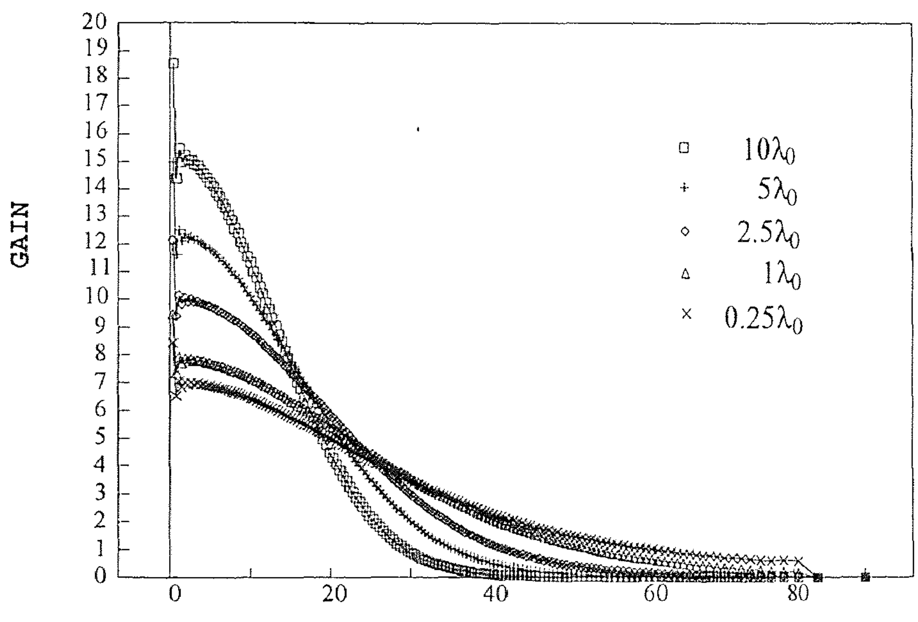

(a)

Figure 10 Radiation pattern of power gain of the slab/wedge for $\varepsilon_r = 2.56$, $D_1 / \lambda_0 = 1/(2\pi)$, $u_N = k_0 D_1$, Step = 64, and N = 150 for (a) z > L, 0° < θ < 90°; (b) z > 0, 90° < θ < 180°; (c) 0° < θ < 180° in dB scale.

Figure 10 (Continued)

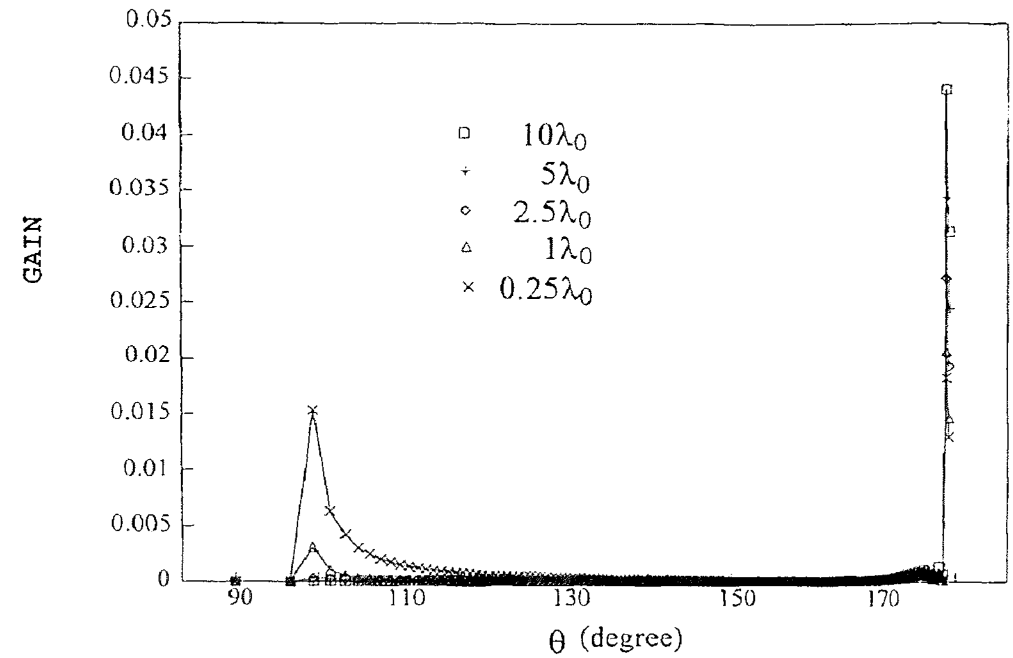

(b)

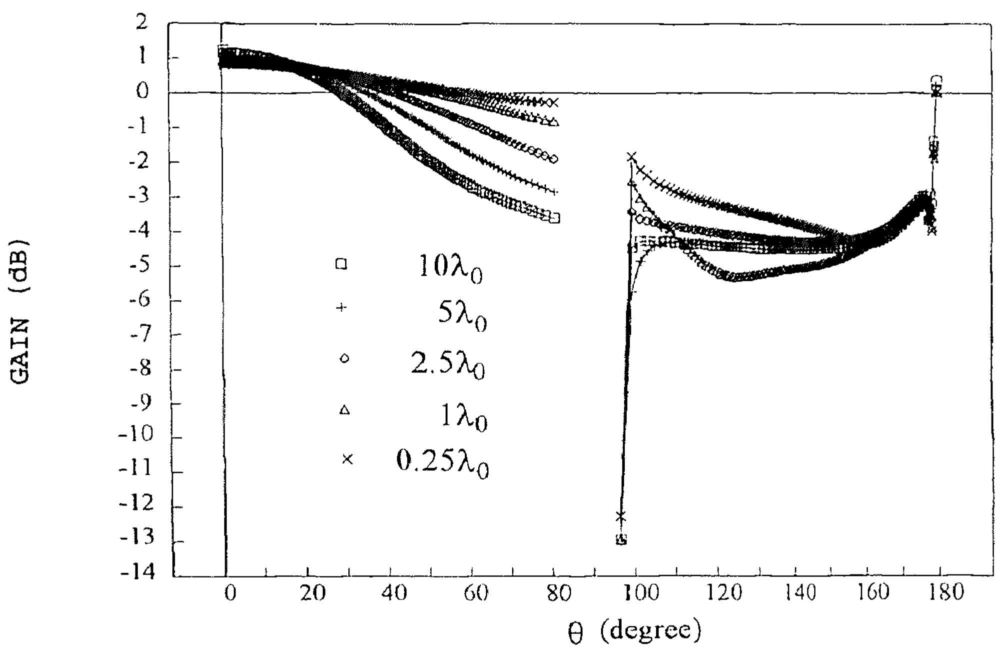

(c)

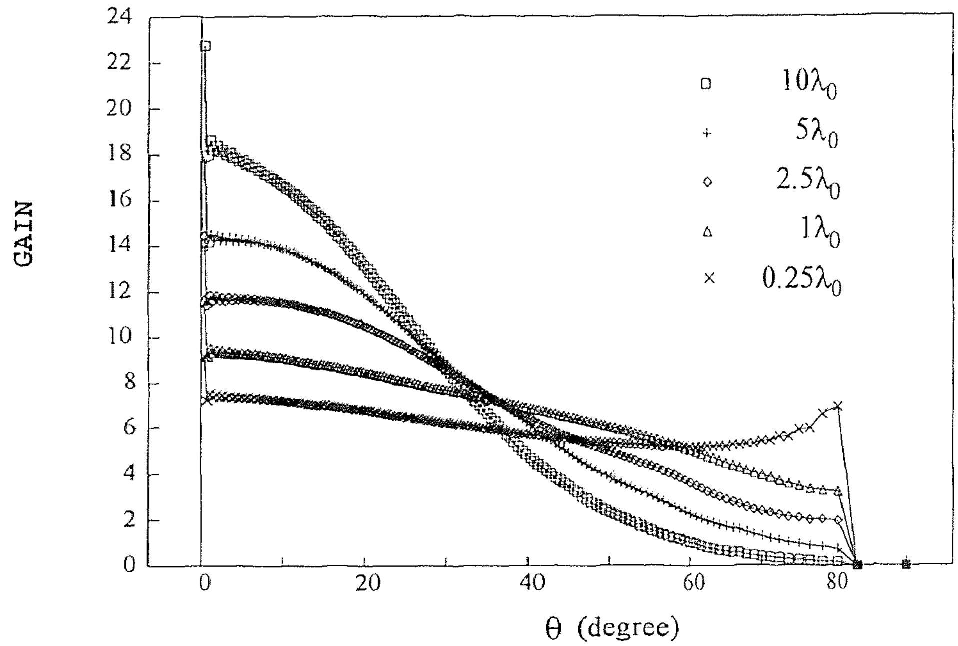

(a)

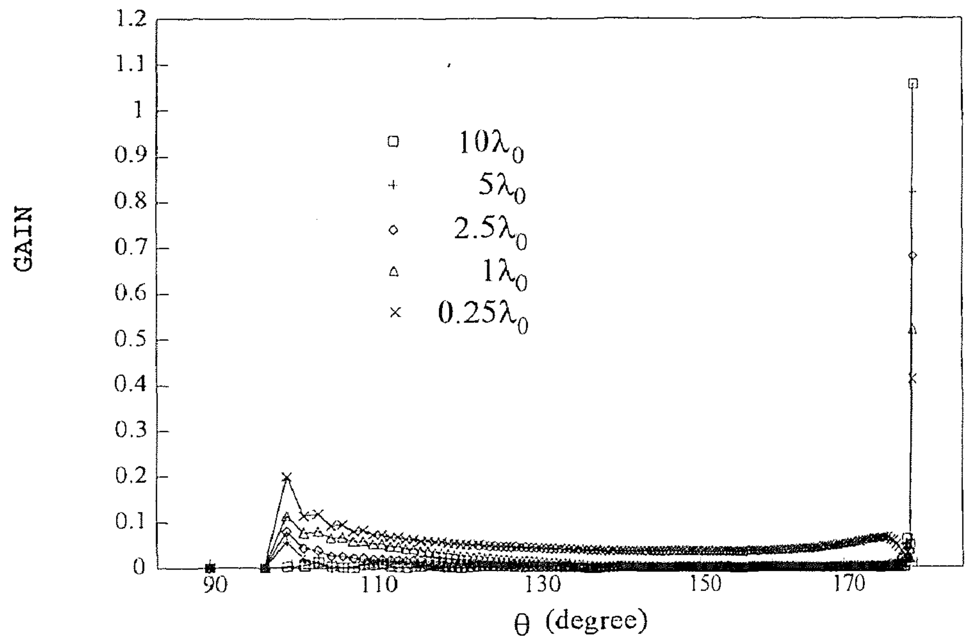

(b)

Figure 11 Radiation pattern of power gain of the slab/wedge for $\varepsilon_r = 12$, $D_1 / \lambda_0 = 1/(2\pi)$, $u_N = k_0 D_1$, Step = 64, and N = 150 for (a) z > L, 0° < θ < 90°; (b) z > 0, 90° < θ < 180°; (c) 0° < θ < 180° in dB scale.

Figure 11 (Continued)

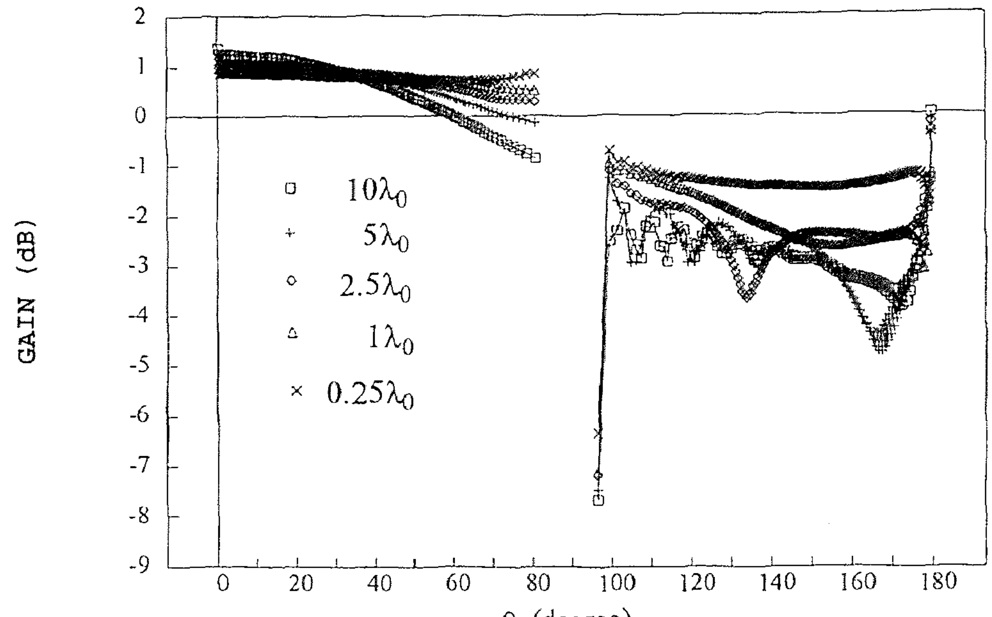

(c)

A closer examination of this particular case is depicted in Figure 12 for $\varepsilon_r = 2.56$ and 12. The choice of 64 steps ensures convergence and truncation at $u_N = k_0 D_1$ is sufficient because of the conclusion that evanescent modes need not be included at each step discontinuity; see Table 2 and 4.

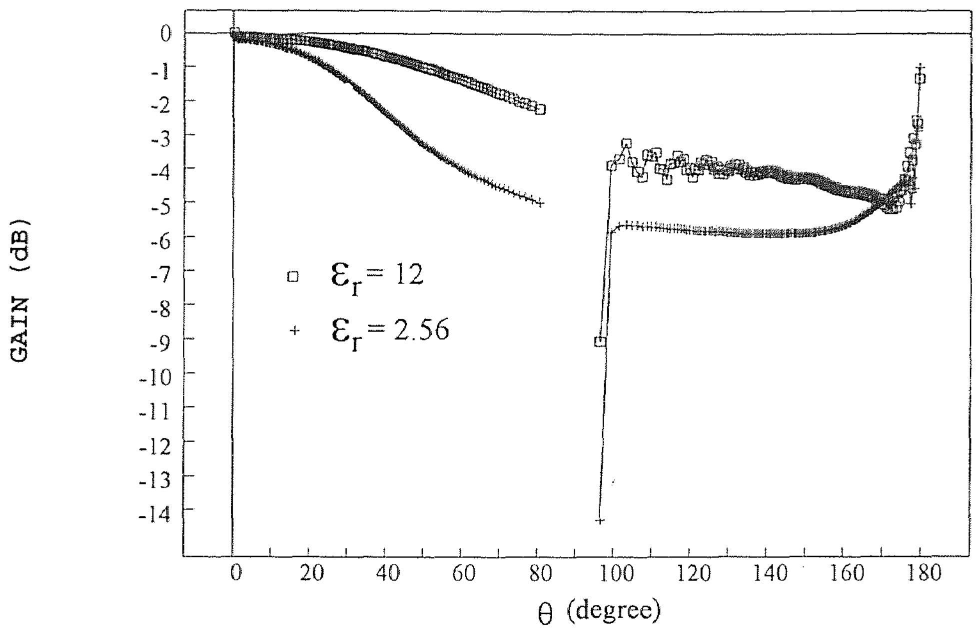

Figure 12 Normalized radiation pattern of power gain (in dB) versus angle θ of the slab/wedge for $\varepsilon_r = 2.56$ and $\varepsilon_r = 12$ with $L/\lambda_0 = 10$, $D_1/\lambda_0 = 1/(2\pi)$, $u_N = k_0 D_1$, Step = 64 and N = 150 .

CHAPTER 5

CONCLUSIONS

The radiation pattern of power gain for a dielectric slab feeding the staircase model of a dielectric wedge has been determined rigorously. In the model, the wedge region is approximated by short, uniform slab waveguide segments. Using the rigorous solution to scattering from a single step discontinuity, the field scattered by multiple steps is found in term of partial fields. The partial fields are determined by first considering waves progressing toward the tip, then back from the tip toward the semi-infinite slab waveguide region, toward the tip a second time, and so on until sufficient accuracy is reached. In this way, the total field, be it in the near or far zone, is found as a superposition of partial fields. The result is approximate only in that infinite integrals are truncated and numerically determined. The radiation pattern in the forward direction was shown to be smooth and highly directive. These results had not been previous proved [2]. The procedure can be applied to a considerable array of different geometries and is currently being applied to the dielectric cylindrical waveguide feeding the staircase model of the dielectric cone radiator.

APPENDIX A

DERIVATION OF (2.22)

Multiplying (2.18a) by $\overline{\Phi}_1(\bar{x},\bar{u}_j)$ and integrating over $\bar{x}$ from $-\infty$ to $+\infty$ gives

$$\begin{aligned}(1+\overline{\Gamma}_1)\int_{-\infty}^{\infty}\overline{\Phi}_1(\bar{x})\overline{\Phi}_1(\bar{x},\bar{u}_j)d\bar{x}+\int_{-\infty}^{\infty}[\int_0^{\infty}\overline{\Gamma}_1(\bar{u})\overline{\Phi}_1(\bar{x},\bar{u})d\bar{u}]\overline{\Phi}_1(\bar{x},\bar{u}_j)d\bar{x}\\ =\bar{\tau}_1\int_{-\infty}^{\infty}\overline{\Phi}_2(\bar{x})\overline{\Phi}_1(\bar{x},\bar{u}_j)d\bar{x}+\int_{-\infty}^{\infty}[\int_0^{\infty}\bar{\tau}_1(\bar{u})\overline{\Phi}_2(\bar{x},\bar{u})d\bar{u}]\overline{\Phi}_1(\bar{x},\bar{u}_j)d\bar{x}\end{aligned} \tag{A.1}$$

The orthogonality relation (2.11) permits setting the first integral on the left-hand side of (A.1) to zero. The overlap integral $\overline{I}_{21}(\bar{u}_j)$, which is defined in (2.22d), appears in the first integral on the right hand side of (A.1) and is evaluated explicitly in Appendix B. The remaining two double integral must be evaluated carefully because the range of integration over $\bar{u}$ includes $\bar{u}_j$. The last double integral in (A.1) was not evaluated correctly in [12, 14, 28].

Consider the double integral on the right hand side of (A.1) and separate the integration over $\bar{u}$ into three ranges as follows:

$$I_R = 2[I_{R1}+I_{R2}+I_{R3}], \tag{A.2}$$

where

$$I_{R1}=\int_0^{\infty}[\int_0^{\bar{u}_j-\delta}\bar{\tau}_1(\bar{u})\overline{\Phi}_2(\bar{x},\bar{u})d\bar{u}]\overline{\Phi}_1(\bar{x},\bar{u}_j)d\bar{x}, \tag{A.2a}$$

$$I_{R2}=\int_0^{\infty}[\int_{\bar{u}_j-\delta}^{\bar{u}_j+\delta}\bar{\tau}_1(\bar{u})\overline{\Phi}_2(\bar{x},\bar{u})d\bar{u}]\overline{\Phi}_1(\bar{x},\bar{u}_j)d\bar{x}, \tag{A.2b}$$

$$I_{R3}=\int_0^{\infty}[\int_{\bar{u}_j+\delta}^{\infty}\bar{\tau}_1(\bar{u})\overline{\Phi}_2(\bar{x},\bar{u})d\bar{u}]\overline{\Phi}_1(\bar{x},\bar{u}_j)d\bar{x}. \tag{A.2c}$$

Note that the integration over $\bar{x}$ is taken from zero to infinite, which is a consequence of symmetry. In the double integrals (A.2a) and (A.2c), the order of integration can be interchanged because $\bar{u}_j$ is excluded from the range of integration. Hence, they become

$$I_{R1}=\int_0^{\bar{u}_j-\delta}\bar{\tau}_1(\bar{u})\overline{I}_{21}(\bar{u},\bar{u}_j)d\bar{u}, \tag{A.3a}$$

$$I_{R3}=\int_{\bar{u}_j+\delta}^{\infty}\bar{\tau}_1(\bar{u})\overline{I}_{21}(\bar{u},\bar{u}_j)d\bar{u}, \tag{A.3b}$$

where the overlap integral $\overline{I}_{21}(\overline{u},\overline{u}_j)$ is given in (2.22d) and explicitly evaluated in Appendix B. The remaining double integral (A.2b) is evaluated by setting all terms in the integrand of the integral over $\overline{u}$ to their value at $\overline{u}=\overline{u}_j$ except for the oscillatory terms $\cos\overline{u}(\overline{x}-\overline{R}_j)$ and $\sin\overline{u}(\overline{x}-\overline{R}_j)$. This is done because the range of integration over $\overline{u}$ is narrow about $\overline{u}_j$ and the $\overline{x}$-integration range extends to infinity. The sinusoidal terms are obtained from the normalized form of the potential functions which are founded in (2.9). Evaluating the resultant integrals and taking the limit as $\delta \to 0$, yields

$$I_{R2} = \overline{\tau}_1(\overline{u}_j)\overline{T}_{12}(\overline{u}_j), \tag{A.4}$$

where $\overline{T}_{12}(\overline{u}_j)$ is given by (2.22c). The double integral on the left hand side of (A.1) is evaluated in a similar fashion with the result that

$$\int_{-\infty}^{\infty}[\int_0^{\infty}\overline{\Gamma}_1(\overline{u})\overline{\Phi}_1(\overline{x},\overline{u})d\overline{u}]\overline{\Phi}_1(\overline{x},\overline{u}_j)d\overline{x} = 2\overline{\Gamma}_1(\overline{u}_j). \tag{A.5}$$

Hence, (A.1) reduces to (2.22a). In like fashion, (2.22b) can be derived.

APPENDIX B

OVERLAP INTEGRALS

In the linear system of equations (2.19) and (2.22). there are several overlap integrals that are evaluated explicitly. Overlap integrals are defineed below for the n^{th} step discontinuity between regions n and $n+1$, where $n = 1, 2, \ldots$. The n^{th} region contains the larger slab waveguide segment , *i.e.*, $\overline{R}_n > \overline{R}_{n+1}$, where $\overline{R}_n \equiv D_n / D_1$. The integrand of an overlap integral involves a product of the potential solutions given in (2.6) and/or (2.9). The four types of overlap integrals are:

1. Guided modes in both the n and $n+1$ regions

$$\begin{aligned}\overline{I}_{n,n+1} &= \int_{-\infty}^{\infty} \overline{\Phi}_n(\overline{x})\overline{\Phi}_{n+1}(\overline{x})d\overline{x} \\ &= 2\overline{C}_n\overline{C}_{n+1}(\overline{J}_1 + \overline{J}_2 + \overline{J}_3)\end{aligned} \tag{B.1}$$

$$\overline{J}_1 = \frac{[\bar{k}_{x,n}\sin(\bar{k}_{x,n}\overline{R}_{n+1})\cos(\bar{k}_{x,n+1}\overline{R}_{n+1}) - \bar{k}_{x,n+1}\cos(\bar{k}_{x,n+1}\overline{R}_{n+1})\sin(\bar{k}_{x,n}\overline{R}_{n+1})]}{\bar{k}_{x,n}^2 - \bar{k}_{x,n+1}^2} \tag{B.2}$$

$$\begin{aligned}\overline{J}_2 = \frac{\cos(\bar{k}_{x,n+1}\overline{R}_{n+1})}{\bar{k}_{x,n}^2 + \overline{\alpha}_{x,n+1}^2}\{&[\bar{k}_{x,n}\sin(\bar{k}_{x,n}\overline{R}_n) - \overline{\alpha}_{x,n+1}\cos(\bar{k}_{x,n}\overline{R}_n)]e^{-\overline{\alpha}_{x,n+1}(\overline{R}_n - \overline{R}_{n+1})} \\ &- \bar{k}_{x,n}\sin(\bar{k}_{x,n}\overline{R}_{n+1}) - \overline{\alpha}_{x,n+1}\cos(\bar{k}_{x,n}\overline{R}_{n+1})\}\end{aligned} \tag{B.3}$$

$$\overline{J}_3 = \frac{\cos(\bar{k}_{x,n}\overline{R}_n)\cos(\bar{k}_{x,n+1}\overline{R}_{n+1})e^{-\overline{\alpha}_{x,n+1}(\overline{R}_n - \overline{R}_{n+1})}}{\overline{\alpha}_{x,n} + \overline{\alpha}_{x,n+1}} \tag{B.4}$$

2. Guided mode in region n and a radiation mode in region $n+1$

$$\begin{aligned}\overline{I}_{n,n+1}(\overline{u}) &= \int_{-\infty}^{\infty} \overline{\Phi}_n(\overline{x})\overline{\Phi}_{n+1}(\overline{x},\overline{u})d\overline{x} \\ &= 2\overline{C}_n\overline{C}_{n+1}(\overline{u})(\overline{J}_4 + \overline{J}_5 + \overline{J}_6)\end{aligned} \tag{B.5}$$

$$\overline{J}_4 = \frac{\bar{k}_{x,n}\sin(\bar{k}_{x,n}\overline{R}_{n+1})\cos(\bar{v}\overline{R}_{n+1}) - \bar{v}\cos(\bar{k}_{x,n}\overline{R}_{n+1})\sin(\bar{v}\overline{R}_{n+1})}{\bar{k}_{x,n}^2 - \bar{v}^2} \tag{B.6}$$

$$\overline{J}_5 = \frac{1}{(\bar{k}_{x,n}^2 - \bar{u}^2)}\{\cos(\bar{v}\overline{R}_{n+1})[\bar{k}_{x,n}\sin(\bar{k}_{x,n}\overline{R}_n)\cos(\bar{u}(\overline{R}_n - \overline{R}_{n+1}))$$
$$-\bar{u}\cos(\bar{k}_{x,n}\overline{R}_n)\sin(\bar{u}(\overline{R}_n - \overline{R}_{n+1})) - \bar{k}_{x,n}\sin(\bar{k}_{x,n}\overline{R}_{n+1})]$$
$$-\frac{\bar{v}}{\bar{u}}\sin(\bar{v}\overline{R}_{n+1})[\bar{k}_{x,n}\sin(\bar{k}_{x,n}\overline{R}_n)\sin(\bar{u}(\overline{R}_n - \overline{R}_{n+1}))$$
$$+\bar{u}\cos(\bar{k}_{x,n}\overline{R}_n)\cos(\bar{u}(\overline{R}_n - \overline{R}_{n+1})) - \bar{u}\cos(\bar{k}_{x,n}\overline{R}_{n+1})]\} \tag{B.7}$$

$$\overline{J}_6 = \frac{-\cos(\bar{k}_{x,n}\overline{R}_n)}{\bar{u}^2 + \bar{\alpha}_{x,n}^2}\{\cos(\bar{v}\overline{R}_{n+1})[\bar{u}\sin(\bar{u}(\overline{R}_n - \overline{R}_{n+1})) - \bar{\alpha}_{x,n}\cos(\bar{u}(\overline{R}_n - \overline{R}_{n+1}))]$$
$$+\frac{\bar{v}}{\bar{u}}\sin(\bar{v}\overline{R}_{n+1})[\bar{\alpha}_{x,n}\sin(\bar{u}(\overline{R}_n - \overline{R}_{n+1})) + \bar{u}\cos(\bar{u}(\overline{R}_n - \overline{R}_{n+1}))]\} \tag{B.8}$$

3. Radiation mode in region n and a guided mode in region $n+1$

$$\overline{I}_{n+1,n}(\bar{u}) = \int_{-\infty}^{\infty}\overline{\Phi}_{n+1}(\bar{x})\overline{\Phi}_n(\bar{x},\bar{u})d\bar{x}$$
$$= 2\overline{C}_{n+1}\overline{C}_n(\bar{u})(\overline{J}_7 + \overline{J}_8 + \overline{J}_9) \tag{B.9}$$

$$\overline{J}_7 = \frac{\bar{k}_{x,n+1}\sin(\bar{k}_{x,n+1}\overline{R}_{n+1})\cos(\bar{v}\overline{R}_{n+1}) - \bar{v}\cos(\bar{k}_{x,n+1}\overline{R}_{n+1})\sin(\bar{v}\overline{R}_{n+1})}{\bar{k}_{x,n+1}^2 - \bar{v}^2} \tag{B.10}$$

$$\overline{J}_8 = \frac{\cos(\bar{k}_{x,n+1}\overline{R}_{n+1})}{\bar{v}^2 + \bar{\alpha}_{x,n+1}^2}\{[\bar{v}\sin(\bar{v}\overline{R}_n) - \bar{\alpha}_{x,n+1}\cos(\bar{v}\overline{R}_n)]e^{-\alpha_{x,n+1}(\overline{R}_n - \overline{R}_{n+1})}$$
$$-\bar{v}\sin(\bar{v}\overline{R}_{n+1}) + \bar{\alpha}_{x,n+1}\cos(\bar{v}\overline{R}_{n+1})\} \tag{B.11}$$

$$\overline{J}_9 = \frac{\cos(\bar{k}_{x,n+1}\overline{R}_{n+1})}{\bar{u}^2 + \bar{\alpha}_{x,n+1}^2}[\bar{\alpha}_{x,n+1}\cos(\bar{v}\overline{R}_n) - \bar{v}\sin(\bar{v}\overline{R}_n)]e^{-\bar{\alpha}_{x,n+1}(\overline{R}_n - \overline{R}_{n+1})} \tag{B.12}$$

4. Radiation modes in both the n and $n+1$ regions

$$\overline{I}_{n,n+1}(\overline{u},\overline{u}_j) = \int_{-\infty}^{\infty} \overline{\Phi}_n(\overline{x},\overline{u})\overline{\Phi}_{n+1}(\overline{x},\overline{u}_j)d\overline{x}$$

$$= 2\overline{C}_n(\overline{u})\overline{C}_{n+1}(\overline{u}_j)\begin{cases} \overline{J}_{10} + \overline{J}_{11} + \overline{J}_{12} & \text{, when } \overline{u} \neq \overline{u}_j \\ \overline{T}_{n,n+1} & \text{, when } \overline{u} = \overline{u}_j \end{cases} \tag{B.13}$$

$$\overline{J}_{10} = \frac{\overline{v}\sin(\overline{v}\overline{R}_{n+1})\cos(\overline{v}_j\overline{R}_{n+1}) - \overline{v}_j\cos(\overline{v}\overline{R}_{n+1})\sin(\overline{v}_j\overline{R}_{n+1})}{\overline{v}^2 - \overline{v}_j^2} \tag{B.14}$$

$$\overline{J}_{11} = \frac{\overline{v}\sin(\overline{v}\overline{R}_n)\cos(\overline{u}_j(\overline{R}_n - \overline{R}_{n+1})) - \overline{u}_j\cos(\overline{v}\overline{R}_n)\sin(\overline{u}_j(\overline{R}_n - \overline{R}_{n+1})) - \overline{v}\sin(\overline{v}\overline{R}_{n+1})}{\overline{v}^2 - \overline{u}_j^2} \tag{B.15}$$

$$\overline{J}_{12} = \frac{1}{(\overline{u}^2 - \overline{u}_j^2)}\{\sin(\overline{u}_j(\overline{R}_n - \overline{R}_{n+1}))[\overline{u}_j\cos(\overline{v}\overline{R}_n)\cos(\overline{v}_j\overline{R}_{n+1}) + \frac{\overline{v}\overline{v}_j}{\overline{u}_j}\sin(\overline{v}\overline{R}_n)\sin(\overline{v}_j\overline{R}_{n+1})]$$
$$+\cos(\overline{u}_j(\overline{R}_n - \overline{R}_{n+1}))[\overline{v}_j\cos(\overline{v}\overline{R}_n)\sin(\overline{v}_j\overline{R}_{n+1}) - \overline{v}\sin(\overline{v}\overline{R}_n)\cos(\overline{v}_j\overline{R}_{n+1})]\} \tag{B.16}$$

$$\overline{T}_{n,n+1} = \frac{\pi}{2}\{\cos(\overline{u}_j(\overline{R}_n - \overline{R}_{n+1}))[\cos(\overline{v}_j\overline{R}_n)\cos(\overline{v}_jR_{n+1}) + (\frac{\overline{v}_j}{\overline{u}_j})^2\sin(\overline{v}_j\overline{R}_n)\sin(\overline{v}_jR_{n+1})]$$
$$+\frac{\overline{v}_j}{\overline{u}_j}\sin(\overline{u}_j(\overline{R}_n - \overline{R}_{n+1}))\sin(\overline{v}_j(\overline{R}_n - \overline{R}_{n+1}))]\} \tag{B.17}$$

where $j = 1, 2, \ldots, N$

APPENDIX C

POWER CALCULATIONS

In Chapter 4, calculations of the various powers scattered at a single step discontinuity are presented. The expressions for these power calculations will now be derived. Consider the single step discontinuity between region 1 with slab thickness $2D_1$ and region 2 with slab thickness $2D_2$ in Figure 2. The even, transverse TE field components in these regions for the first forward progression are given by (2.14a), (2.14b), (2.15a) and (2.15b). Let

$$E_{y1}^{f1} = E_{y1,inc}^{G} + E_{y1,ref}^{G} + \int_0^\infty E_{y1,ref}^{RAD}\, du, \tag{C.1a}$$

$$H_{x1}^{f1} = H_{x1,inc}^{G} + H_{x1,ref}^{G} + \int_0^\infty H_{x1,ref}^{RAD}\, du, \tag{C.1b}$$

where

$$E_{y1,inc}^{G} = A_1 e^{-j\beta_1 z}\Phi_1(x), \tag{C.1c}$$

$$E_{y1,ref}^{G} = A_1\Gamma_1 e^{j\beta_1 z}\Phi_1(x), \tag{C.1d}$$

$$E_{y1,ref}^{RAD} = A_1\Gamma_1(u) e^{j\beta_1(u) z}\Phi_1(x,u), \tag{C.1e}$$

$$H_{x1,inc}^{G} = -\frac{A_1\beta_1}{\eta_0 k_0} e^{-j\beta_1 z}\Phi_1(x), \tag{C.1f}$$

$$H_{x1,ref}^{G} = \frac{A_1\beta_1}{\eta_0 k_0}\Gamma_1 e^{j\beta_1 z}\Phi_1(x), \tag{C.1g}$$

$$H_{x1,ref}^{RAD} = \frac{A_1\beta_1(u)}{\eta_0 k_0}\Gamma_1(u) e^{j\beta_1(u) z}\Phi_1(x,u), \tag{C.1h}$$

and let

$$E_{y2}^{f1} = E_{y2,trans}^{G} + \int_0^\infty E_{y2,trans}^{RAD}\, du, \tag{C.2a}$$

$$H_{x2}^{f1} = H_{x2,trans}^{G} + \int_0^\infty H_{x2,trans}^{RAD}\, du, \tag{C.2b}$$

where

$$E_{y2,trans}^{G} = A_1\tau_1 e^{-j\beta_2 z}\Phi_2(x), \tag{C.2c}$$

$$E_{y2,trans}^{RAD} = A_1\tau_1(u) e^{-j\beta_2(u) z}\Phi_2(x,u), \tag{C.1d}$$

$$H_{x2,trans}^{G} = -\frac{A_1\beta_2}{\eta_0 k_0}\tau_1 e^{-j\beta_2 z}\Phi_2(x), \tag{C.2e}$$

$$H_{x2,trans}^{RAD} = -\frac{A_1\beta_2(u)}{\eta_0 k_0}\tau_1(u) e^{-j\beta_2(u) z}\Phi_2(x,u). \tag{C.2f}$$

From conservation of power,

$$P_{in} = P_{out}, \tag{C.3}$$

where the power into a volume bounded by a surface S enclosing the step discontinuity equals the incident power carried by the even TE_0 mode and the power out of the volume is determined from the Poynting Vector by the expression

$$P_{out} = \frac{1}{2}\oint\!\!\oint_S \mathrm{Re}(\underline{E^S} \times \underline{H^{S^*}}) \cdot \hat{n}\, dS, \tag{C.4}$$

where the scattered field $(\underline{E^S}, \underline{H^S})$ is defined to be the total field minus the incident field and the underbars signify vector quantities. For convenience, choose $S = S_1 + S_2$, where S_1 is the planar surface $z = 0 - \delta$, $-\infty < x < \infty$, $0 \le y \le 1$ and S_2 is the planar surface $z = 0 + \delta$, $-\infty < x < \infty$, $0 \le y \le 1$ with $0 < \delta << 1$, and take S_1 and S_2 to close at infinity. Hence, (C.4) reduces to

$$P_{out} = P_{1,out} + P_{2,out}, \tag{C.5}$$

where

$$P_{1,out} = \frac{1}{2}\int_0^1\int_{-\infty}^{\infty} \mathrm{Re}(\underline{E_1^s} \times \underline{H_1^{s^*}})\big|_{0-\delta} \cdot (-\hat{z})\, dx\, dy, \tag{C.5a}$$

$$P_{2,out} = \frac{1}{2}\int_0^1\int_{-\infty}^{\infty} \mathrm{Re}(\underline{E_2^s} \times \underline{H_2^{s^*}})\big|_{0+\delta} \cdot \hat{z}\, dx\, dy, \tag{C.5b}$$

Substituting (C.1a), (C.1b), (C.2a) and (C.2b) into (C.5a) and (C.5b) give

$$P_{1,out} = \int_0^{\infty} \mathrm{Re}[(E_{y1,ref}^{G} + \int_0^{\infty} E_{y1,ref}^{RAD}\, du)(H_{x1,ref}^{G} + \int_0^{\infty} H_{x1,ref}^{RAD}\, du)^*]_{z=0-\delta}\, dx, \tag{C.6a}$$

$$P_{2,out} = \int_0^{\infty} \mathrm{Re}[(E_{y2,trans}^{G} + \int_0^{\infty} E_{y2,trans}^{RAD} du)(H_{x1,trans}^{G} + \int_0^{\infty} H_{x1,trans}^{RAD} du)^*]_{z=0+\delta}\, dx. \tag{C.6b}$$

Using (C.1c) - (C.1h), (C.2c) - (C.2f), the orthogonality relations (2.8) and (2.11) and the normalization (2.14d) give

$$P_{1,out} = P^{G}_{1,ref} + P^{RAD}_{1,ref}, \qquad P_{2,out} = P^{G}_{2,trans} + P^{RAD}_{2,trans}, \tag{C.7}$$

where

$$P^{G}_{1,ref} = \left|\Gamma_1\right|^2 \tag{C.7a}$$

$$P^{RAD}_{1,ref} = \frac{2}{\beta_1}\int_0^{k_0} \beta_1(u)\left|\Gamma_1(u)\right|^2 du \tag{C.7b}$$

$$P^{G}_{2,trans} = \frac{\beta_2}{\beta_1}\left|\tau_1\right|^2 \tag{C.7d}$$

$$P^{RAD}_{2,trans} = \frac{2}{\beta_1}\int_0^{k_0} \beta_2(u)\left|\tau_1(u)\right|^2 du \tag{C.7e}$$

APPENDIX D

POWER GAIN

The radiation pattern of power gain for the slab/wedge geometry of Figure 1 is given by the power gain formula

$$G_5(\theta) = \frac{2\pi\rho S_5^{ff}(\rho,\theta)}{P_{IN}}, \qquad z > L\,, \qquad \text{(D.1)}$$

and

$$G_1(\theta) = \frac{2\pi\rho S_1^{ff}(\rho,\theta)}{P_{IN}}, \qquad z < 0\,, \qquad \text{(D.2)}$$

where the observation point P in polar coordinate (ρ, θ) is measured from the origin of the xz-plane; $P_{IN} = P_{inc} = 1$ and $S_{1,5}^{ff}$ represent the time-average power density or Poynting Vectors in the far field in region 1 and 5, respectively. Since

$$S_{1,5}^{ff} = \frac{1}{2\eta_0}\left|E_{y1,5}^{ff}\right|^2, \qquad \text{(D.3)}$$

it is necessary to find the far field intensities E_{y1}^{ff} and E_{y5}^{ff} in region 1 and 5, respectively.

Considering only the first forward progression and the partial wave fields of Figure 3(a), the radiation electric fields in region 1 and 5 using the normalized quantities defined in (2.16) give, respectively,

$$\bar{E}_{y1}(\bar{x},\bar{z}) = \bar{A}_1 \int_0^\infty \bar{\Gamma}_1(\bar{u}) e^{j\bar{\beta}_1(\bar{u})\bar{z}} \bar{\Phi}_1(\bar{x},\bar{u})\,d\bar{u}, \qquad z < 0, \qquad \text{(D.4a)}$$

and

$$\bar{E}_{y5}(\bar{x},\bar{z}) = \bar{A}_4 \int_0^\infty \bar{\tau}_4(\bar{u}) e^{-j\bar{\beta}_5(\bar{u})\bar{z}} \bar{\Phi}_5(\bar{x},\bar{u})\,d\bar{u}, \qquad z > L\,, \qquad \text{(D.4b)}$$

where

$$\left|\bar{A}_1\right| = \left(\frac{2\eta_0 \bar{k}_0}{\bar{\beta}_1}\right)^{1/2}, \qquad \bar{A}_4 = \bar{\tau}_1\bar{\tau}_2\bar{\tau}_3\bar{A}_1. \qquad \text{(D.4c)}$$

A first-order stationary phase [29] evaluation of (D.4a) and (D.4b) and using (D.3) give for (D.1) and (D.2)

$$G_5(\theta) = 2\pi \frac{\bar{k}_0^2}{\bar{\beta}_1} \cos^2\theta \left| \bar{\tau}_1 \bar{\tau}_2 \bar{\tau}_3 \bar{\tau}_4 (\bar{k}_0 \sin\theta) \right|^2, \qquad 0 < \theta < \pi/2, \qquad \text{(D.5a)}$$

$$G_1(\theta) = 2\pi \frac{\bar{k}_0^2}{\bar{\beta}_1} \cos^2\theta \left| \bar{\Gamma}_1 (\bar{k}_0 \sin\theta) \right|^2, \qquad \pi/2 < \theta < \pi. \qquad \text{(D.5b)}$$

Because only the first-order stationary phase formula was used, the result in (D.5a) is not valid near $\theta = 0°$ and in (D.5b), it is not valid near $\theta = \pi$. Note that the gain functions are symmetric about the z-axis.

In the above, only the first forward progression is considered. If the first forward, first backward and second forward partial fields are included in the expressions for the radiation intensities $\bar{E}_{y1,5}$, then the gain functions $G_{1,5}(\theta)$ can be shown to take the forms

$$G_5(\theta) = 2\pi \frac{\bar{k}_0^2}{\bar{\beta}_1} \cos^2\theta \left| P_{f1} \bar{\tau}_4^{f1} (\bar{k}_0 \sin\theta) + P_{f1b1f2} \bar{\tau}_4^{f2} (\bar{k}_0 \sin\theta) \right|^2, \quad 0 < \theta < \pi/2, \qquad \text{(D.6a)}$$

$$G_1(\theta) = 2\pi \frac{\bar{k}_0^2}{\bar{\beta}_1} \cos^2\theta \left| \bar{\Gamma}_1^{f1} (\bar{k}_0 \sin\theta) + P_{f1b1} \bar{\tau}_1^{b1} (\bar{k}_0 \sin\theta) \right|^2, \qquad \pi/2 < \theta < \pi, \qquad \text{(D.6b)}$$

where

$$P_{f1} = \bar{\tau}_3^{f1} \bar{\tau}_2^{f1} \bar{\tau}_1^{f1}, \qquad P_{f1b1} = \bar{\tau}_2^{b1} \bar{\tau}_3^{b1} \bar{\Gamma}_4^{f1} P_{f1}, \qquad P_{f1b1f2} = \bar{\tau}_3^{f2} \bar{\tau}_2^{f2} \bar{\Gamma}_1^{b1} P_{f1b1}. \qquad \text{(D.6c)}$$

APPENDIX E

PROGRAM for SINGLE STEP DISCONTINUITY

(Wave Incident from Wider Waveguide to Narrower Waveguide)

```
PROGRAM NORMALIZED


REAL*8 KD, NO
PARAMETER (N=400, NO=2, C=2*N+2,PI=3.14159265358979)
REAL*8 LENDA
REAL*8 K0, ER, D1, D2, NS, NF, RATIO
REAL*8 KX1, KX2, AX1, AX2, BETA1, BETA2
REAL*8 KEPAF, KEPA
REAL*8 DELTU, D, DELTUN

REAL*8 UN(N), VN(N)
COMPLEX*16 BNC(N)

REAL*8 S1, S2, S3, S4, S5
REAL*8 P(N)
REAL*8 Q1, Q2
REAL*8 AU1(N), AU2(N)
REAL*8 AMP1, AMP2
REAL*8 G, R, GG
REAL*8 F(N), DY
REAL*8 GR(N), RG(N)
REAL*8 RR(0:N, 0:N), RY(0:N, 0:N)

COMPLEX*16 A(C,C), B(C), COEFY(C), COEFX(C), COEF(C)
COMPLEX*16 XR
REAL*8 PREF, PTRANS, RPREF, RPTRANS, PTOTAL
REAL*8 PREFS, PTRANSS, RPREFS, RPTRANSS
COMPLEX*16 AL(C,C)

INTEGER*4 W, X, Y, Z, T, TK0, CK0, L, FLAG


COMMON /SET1/ KEPAS, ER, KEPAF
COMMON /SET2/ KX1, KX2, AX1, AX2
COMMON /SET3/ S1, S2, S3, S4, S5
COMMON /SET4/ DELTU
COMMON /SET5/ RATIO
COMMON /SET6/ P
COMMON /SET7/ UN, VN, BNC
COMMON /SET8/ GG
COMMON /SET9/ G, R


****** OPEN THE DATA FILE

OPEN (5, FILE='CEFNORM.DAT', STATUS='NEW', FORM='FORMATTED')
OPEN (6, FILE='NORM.DAT', STATUS='NEW', FORM='FORMATTED')
OPEN (7, FILE='COEFN.DAT', STATUS='NEW', FORM='FORMATTED')
```

```
      OPEN (8, FILE='BOUNDN.DAT', STATUS='NEW', FORM='FORMATTED')
```

WRITES OUT ALL OF THE INITIAL VALUES

```
      KD = 1.d0
      NS = 1.D0
      NF = DSQRT(5.D0)
      RATIO = .02

       KEPAF = KD * NF
       KEPAS = KD * NS
       ER = NF ** 2 / NS ** 2


      WRITE(5,5)
 5    FORMAT(7X, 'Initial Values:')
      WRITE(5,15) 'KD=', KD, 'Er=', ER, 'N= ', N
      WRITE(5,14) 'KEPAF=', KEPAF, 'KEPAS=', KEPAS
15    FORMAT(3X, A3, 1X, D15.8, 3X, A3, 1X, D15.8, 3X, A3, I4)
14    FORMAT(3X, A6, 1X, D15.8, 3X, A6, 1X, D15.8)
      WRITE(5,*)
```

CALCULATES THE GUIDED PROPAGATION COEFFICIENTS IN DIFFERENT REGIONS

```
      WRITE (5,25)
25    FORMAT(7X, 'In Guided Mode:')

      D = 1.
       CALL DISPER(KX1, AX1, BETA1, D)

        WRITE(5,35) 'D1=', D, 'Kx1=', KX1, 'Ax1=', AX1,
     C       'BETA1=', BETA1

      D = RATIO
       IF (D .EQ. 0) THEN
        KX2 = 0.
        AX2 = 0.
        BETA2 = 0.
       ELSE
        CALL DISPER(KX2, AX2, BETA2, D)
       ENDIF

        WRITE(5,35) 'D2=', D, 'Kx2=', KX2, 'Ax2=', AX2,
     C       'BETA2=', BETA2
35     FORMAT(3X, A3, 1X, D15.8, 2(3X, A4, 1X, D15.8),
     C       3X, A6, 1X, D15.8 )
       WRITE(5,*)
```

CALCULATES THE RADIATION PROPAGATION COEFFICIENTS
IN DIFFERENT STEPS

```
      DELTU = NO * KEPAS / FLOATJ(N)
      CK0 = N

      DO 10 I = 1, N
       UN(I) = I * DELTU

       CALL FINDUN(UN(I), VN(I), BNC(I), FLAG)

       IF (FLAG .EQ. 1) THEN
        CK0 = I
       ENDIF

10    CONTINUE

      S1 = KX1
      S2 = KX1 * RATIO
      S3 = KX2
      S4 = KX2 * RATIO
      S5 = AX2 * (RATIO - 1)
      S5 = DEXP(S5)
```

CALCULATES THE AMPLITUDE OF THE GUIDED MODE

```
      AMP1 = (AX1) / (1 + AX1)
       AMP1 = DSQRT(AMP1)

      AMP2 = (AX2) / (1 + (AX2 * RATIO))
       AMP2 = DSQRT(AMP2)

      WRITE(5,105) 'AMP1= ', AMP1, 'AMP2= ', AMP2
105   FORMAT(7X, A6, D12.6, 3X, A6, D12.6)
      WRITE(5,*)
```

CALCULATES THE OVERLAP INTEGRAL
BOTH SIDES OF STEP HAVE IN GUIDED MODE

```
      CALL GUIDE
      GG = 2 * AMP1 * AMP2 * GG

       WRITE(5,65) 'I12=', GG
65    FORMAT(7X, A4, 1X, D12.6)
       WRITE(5,*)
```

CALCULATES THE OVERLAP INTEGRAL

ONE SIDE OF STEP HAS GUIDED MODE AND
THE OTHER HAS RADIATION MODE

```
      DO 20 I = 1, N
       P(I) = VN(I) / UN(I)
        Q1 = VN(I)
         Q2 = VN(I) * RATIO
```

CALCULATES THE AMPLITUDE OF RADIATION MODE

```
      AU1(I) = DCOS(Q1) * DCOS(Q1) + P(I) * P(I) * DSIN(Q1) * DSIN(Q1)
        AU1(I) = PI * AU1(I) / 2.
         AU1(I) = DSQRT(AU1(I))
          AU1(I) = 1. / AU1(I)

      AU2(I) = DCOS(Q2) * DCOS(Q2) + P(I) * P(I) * DSIN(Q2) * DSIN(Q2)
       AU2(I) = PI * AU2(I) / 2.
        AU2(I) = DSQRT(AU2(I))
         AU2(I) = 1. / AU2(I)

       CALL GDRAD(UN(I), VN(I), P(I), G, R)

       GR(I) = 2 * AMP1 * AU2(I) * G
       RG(I) = 2 * AU1(I) * AMP2 * R

 20   CONTINUE
```

CALCULATES THE OVERLAP INTEGRAL
BOTH SIDES OF STEP HAVE RADIATION MODE

```
      RR(0,0) = 0.
      RY(0,0) = 0.

      DO 40  I = 1, N
       DO 50  J = 1, N


      CALL RADRAD( UN(I), UN(J), VN(I), VN(J), P(J)
 C          , AU1(I), AU2(J), RY(I,J))

      RR(I,J) = G

      IF (R .NE. 0.) THEN
       F(I) = R
      ENDIF

 50    CONTINUE
 40   CONTINUE

      DO 41 I = 1, N-1
      WRITE(5,51) 'RY(', I, I, ')= ', RY(I,I)
      WRITE(5,51) 'RR(', I, I, ')= ', RR(I,I)

       DY = (RY(I+1,I+1) - RY(I-1, I-1)) / (2. * DELTU)
       RR(I,I) = RR(I,I) + DY
```

```
 41     CONTINUE
```

WRITES DOWN THE NUMERCIAL MATRIX

```
****** THE FIRST FOUR TERMS: A(1,1) , A(1,2) , A(2,1), A(2,2)

         A(1,1) = -1.D0
         A(1,2) = GG
         A(2,1) = BETA1 * GG
         A(2,2) = BETA2

****** CALCULATE SOME CONSTANT COEFFICIENCES

         DELTUN = DELTU / 3.D0

         X = N + 2
         Y = X + 1

****** CALCULATE FROM A(1,3) ... A(2,(N+2))

         DO 60 J = 3, X
          M = J - 2

          IF (M .EQ. N) THEN
           A(1,J) = DELTUN * GR(M)
          ELSE

            L = JMOD(M , 2)
             IF (L .EQ. 0) THEN
                   A(1,J) = DELTUN * GR(M) * 2.D0
             ELSE
                   A(1,J) = DELTUN * GR(M) * 4.D0
             ENDIF

          ENDIF

          A(2,J) = 0.D0
 60     CONTINUE

****** CALCULATE FROM A(1,N+3) ... A(2,2N+2)

         DO 70 J = Y, C
          A(1,J) = 0.D0
           M = J - X

             L = JMOD(M ,2)

                   IF (L .EQ. 0) THEN
                     A(2,J) = DELTUN * BNC(M) * RG(M) * 2.D0
                   ELSE
                     A(2,J) = DELTUN * BNC(M) * RG(M) * 4.D0
                   ENDIF

 70     CONTINUE
```

```
****** CALCULATE FROM A(3,1) ... A((N+2), 2)

        DO 80 I = 3, X
         M = I - 2
         A(I,1) = 0.D0
         A(I,2) = RG(M)
 80   CONTINUE

****** CALCULATE FROM A((N+3), 1) ... A(2N+2, 2)

        DO 90 I = Y, C
         M = I - X
         A(I,2) = 0.D0
         A(I,1) = BETA1 * GR(M)
 90   CONTINUE

****** CALCULATE FROM A(3, (N+3)) ... A((N+3), 2N+2)

        DO 110 I = 3, X

        DO 120 J = Y, C
          M = J - X
          L = I - 2

          IF ( M .EQ. L) THEN
                A(I,J) = -2.D0
          ELSE
           A(I,J) = 0.D0
          ENDIF

 120  CONTINUE

 110  CONTINUE

****** CALCULATE FROM A((N+3), 3) ... A(2N+2, (N+2))

        DO 130 I = Y, C

        DO 140  J = 3, X
         M = J - 2
         L = I - X

         IF ( M .EQ. L) THEN
               A(I,J) = 2. * BNC(M)
         ELSE
               A(I,J) = 0.D0
         ENDIF

 140  CONTINUE

 130  CONTINUE


****** CALCULATE FROM A(3,3) ... A((N+2), (N+2))
              and A((N+3), (N+3)) ... A((2N+2), (2N+2))

        DO 150 I = 3, X
```

```
      DO 160 J = 3, X
       L = I - 2
        M = J - 2
         T = I + N
          W = J + N

      IF (M .EQ. N) THEN
       CI = 1.D0
      ELSE

        Z = JMOD(M,2)
        IF (Z .EQ. 0) THEN
         CI = 2.D0
        ELSE
         CI = 4.D0
        ENDIF

      ENDIF

        IF (L .EQ. M) THEN
         A(I,J) = DELTUN * RR(L,M) * CI + F(L)
         A(T,W) = (DELTUN * RR(M,L) * CI + F(L)) * BNC(M)
        ELSE
         A(I,J) = DELTUN * RR(L,M) * CI
         A(T,W) = (DELTUN * RR(M,L) * CI) * BNC(M)
        ENDIF


160   CONTINUE

150   CONTINUE

****** THE MATRIX ON THE RIGHT HAND SIDE

      B(1) = 1.D0
      B(2) = BETA1 * GG

      DO 180 I = 3, X
       B(I) = 0.D0
180   CONTINUE

      DO 190 I = Y, C
       M = I - X
       B(I) = BETA1 * GR(M)
190   CONTINUE

****** ADJUST THE MATRIX (ERASE TAU(K0) ITEM)

      IF (CK0 .NE. N) THEN
       Z = C - 1
       T = CK0 + N + 3
       GO TO 199
      ELSE
       Z = C - 1
       GO TO 201
      ENDIF
```

```
199   DO 191 I = 1, C
        DO 192 J = T, C
         A(I,J-1) = A(I,J)
192    CONTINUE
191   CONTINUE


       DO 193 J = 1, C-1
        DO 194 I = T, C
         A(I-1, J) = A(I,J)
194    CONTINUE
193   CONTINUE


       DO 195 I = T, C
        B(I-1) = B(I)
195   CONTINUE
```

USING GAUSSIAN ELIMINATION TO SOLVE THE MATRIX

```
201   IF (RATIO .EQ. 0) THEN

        DO 202 I = 1, Z
         DO 203 J = 3, Z
          A(I,J-1) = A(I,J)
203    CONTINUE
202   CONTINUE

        DO 204 J = 1, Z-1
         DO 205 I = 3, Z
          A(I-1, J) = A(I,J)
205    CONTINUE
204   CONTINUE

        DO 206 I = 3, Z
         B(I-1) = B(I)
206   CONTINUE

        Z = Z - 1
        ENDIF

       DO 200 W = 1, Z

        DO 210 X = (W+1), Z
         AL(X,W) = A(X,W) / A(W,W)

          DO 220 Y = W, Z
           A(X,Y) = A(X,Y) - AL(X,W) * A(W,Y)
220     CONTINUE

210   CONTINUE

200   CONTINUE

       DO 221 I = 1, Z
       AL(I,I) = 1.D0
```

```
221   CONTINUE


****** LU FACTORY CALCULATION

        COEFY(1) = B(1) / AL(1,1)

        DO 230 I = 2, Z
         XR = 0.

         DO 240 J = 1, I-1
          XR = AL(I,J) * COEFY(J) + XR
          COEFY(I) = (B(I) - XR) / AL(I,I)
240     CONTINUE

230   CONTINUE


        COEFX(Z) = COEFY(Z) / A(Z,Z)

        DO 250 I = Z-1, 1, -1
         XR = 0.

         DO 260 J = Z, I+1, -1
          XR = A(I,J) * COEFX(J) + XR
          COEFX(I) = (COEFY(I) - XR) / A(I,I)
260     CONTINUE


250   CONTINUE

        IF (RATIO .EQ. 0) THEN

         DO 251 I = Z, 2, -1
          COEFX(I+1) = COEFX(I)
251     CONTINUE

         COEFX(2) = 0.
         Z = Z + 1
        ENDIF

        TK0 = CK0 + N + 2

         IF (Z .EQ. C-1) THEN

          DO 270 I = Z, TK0, -1
           COEFX(I+1) = COEFX(I)
270      CONTINUE

          COEFX(TK0) = 0.

         ENDIF

        WRITE(7,124) 'GUIDED REFLECTED COEF. =', COEFX(1)
        WRITE(7,124) 'GUIDED TRANSMITTED COEF. =', COEFX(2)
124    FORMAT(2X, A30, (D15.8, 3X, D15.8))
```

```
      WRITE(7,*) 'TRANSMITTED RADIATION COEFFICIENTS :'

      DO 280 I = 1, N
       J = I + 2
      WRITE(7, 125) 'COEF(', I, ')= ', COEFX(J)
125   FORMAT(2X, A6, I4, A3, (D15.8, 3X, D15.8))
280   CONTINUE

      WRITE(7,*)
      WRITE(7,*) 'REFLECTED RADIATION COEFFICIENTS :'

      DO 281 I = 1, N
       J = I + N + 2
      WRITE(7,125) 'COEF(', I, ')= ', COEFX(J)
281   CONTINUE
```

CALCULATES THE TRANSMITTED & REFLECTED POWER of GUIDED & RADIATION MODES

```
      PREF = (CDABS(COEFX(1))) ** 2
      PTRANS = ((CDABS(COEFX(2))) ** 2) * BETA2 / BETA1

      RPTRANS = 0.
      RPREF = 0.


      DO 1000 I = 3, CK0+1
       L = I - 2
       RPTRANS = RPTRANS + ((CDABS(COEFX(I))) ** 2) * CDABS(BNC(L))
1000  CONTINUE


      DO 1100 I = N+3, TK0-1
       L = I - N - 2
       RPREF = RPREF + ((CDABS(COEFX(I)))** 2) * CDABS(BNC(L))
1100  CONTINUE


      RPTRANS = 2. * RPTRANS * DELTU / BETA1
      RPREF = 2. * RPREF * DELTU / BETA1
      PTOTAL = PTRANS + PREF + RPTRANS + RPREF



      WRITE(6,2) 'K0D =', KD, '?*K0 =', NO
2     FORMAT(5X, 2(A6, F5.2, 6X))
      WRITE(6,*)
      WRITE(6,1) 'D1= ', KD*2., 'D2= ', KD*RATIO, 'NS= ', NS, 'NF= ', NF
   C            , 'N= ', N
1     FORMAT (2(A4, D10.4, 2X), 2(A4, F10.8, 2X), A3, I3)
      WRITE(6,*)


      WRITE(6,1005) 'TRANSMITTED POWER IN GUIDED MODE = ', PTRANS
      WRITE(6,*)
      WRITE(6,1005) 'REFLECTED POWER IN GUIDED MODE = ', PREF
```

```
      WRITE(6,*)
      WRITE(6,1005) 'TRANSMITTED POWER IN RADIATION MODE = ', RPTRANS
      WRITE(6,*)
      WRITE(6,1005) 'REFLECTED POWER IN RADIATION MODE = ', RPREF
      WRITE(6,*)
      WRITE(6,1005) 'TOTAL POWER IN THIS MODEL = ', PTOTAL
1005  FORMAT(3X, A40, F12.8)
      WRITE(6,*)

      CASEI = 1.0D0 - PTRANS - PREF
      CASEII = RPTRANS + RPREF
      DIFF = CASEI - CASEII

      WRITE(6,*) 'FOR CASE I: '
      WRITE(6,*) '   RADIATION POWER = 1 - GUIDED MODE POWER '
      WRITE(6,1006) 'RADIATION POWER = ', CASEI

      WRITE(6,*)
      WRITE(6,*) 'FOR CASE II: '
      WRITE(6,*) '   RADIATION POWER = TRANSMISSION POWER + REFLECTION
     C POWER IN RADIATION MODE'
      WRITE(6,*)
      WRITE(6,1006) 'RADIATION POWER = ', CASEII
      WRITE(6,*)
      WRITE(6,*) 'THE DIFFERENCE BETWEEN TWO CASES IS :', DIFF

1006  FORMAT(3X, A20, F10.8)
```

CLOSES THE DATA FILE

```
      CLOSE(8)
      CLOSE(7)
      CLOSE(6)
      CLOSE(5)

      STOP
      END
```

SUBROUTINE FOR
CALCULATING THE OVERLAP INTEGRAL
BOTH SIDES OF STEP HAVE RADIATION MODE

```
      SUBROUTINE RADRAD(U1, U2, V1, V2, P, A1, A2, T12)

      PARAMETER (PI = 3.14159265358979)
      REAL*8 U1, U2, V1, V2, P, A1, A2
      REAL*8 W1, W2, W3, W4, W5
      REAL*8 T10, T11, T12, F, Y
      REAL*8 RR, RATIO

      COMMON /SET5/ RATIO
      COMMON /SET9/ RR, F
```

```
      W1 = V1
      W2 = V1 * RATIO
      W3 = V2
      W4 = V2 * RATIO
      W5 = U2 * (1. - RATIO)

      IF (V1 .EQ. U2) THEN
       T11 = 0.
      ELSE
       T11 = (DCOS(W4) * ( V1 * DSIN(W1) * DCOS(W5) - U2 * DCOS(W1)
C       * DSIN(W5) - V1 * DSIN(W2) ) - P * DSIN(W4) *
C       ( V1 * DSIN(W1) * DSIN(W5) + U2 * DCOS(W1) * DCOS(W5)
C       - U2 * DCOS(W2) ) ) / ( V1 * V1 - U2 * U2 )
      ENDIF


      Y = (  U2 * DCOS(W1) * DCOS(W4) * DSIN(W5)
C      + V2 * DCOS(W1) * DSIN(W4) * DCOS(W5)
C      - V1 * DSIN(W1) * DCOS(W4) * DCOS(W5)
C      + P * V1 * DSIN(W1) * DSIN(W4) * DSIN(W5)) / (U1 + U2)

       IF ( U1 .EQ. U2 ) THEN
        F = (( DCOS(W1) * DCOS(W4) + (V1 / U1) * P * DSIN(W1) *
C        DSIN(W4)) * DCOS(W5) + ((V1 / U1) * DSIN(W1) *
C        DCOS(W4) - P * DCOS(W1) * DSIN(W4)) * DSIN(W5))
C        * PI * A1 * A2

        T10 = ( ( DSIN(2 * W2) / (2 * V1) ) + RATIO ) / 2.

        T12 = Y * 2. * A1 * A2
        RR = 2. * A1 * A2 * (T10 + T11)

       ELSE
        F = 0.
        T10 = (V1 * DSIN(W2) * DCOS(W4) - V2 * DCOS(W2) * DSIN(W4))
C        / (V1 * V1 - V2 * V2)
        T12 = Y / (U1 - U2)

         RR = A1 * A2 * 2. * (T10 + T11 + T12)
       ENDIF


       RETURN
       END
```

SUBROUTINE FOR
CALCULATING THE OVERLAP INTEGRAL
ONE SIDE OF STEP HAS GUIDED MODE AND
THE OTHER HAS RADIATION MODE

```
       SUBROUTINE  GDRAD(U, V, P, G, R)

       REAL*8 K1, K2, D1, D2, A1, A2, RATIO
       REAL*8 S6, S7, S8
```

```
      REAL*8 T4, T5, T6, T7, T8, T9
      REAL*8 U, V, P
      REAL*8 G, R
      REAL*8 S1, S2, S3, S4, S5

      COMMON /SET2/ K1, K2, A1, A2
      COMMON /SET3/ S1, S2, S3, S4, S5
      COMMON /SET5/ RATIO

      S6 = V
      S7 = V * RATIO
      S8 = U * (1. - RATIO)
```

GUIDED MODE IN REGION I & RADIATION MODE IN REGION II

```
      T4 = (K1 * DSIN(S2) * DCOS(S7) - V * DCOS(S2) * DSIN(S7))
c      / (K1 * K1 - V * V)

      T5 = ( DCOS(S7) * ( K1 * DSIN(S1) * DCOS(S8) - U * DCOS(S1)
C                 * DSIN(S8) - K1 * DSIN(S2) )
C      - P * DSIN(S7) * (K1 * DSIN(S1) * DSIN(S8) +
C             U * DCOS(S1) * DCOS(S8) - U * DCOS(S2) ) )
C      / (K1 * K1 - U * U)

      T6 = -1.* DCOS(S1) * (DCOS(S7) * (U *DSIN(S8) - A1 * DCOS(S8))
C           + P * DSIN(S7) * ( A1 * DSIN(S8) + U * DCOS(S8)))
C       / ( A1 * A1 + U * U )

      G = T4 + T5 + T6
```

RADIATION MODE IN REGION I & GUIDED MODE IN REGION II

```
      T7 = ( K2 * DSIN(S4) * DCOS(S7) - V * DCOS(S4) * DSIN(S7) )
C       / (K2 * K2 - V * V)

      T8 = DCOS(S4) * ( ( V * DSIN(S6) - A2 * DCOS(S6) ) * S5
C            - ( V * DSIN(S7) - A2 * DCOS(S7) ) )
C       / (A2 * A2 + V * V)

      T9 = ( A2 * DCOS(S6) - V * DSIN(S6) ) * DCOS(S4) * S5
C       / (A2 * A2 + U * U)

      R = T7 + T8 + T9

      RETURN
      END
```

SOLVE THE DISPERSION EQUATION $K_{xn}\mathrm{Tan}(K_{xn}D) = \alpha_{xn}$ FOR GUIDED MODES

```
      SUBROUTINE DISPER(KX, AX, B, R)

      PARAMETER(PI = 3.14159265358979)
```

```
      REAL*8 K0, K1, R
      REAL*8 KX, AX, B
      REAL*8 HN, VAR1, VAR2
      REAL*8 K, EN, T
      REAL*8 KEPAS, ER, KEPAF, P
      REAL*8 KLEFT, KRIGHT

      COMMON /SET1/ KEPAS, ER, KEPAF

      K0 = KEPAS
      ER = ER
      K1 = KEPAF

       K0 = K0 * R
       EN = ER - 1
       K1 = K1 * R

      T = 1 + ( PI * PI / 4.)
      KRIGHT = DSQRT(EN) * K0
      KLEFT = KRIGHT / DSQRT(T)


      DO 20 I = 1, 100

      KX = (KLEFT + KRIGHT) / 2.

       VAR1 = KX - K0 * DSQRT(EN) * COS(KX)
       P = DABS(VAR1)

          IF (P .LT. 0.5D-6) THEN
           GO TO 95
          ENDIF

      IF (VAR1 .GT. 0) THEN
       KRIGHT = KX
      ELSE
       KLEFT = KX
      ENDIF

20    CONTINUE

95         KX = KX / R
       K0 = K0 / R
        K1 = K1 / R

       B = K1 * K1 - KX * KX
         AX = B - K0 * K0
          B = DSQRT(B)

        IF (AX .LT. 0.) THEN
         AX = KX * KX * R
         ELSE
          AX = DSQRT(AX)
        ENDIF
        RETURN
       END
```

SUBROUTINE FOR CALCULATING

THE RADIATION PROPAGATION COEFFICIENTS IN DIFFERENT REGIONS

```
SUBROUTINE FINDUN(X, Y, Z, C)


REAL*8 X, Y
COMPLEX*16 Z, IMAGE
REAL*8 P, S
REAL*8 K0, K
REAL*8 DU
REAL*8 KEPAS, ER, KEPAF
INTEGER*4 C


COMMON /SET1/ KEPAS, ER, KEPAF

K0 = KEPAS
K = KEPAF

IMAGE = CMPLX(0,-1)

P = K0 * K0 - X * X
 Y = K * K - P
  Y = DSQRT(Y)


IF (DABS(P) .LT. 0.5D-2) THEN
 Z = 0.
 C = 1
ELSE

  IF (P .LT. 0) THEN
     S = DABS(P)
    S = DSQRT(S)
   Z = IMAGE * S
  ELSE
    Z = DSQRT(P)
  ENDIF
 C = 0
ENDIF

RETURN
END
```

SUBROUTINE FOR CALCULATING THE OVERLAP INTEGRAL
BOTH REGIONS HAVE GUIDED MODE

```
      SUBROUTINE GUIDE

      REAL*8 K1, K2
      REAL*8 T1, T2, T3
      REAL*8 A1, A2
      REAL*8 S1, S2, S3, S4, S5
      REAL*8 GG

      COMMON /SET2/ K1, K2, A1, A2
      COMMON /SET3/ S1, S2, S3, S4, S5
      COMMON /SET8/ GG


      T1 = ( K1 * DSIN(S2) * DCOS(S4) - K2 * DCOS(S2) * DSIN(S4))
C     / ( K1 * K1 - K2 * K2 )

      T2 = DCOS(S4) * ( (K1 * DSIN(S1) - A2 * DCOS(S1) ) * S5 -
C                 (K1 * DSIN(S2) - A2 * DCOS(S2)))
C     / (K1 * K1 + A2 * A2)
      T3 = ( DCOS(S1) * DCOS(S4) * S5 ) / (A1 + A2)

      GG = T1 + T2 + T3

      RETURN
      END
```

APPENDIX F

PROGRAM for MANY STEPS DISCONTINUITIES

```
PROGRAM NORM_MAIN

INTEGER*4 STEP, ITER, N, NO, C, DIR, X, FLAG, CK0, FLAGP, RATION
REAL*8 PI, KD, ER, NS, LENGTH, RATIO

PARAMETER(STEP=128, ITER=3, N=150, NO=1, C=2*N+2, PI=3.14159265)
PARAMETER(KD=1, ER=2.56, NS=1)


REAL*8 KEPAS, KEPAF, DELTA_Z, DELTA_U, RATIO1, RATIO2
REAL*8 ZZ, DELTA_UN, B1, B2
REAL*8 UN(N), VN(N), R(STEP+1) , P(N)
REAL*8 KX(STEP+1), AX(STEP+1), BETA(STEP+1)
COMPLEX*16 BNC(N)
REAL*8 AU1(N), AU2(N), Q1, Q2, AMP1, AMP2
REAL*8 S1, S2, S3, S4, S5, SS
REAL*8 GG, GR(N), RG(N), RR(N,N), RY(0:N,0:N), DY
COMPLEX*16 A(C,C), B(C), COEFX(C), PREV(C)
COMPLEX*16 PEXPB1Z, PEXPB2Z, NEXPB1Z, NEXPB2Z
COMPLEX*16 PEXPBU(N), NEXPBU(N), IMAGE
REAL*8 G, H
COMPLEX*16 TRANS(N), REF(N), TCOEF
REAL*8 PREF, PTRANS, RPTRANS, RPREF, PTOTAL, DIF_P
REAL*8 PINC, PTPREV

COMMON /SET1/ KEPAS, KEPAF
COMMON /SET3/ S1, S2, S3, S4, S5
COMMON /SET4/ RATIO1, RATIO2
COMMON /SET5/ GG, GR, RG, RR
COMMON /SET6/ A, B
COMMON /SET7/ PEXPB1Z, PEXPB2Z, NEXPB1Z, NEXPB2Z, PEXPBU, NEXPBU
COMMON /SET9/ PREV
COMMON /SET10/ COEFX
COMMON /SET11/ TRANS
COMMON /SET12/ REF
COMMON /SET13/ BNC



OPEN (6, FILE='CONSERV.DAT', STATUS='NEW', FORM='FORMATTED')
OPEN (7, FILE='PATTER.DAT' , STATUS='NEW', FORM='FORMATTED')
OPEN (8, FILE='COEF.DAT',    STATUS='NEW', FORM='FORMATTED')

KEPAS = KD * NS
KEPAF = KD * DSQRT(ER)
LENGTH = PI * 10.

Z = STEP

IF (Z .EQ. 1) THEN
 DELTA_Z = 0.
ELSE
```

```
      DELTA_Z = LENGTH / (Z - 1)
     ENDIF

     DELTA_U = NO * KEPAS / N
     RATIO = KD / STEP

     CK0 = N
     RATION = N / NO
     DO 100 I = 1, N
      UN(I) = I * DELTA_U
       IF (I .EQ. RATION) THEN
        BNC(I) = 0.
        VN(I) = KEPAF
        CK0 = I
       ELSE
        CALL FINDUN (UN(I), VN(I), BNC(I))
       ENDIF
100  CONTINUE

     R(1) = 1.
     WRITE(8,2) 'R(', 1, ') = ', R(1)
     DO 120 I = 2, STEP
      R(I) = R(I-1) - RATIO
120  CONTINUE

     DO 130 I = 1, STEP
      CALL DISPER(KX(I), AX(I), BETA(I), R(I), ER)
130  CONTINUE

     R(STEP+1) = 0.
     KX(STEP+1) = 0.
     AX(STEP+1) = 0.
     BETA(STEP+1) = 0.

     PTPREV = 1.
     PREV(1) = 0.
     PREV(2) = 1.
     PINC = 1.
     TCOEF = 1.
     DO 140 I = 3, C
      PREV(I) = 0.
140  CONTINUE

     DO 1000 X = 1, ITER
      DIR = JMOD(X,2)
       IF (X .EQ. 1) THEN
        II = 1
        JJ = STEP
        KK = 1
        FLAGP = 1
       ELSE
        IF (DIR .EQ. 0) THEN
         II = STEP - 1
         JJ = 1
         KK = -1
         FLAGP = 2
        ELSE
         II = 2
```

```
        JJ = STEP
        KK = 1
        FLAGP = 3
       ENDIF
      ENDIF

     DO 150 I = II, JJ, KK
      RATIO1 = R(I)
      RATIO2 = R(I+1)

      S1 = KX(I) * RATIO1
      S2 = KX(I) * RATIO2
      S3 = KX(I+1) * RATIO1
      S4 = KX(I+1) * RATIO2
      S5 = AX(I+1) * (RATIO2 - RATIO1)
      S5 = DEXP(S5)

      AMP1 = AX(I) / (1 + AX(I) * RATIO1)
      AMP1 = DSQRT(AMP1)
      AMP2 = AX(I+1) / (1 + AX(I+1) * RATIO2)
      AMP2 = DSQRT(AMP2)

      CALL GUIDE(KX(I), AX(I), KX(I+1), AX(I+1), GG)
       GG = 2. * AMP1 * AMP2 * GG

      DO 170 J = 1, N
       P(J) = VN(J) / UN(J)
       Q1 = VN(J) * RATIO1
       Q2 = VN(J) * RATIO2

       AU1(J) = DCOS(Q1) *DCOS(Q1) +P(J) *P(J) *DSIN(Q1) *DSIN(Q1)
       AU1(J) = PI * AU1(J) / 2.
       AU1(J) = 1. / DSQRT(AU1(J))

       AU2(J) = DCOS(Q2) *DCOS(Q2) +P(J) *P(J) *DSIN(Q2) *DSIN(Q2)
       AU2(J) = PI * AU2(J) / 2.
       AU2(J) = 1. / DSQRT(AU2(J))

       CALL GDRAD(KX(I),AX(I),KX(I+1),AX(I+1),VN(J),UN(J),P(J),G,H)

        GR(J) = 2. * AMP1 * AU2(J) * G
        RG(J) = 2. * AU1(J) * AMP2 * H

170   CONTINUE

        DO 190 L = 1, N
         DO 200 M = 1, N

          CALL RADRAD(UN(L), UN(M), VN(L), VN(M), P(M),
 C           AU1(L), AU2(M), RR(L,M), L, M)

200     CONTINUE
190    CONTINUE

       ZZ = DELTA_Z * (I-1)
       IMAGE = CMPLX(0,1)
       PEXPB1Z = DCOS(BETA(I) * ZZ) + IMAGE * DSIN(BETA(I) * ZZ)
       PEXPB2Z = DCOS(BETA(I+1) * ZZ) + IMAGE * DSIN(BETA(I+1) *ZZ)
```

```
      NEXPB1Z = DCOS(BETA(I) * ZZ) - IMAGE * DSIN(BETA(I) * ZZ)
      NEXPB2Z = DCOS(BETA(I+1) * ZZ) - IMAGE * DSIN(BETA(I+1) *ZZ)
      IF (CK0 .NE. N) THEN
       DO 210 J = 1, CK0
        SS = CDABS(BNC(J) * ZZ)
        PEXPBU(J) = DCOS(SS) + IMAGE * DSIN(SS)
        NEXPBU(J) = DCOS(SS) - IMAGE * DSIN(SS)
210    CONTINUE

       DO 220 J = CK0+1, N
        SS = DIMAG(BNC(J) * ZZ)
        PEXPBU(J) = DEXP(SS)
        NEXPBU(J) = DEXP(-1. * SS)

220    CONTINUE

      ELSE

       DO 230 J = 1, N
        SS = CDABS(BNC(J) * ZZ)
        PEXPBU(J) = DCOS(SS) + IMAGE * DSIN(SS)
        NEXPBU(J) = DCOS(SS) - IMAGE * DSIN(SS)
230    CONTINUE
      ENDIF

      DELTA_UN = DELTA_U / 3.

      IF (DIR .EQ. 0) THEN
       CALL BACKWARD(BETA(I), BETA(I+1), DELTA_UN)
       B1 = BETA(I+1)
       B2 = BETA(I)
       WRITE(6,*) 'IT''S BACKWARD ON BOUNDARY', I, ' , THE', X,
C     ' TIME''S PROPAGATION!'
      ELSE
       CALL FORWARD(BETA(I), BETA(I+1), DELTA_UN)
       B1 = BETA(I)
       B2 = BETA(I+1)
       WRITE(6,*) 'IT''S FORWARD ON BOUNDARY', I, ' , THE', X,
C     ' TIME''S PROPAGATION!'
      ENDIF

      IF (I .EQ. STEP) THEN
       FLAG = 1
      ELSE
       FLAG = 0
      ENDIF
      CALL CAL_COEF(FLAG, CK0)

      PREF = ((CDABS(COEFX(1))) ** 2) * PTPREV
      PTRANS = ((CDABS(COEFX(2))) ** 2) * PTPREV * B2 / B1
      RPTRANS = 0.
      RPREF = 0.

      DO 240 J = 3, CK0+2
       L = J - 2
       K = J + N
       RPTRANS = RPTRANS + ((CDABS(COEFX(J))) ** 2) * CDABS(BNC(L))
       RPREF = RPREF + ((CDABS(COEFX(K))) ** 2) * CDABS(BNC(L))
```

```
240     CONTINUE

          RPTRANS = 2. * RPTRANS * DELTA_U * PTPREV / B1
          RPREF = 2. * RPREF * DELTA_U * PTPREV/ B1
          PTOTAL = PTRANS + PREF + RPTRANS + RPREF
          DIF_P = (PINC - PTOTAL) / PINC

        WRITE(6,*)
        WRITE(6,*) 'POWER DISTRIBUTION :'
        WRITE(6,*) 'GUIDED TRANSMITTED POWER =', PTRANS
        WRITE(6,*) 'GUIDED REFLECTED POWER =', PREF
        WRITE(6,*) 'RADIATED TRANSMITTED POWER =', RPTRANS
        WRITE(6,*) 'RADIIATED REFLECTED POWER =', RPREF
        WRITE(6,*) 'TOTAL POWER AT THIS STAGE =', PTOTAL
        WRITE(6,*)
        WRITE(6,*) 'INCIDENT POWER FROM PREVIOUS STAGE =', PINC
        WRITE(6,*)
        WRITE(6,*) 'THE PERCENTAGE ERROR OF TOTAL POWER =', DIF_P


        WRITE(8,*) 'PREVIOUS GUIDED POWER = ', PTPREV
        WRITE(8,*) 'PREVIOUS INCIDENT POWER = ', PINC
        WRITE(8,*) 'GUIDED TRANSMITTED COEFFICIENT = ', COEFX(2)
        WRITE(8,*) 'GUIDED REFLECTED COEFFICIENT = ', COEFX(1)
        WRITE(8,*) 'TRANSMITTED COEFFICIENT = ', TCOEF

        IF (FLAGP .EQ. 1) THEN
         IF (I .EQ. 1) THEN
          PREV(1) = COEFX(1)
          PREV(2) = COEFX(2)
          DO 245 J = 3, N+2
           L = J + N
           REF(J-2) = COEFX(L)
           PREV(J) = COEFX(J)
245       CONTINUE
          CALL PATTERNR(DELTA_U, B1, X, RATION, TCOEF)
          PTPREV = PTRANS
          PINC = PTRANS + RPTRANS
          TCOEF = TCOEF * PREV(2)
         ELSE
          IF (I .EQ. STEP) THEN
           PREV(1) = COEFX(1)
           PREV(2) = COEFX(1)
          DO 250 J = 3, N
           L = J + N
           TRANS(J-2) = COEFX(J)
           PREV(J) = COEFX(L)
250       CONTINUE
           CALL PATTERNT(DELTA_U, B1, X, RATION, TCOEF)
           PTPREV = PREF
           PINC = PREF + RPREF
           TCOEF = TCOEF * PREV(2)
          ELSE
           PTPREV = PTRANS
           PINC = PTRANS + RPTRANS
           TCOEF = TCOEF * COEFX(2)
           DO 260 J = 1, C
                PREV(J) = COEFX(J)
```

```
260         CONTINUE
           ENDIF
          ENDIF
         ELSE
         IF ((FLAGP .EQ. 2) .AND. (I .EQ. 1)) THEN
          PREV(1) = COEFX(1)
          PREV(2) = COEFX(1)
          DO 265 J = 3, N
           L = J + N
           REF(J-2) = COEFX(J)
           PREV(J) = COEFX(L)
265       CONTINUE
          CALL PATTERNR(DELTA_U, B1, X, RATION ,TCOEF)
          PTPREV = PREF
          PINC = PREF + RPREF
          TCOEF = TCOEF * PREV(2)
         ELSE
          IF ((FLAGP .EQ. 3) .AND. (I .EQ. STEP)) THEN
           PREV(1) = COEFX(1)
           PREV(2) = COEFX(1)
           DO 270 J = 3, N
            L = J + N
            TRANS(J-2) = COEFX(J)
            PREV(J) = COEFX(L)
270        CONTINUE
            CALL PATTERNT(DELTA_U, B1, X, RATION, TCOEF)
            PTPREV = PREF
            PINC = PREF + RPREF
            TCOEF = TCOEF * PREV(2)
          ELSE
           PTPREV = PTRANS
           PINC = PTRANS + RPTRANS
           TCOEF = TCOEF * COEFX(2)
           DO 280 J = 1, C
            PREV(J) = COEFX(J)
280        CONTINUE
           ENDIF
          ENDIF
         ENDIF


150   CONTINUE
1000  CONTINUE

        CLOSE(6)
        CLOSE(7)
        CLOSE(8)

        STOP
        END
```

THE RADIATION PROPAGATION COEFFICIENTS
IN DIFFERENT REGIONS

```
SUBROUTINE FINDUN(X, Y, Z)


REAL*8 X, Y
COMPLEX*16 Z, IMAGE
REAL*8 P, S
REAL*8 K0, K
REAL*8 KEPAS, KEPAF

COMMON /SET1/ KEPAS, KEPAF

K0 = KEPAS
K = KEPAF

IMAGE = CMPLX(0,-1)

P = K0 * K0 - X * X
 Y = K * K - P
  Y = DSQRT(Y)

  IF (P .LT. 0) THEN
      S = DABS(P)
     S = DSQRT(S)
    Z = IMAGE * S
  ELSE
     Z = DSQRT(P)
  ENDIF

RETURN
END
```

SOLVES THE DISPERSION EQUATION
$K_{xn}\mathrm{Tan}(K_{xn}D) = \alpha_{xn}$
FOR GUIDED MODES

```
SUBROUTINE DISPER(KX, AX, B, R, ER)

PARAMETER(PI = 3.14159265358979)
REAL*8 K0, K1, R
REAL*8 KX, AX, B
REAL*8 HN, VAR1
REAL*8 K, EN, T, P
REAL*8 KEPAS, KEPAF, ER
REAL*8 KLEFT, KRIGHT

COMMON /SET1/ KEPAS, KEPAF

K0 = KEPAS
ER = ER
K1 = KEPAF
```

```
      K0 = K0 * R
      EN = ER - 1
      K1 = K1 * R

      T = (( PI * PI / 4.) - 1.) / EN
      KRIGHT = K1
      KLEFT = 0.


      DO 10 I = 1, 100

      KX = (KLEFT + KRIGHT) / 2.

      VAR1 = KX - K0 * DSQRT(EN) * COS(KX)
      P = DABS(VAR1)

         IF (P .LT. 0.5D-6) THEN
          GO TO 95
         ENDIF

      IF (VAR1 .GT. 0) THEN
       KRIGHT = KX
      ELSE
       KLEFT = KX
      ENDIF

10    CONTINUE

95    KX = KX / R
       K0 = K0 / R
        K1 = K1 / R

      B = K1 * K1 - KX * KX
        AX = B - K0 * K0
         B = DSQRT(B)

       IF (AX .LT. 0.) THEN
        AX = KX * KX * R
        ELSE
         AX = DSQRT(AX)
       ENDIF
       RETURN
      END
```

SUBROUTINE FOR CALCULATING THE OVERLAP INTEGRAL
BOTH SIDES OF STEP HAVE GUIDED MODE

```
      SUBROUTINE GUIDE(K1, A1, K2, A2, GG)

      REAL*8 K1, K2, A1, A2
      REAL*8 T1, T2, T3
```

```
      REAL*8 S1, S2, S3, S4, S5
      REAL*8 GG

      COMMON /SET3/ S1, S2, S3, S4, S5


      T1 = ( K1 * DSIN(S2) * DCOS(S4) - K2 * DCOS(S2) * DSIN(S4))
C     / ( K1 * K1 - K2 * K2 )

      T2 = DCOS(S4) * ( (K1 * DSIN(S1) - A2 * DCOS(S1) ) * S5 -
C                  (K1 * DSIN(S2) - A2 * DCOS(S2)))
C     / (K1 * K1 + A2 * A2)
      T3 = ( DCOS(S1) * DCOS(S4) * S5 ) / (A1 + A2)

      GG = T1 + T2 + T3

      RETURN
      END
```

SUBROUTINE FOR CALCULATING THE OVERLAP INTEGRAL ONE SIDE OF STEP HAS GUIDED MODE & THE OTHER SIDE HAS RADIATION MODE

```
      SUBROUTINE  GDRAD(K1, A1, K2, A2, V, U, P, G, R)

      REAL*8 K1, K2, A1, A2, RATIO1, RATIO2
      REAL*8 S6, S7, S8
      REAL*8 T4, T5, T6, T7, T8, T9
      REAL*8 U, V, P
      REAL*8 G, R
      REAL*8 S1, S2, S3, S4, S5


      COMMON /SET3/ S1, S2, S3, S4, S5
      COMMON /SET4/ RATIO1, RATIO2

      S6 = V * RATIO1
      S7 = V * RATIO2
      S8 = U * (RATIO1 - RATIO2)
```

GUIDED MODE IN REGION I & RADIATION MODE IN REGION II

```
      T4 = (K1 * DSIN(S2) * DCOS(S7) - V * DCOS(S2) * DSIN(S7))
c     / (K1 * K1 - V * V)

      T5 = ( DCOS(S7) * ( K1 * DSIN(S1) * DCOS(S8) - U * DCOS(S1)
C             * DSIN(S8) - K1 * DSIN(S2) )
C     - P * DSIN(S7) * (K1 * DSIN(S1) * DSIN(S8) +
C           U * DCOS(S1) * DCOS(S8) - U * DCOS(S2) ) )
C     / (K1 * K1 - U * U)

      T6 = -1.* DCOS(S1) * (DCOS(S7) * (U *DSIN(S8) - A1 * DCOS(S8))
C          + P * DSIN(S7) * ( A1 * DSIN(S8) + U * DCOS(S8)))
C     / ( A1 * A1 + U * U )

      G = T4 + T5 + T6
```

RADIATION MODE IN REGION I & GUIDED MODE IN REGION II

```
      T7 = ( K2 * DSIN(S4) * DCOS(S7) - V * DCOS(S4) * DSIN(S7) )
C       / (K2 * K2 - V * V)

      T8 = DCOS(S4) * ( ( V * DSIN(S6) - A2 * DCOS(S6) ) * S5
C             - ( V * DSIN(S7) - A2 * DCOS(S7) ) )
C       / (A2 * A2 + V * V)

      T9 = ( A2 * DCOS(S6) - V * DSIN(S6) ) * DCOS(S4) * S5
C       / (A2 * A2 + U * U)

      R = T7 + T8 + T9

      RETURN
      END
```

SUBROUTINE FOR
CALCULATING THE OVERLAP INTEGRAL
BOTH SIDES OF STEP HAVE RADIATION MODE

```
      SUBROUTINE RADRAD(U1, U2, V1, V2, P, A1, A2, RR, I, J)

      PARAMETER (PI = 3.14159265358979)
      REAL*8 U1, U2, V1, V2, P, A1, A2
      REAL*8 W1, W2, W3, W4, W5
      REAL*8 T10, T11, T12, Y
      REAL*8 RR, RATIO1, RATIO2

      COMMON /SET4/ RATIO1, RATIO2

      W1 = V1 * RATIO1
      W2 = V1 * RATIO2
      W3 = V2 * RATIO1
      W4 = V2 * RATIO2
      W5 = U2 * (RATIO1 - RATIO2)


      IF (V1 .EQ. U2) THEN
       T11 = 0.
      ELSE
       T11 = (DCOS(W4) * ( V1 * DSIN(W1) * DCOS(W5) - U2 * DCOS(W1)
C       * DSIN(W5) - V1 * DSIN(W2) ) - P * DSIN(W4) *
C       ( V1 * DSIN(W1) * DSIN(W5) + U2 * DCOS(W1) * DCOS(W5)
C       - U2 * DCOS(W2) ) ) / ( V1 * V1 - U2 * U2 )
      ENDIF

      Y = (  U2 * DCOS(W1) * DCOS(W4) * DSIN(W5)
C      + V2 * DCOS(W1) * DSIN(W4) * DCOS(W5)
C      - V1 * DSIN(W1) * DCOS(W4) * DCOS(W5)
C      + P * V1 * DSIN(W1) * DSIN(W4) * DSIN(W5)) / (U1 + U2)

       IF ( I .EQ. J) THEN
```

```
       RR = (( DCOS(W1) * DCOS(W4) + (V1 / U1) * P * DSIN(W1) *
C       DSIN(W4)) * DCOS(W5) + ((V1 / U1) * DSIN(W1) *
C       DCOS(W4) - P * DCOS(W1) * DSIN(W4)) * DSIN(W5))
C       * PI * A1 * A2

      ELSE
       T10 = (V1 * DSIN(W2) * DCOS(W4) - V2 * DCOS(W2) * DSIN(W4))
C      / (V1 * V1 - V2 * V2)
       T12 = Y / (U1 - U2)

       RR = A1 * A2 * 2. * (T10 + T11 + T12)
      ENDIF


      RETURN
      END
```

SUBROUTINE FOR FORWARD PROPAGATION
MATRIX CALCULATION

```
      SUBROUTINE FORWARD(B1, B2, DELTA_UN)

      PARAMETER(N = 150, C = 2*N+2)
      INTEGER*4 X, Y, Z, CI
      COMPLEX*16 REF, REF1
      COMPLEX*16 A(C,C), B(C)
      COMPLEX*16 PB1Z, PB2Z, NB1Z, NB2Z, PBU(N), NBU(N)
      REAL*8 GG, GR(N), RG(N), RR(N,N)
      COMPLEX*16 PREV(C)
      COMPLEX*16 BNC(N)

      COMMON /SET5/ GG, GR, RG, RR
      COMMON /SET6/ A, B
      COMMON /SET7/ PB1Z, PB2Z, NB1Z, NB2Z, PBU, NBU
      COMMON /SET9/ PREV
      COMMON /SET13/ BNC

      A(1,1) = -1. * PB1Z
      A(1,2) = NB2Z * GG
      A(2,1) = PREV(2) * PB1Z * B1 * GG
      A(2,2) = PREV(2) * NB2Z * B2

      X = N + 2
      Y = X + 1

      DO 10 J = 3, X
       M = J - 2
       Z = JMOD(M, 2)
        IF (M .EQ. N) THEN
         A(1,J) = NBU(M) * DELTA_UN * GR(M)
        ELSE
         IF (Z .EQ. 0) THEN
          A(1,J) = NBU(M) * DELTA_UN * GR(M) * 2.
         ELSE
```

```
        A(1,J) = NBU(M) * DELTA_UN * GR(M) * 4.
       ENDIF
      ENDIF
     A(2,J) = 0.
10   CONTINUE


     DO 20 J = Y, C
      A(1, J) = 0.
      M = J - X
      Z = JMOD(M, 2)
       IF (M .EQ. N) THEN
        A(2,J) = PREV(2) * PBU(M) * BNC(M) * DELTA_UN * RG(M)
       ELSE
        IF (Z .EQ. 0) THEN
         A(2,J) = PREV(2) * PBU(M) * BNC(M) * DELTA_UN * RG(M) * 2.
        ELSE
         A(2,J) = PREV(2) * PBU(M) * BNC(M) * DELTA_UN * RG(M) * 4.
        ENDIF
       ENDIF
20   CONTINUE


     DO 30 I = 3, X
      L = I - 2
      J = I + N
      A(I,1) = 0.
      A(I,2) = PREV(2) * NB2Z * RG(L)

      A(J,1) = PREV(2) * PB1Z * B1 * GR(L)
      A(J,2) = 0.
30   CONTINUE


     DO 50 I = 3, X
      L = I - 2
      DO 40 J = Y, C
       M = J - X
       IF (M .EQ. L) THEN
        A(I,J) = PREV(2) * PBU(M) * (-2.)
       ELSE
        A(I,J) = 0.
       ENDIF
40    CONTINUE
50   CONTINUE


     DO 70 I = Y, C
      L = I - X
      DO 60 J = 3, X
       M = J - 2
       IF (M .EQ. L) THEN
        A(I,J) = PREV(2) * NBU(M) * 2. * BNC(M)
       ELSE
        A(I,J) = 0.
       ENDIF
60    CONTINUE
70   CONTINUE
```

```
      DO 90 I = 3, X
       L = I - 2
       T = I + N
       DO 80 J = 3, X
        M = J - 2
        W = J + N
        Z = JMOD(M, 2)
         IF (M .EQ. N) THEN
          CI = 1
         ELSE
          IF (Z .EQ. 0) THEN
           CI = 2
          ELSE
           CI = 4
          ENDIF
         ENDIF

         IF (M .EQ. L) THEN

          A(I,J) = PREV(2) * NBU(M) * RR(L,M)
          A(T,W) = PREV(2) * PBU(M) * BNC(M) * RR(M,L)
         ELSE
          A(I,J) = PREV(2) * NBU(M) * DELTA_UN * RR(L,M) * CI
          A(T,W) = PREV(2) * PBU(M) * BNC(M) * DELTA_UN * RR(M,L) * CI
         ENDIF
80     CONTINUE
90    CONTINUE

      B(1) = NB1Z
      REF = 0.
      DO 100 I = 1, N
       Z = JMOD(I, 2)
        IF (I .EQ. N) THEN
         CI = 1
        ELSE
         IF (Z .EQ. 0) THEN
          CI = 2
         ELSE
          CI = 4
         ENDIF
        ENDIF

        REF = REF + PREV(I+2) * NBU(I) * BNC(I) * RG(I) * DELTA_UN*CI
100    CONTINUE

       B(2) = REF + PREV(2) * NB1Z * B1 * GG

      DO 110 I = 3, X
       B(I) = PREV(I) * NBU(I-2) * 2.
110    CONTINUE

      DO 130 I = Y, C
       L = I - X
       REF = 0.
       DO 120 J = 1, N
        Z = JMOD(J, 2)
```

```
      IF (J .EQ. N) THEN
       CI = 1
      ELSE
       IF (Z .EQ. 0) THEN
        CI = 2
       ELSE
        CI = 4
       ENDIF
      ENDIF

      IF (J .EQ. L) THEN
       REF1 = PREV(J+2) * NBU(J) * BNC(J) * RR(J,L)
      ELSE
       REF1 = PREV(J+2) * NBU(J) * BNC(J) * RR(J,L) * DELTA_UN*CI
      ENDIF

      REF = REF + REF1
120   CONTINUE
     B(I) = REF + PREV(2) * NB1Z * B1 * GR(L)
130  CONTINUE

     RETURN
     END
```

SUBROUTINE FOR BACKWARD PROPAGATION
MATRIX CALCULATION

```
     SUBROUTINE BACKWARD(B1, B2, DELTA_UN)

     PARAMETER(N = 150, C = 2*N+2)
     INTEGER*4 X, Y, Z, CI
     COMPLEX*16 REF, REF1
     REAL*8 B1, B2, DELTA_UN
     REAL*8 GG, GR(N), RG(N), RR(N,N)
     COMPLEX*16 A(C,C), B(C)
     COMPLEX*16 PB1Z, PB2Z, NB1Z, NB2Z, PBU(N), NBU(N)
     COMPLEX*16 PREV(C)
     COMPLEX*16 BNC(N)


     COMMON /SET5/ GG, GR, RG, RR
     COMMON /SET6/ A, B
     COMMON /SET7/ PB1Z, PB2Z, NB1Z, NB2Z, PBU, NBU
     COMMON /SET9/ PREV
     COMMON /SET13/ BNC

     A(1,1) = -1. * NB2Z
     A(1,2) = PB1Z * GG
     A(2,1) = PREV(2) * NB2Z * B2 * GG
     A(2,2) = PREV(2) * PB1Z * B1

     X = N + 2
     Y = X + 1

     DO 10 J = 3, X
      M = J - 2
      Z = JMOD(M, 2)
```

```
        IF (M .EQ. N) THEN
         A(1,J) = PBU(M) * DELTA_UN * RG(M)
        ELSE
         IF (Z .EQ. 0) THEN
          A(1,J) = PBU(M) * DELTA_UN * RG(M) * 2.
         ELSE
          A(1,J) = PBU(M) * DELTA_UN * RG(M) * 4.
         ENDIF
        ENDIF
       A(2,J) = 0.
10    CONTINUE

      DO 20 J = Y, C
       A(1, J) = 0.
       M = J - X
       Z = JMOD(M, 2)
        IF (M .EQ. N) THEN
         A(2,J) = PREV(2) * NBU(M) * BNC(M) * DELTA_UN * GR(M)
        ELSE
         IF (Z .EQ. 0) THEN
          A(2,J) = PREV(2) * NBU(M) * BNC(M) * DELTA_UN * GR(M) * 2.
         ELSE
          A(2,J) = PREV(2) * NBU(M) * BNC(M) * DELTA_UN * GR(M) * 4.
         ENDIF
        ENDIF
20    CONTINUE

      DO 30 I = 3, X
       L = I - 2
       J = I + N
       A(I,1) = 0.
       A(I,2) = PREV(2) * PB1Z * GR(L)

       A(J,1) = PREV(2) * NB2Z * B2 * RG(L)
       A(J,2) = 0.
30    CONTINUE

      DO 50 I = 3, X
       L = I - 2
       DO 40 J = Y, C
        M = J - X
        IF (M .EQ. L) THEN
         A(I,J) = PREV(2) * NBU(M) * (-2.)
        ELSE
         A(I,J) = 0.
        ENDIF
40    CONTINUE
50    CONTINUE

      DO 70 I = Y, C
       L = I - X
       DO 60 J = 3, X
        M = J - 2
        IF (M .EQ. L) THEN
```

```
          A(I,J) = PREV(2) * PBU(M) * 2. * BNC(M)
         ELSE
          A(I,J) = 0.
         ENDIF
60     CONTINUE
70    CONTINUE


       DO 90 I = 3, X
        L = I - 2
        T = I + N
        DO 80 J = 3, X
         M = J - 2
         W = J + N
         Z = JMOD(M, 2)
          IF (M .EQ. N) THEN
           CI = 1
          ELSE
           IF (Z .EQ. 0) THEN
            CI = 2
           ELSE
            CI = 4
           ENDIF
          ENDIF

          IF (M .EQ. L) THEN
           A(I,J) = PREV(2) * PBU(M) * RR(M,L)
           A(T,W) = PREV(2) * NBU(M) * BNC(M) * RR(L,M)
          ELSE
           A(I,J) = PREV(2) * PBU(M) * DELTA_UN * RR(M,L) * CI
           A(T,W) = PREV(2) * NBU(M) * BNC(M) * DELTA_UN * RR(L,M) * CI
          ENDIF
80     CONTINUE
90    CONTINUE

       B(1) = PB2Z
       REF = 0.
       DO 100 I = 1, N
        Z = JMOD(I, 2)
         IF (I .EQ. N) THEN
          CI = 1
         ELSE
          IF (Z .EQ. 0) THEN
           CI = 2
          ELSE
           CI = 4
          ENDIF
         ENDIF

         REF = REF + PREV(I+2) * PBU(I) * BNC(I) * GR(I) * DELTA_UN*CI
100   CONTINUE

        B(2) = REF + PREV(2) * PB2Z * B2 * GG

       DO 110 I = 3, X
        B(I) = PREV(I) * PBU(I-2) * 2.
110   CONTINUE
```

```
      DO 130 I = Y, C
       L = I - X
       REF = 0.
       DO 120 J = 1, N
        Z = JMOD(J, 2)
        IF (J .EQ. N) THEN
         CI = 1
        ELSE
         IF (Z .EQ. 0) THEN
          CI = 2
         ELSE
          CI = 4
         ENDIF
        ENDIF


        IF (J .EQ. L) THEN
         REF1 = PREV(J+2) * PBU(J) * BNC(J) * RR(L,J)
        ELSE
         REF1 = PREV(J+2) * PBU(J) * BNC(J) * RR(L,J) * DELTA_UN*CI
        ENDIF

        REF = REF + REF1
120    CONTINUE
       B(I) = REF + PREV(2) * PB2Z * B2 * RG(L)
130   CONTINUE

      RETURN
      END
```

SUBROUTINE FOR CALCULATING MATRIX

```
      SUBROUTINE CAL_COEF(F, CK)

      PARAMETER(N=150, C=2*N+2)
      INTEGER*4 Z, F, CK, T
      COMPLEX*16 AL(C,C), COEFY(C), XR
      COMPLEX*16 A(C,C), B(C), COEFX(C)

      COMMON /SET6/ A, B
      COMMON /SET10/ COEFX


      Z = C - 1

      IF (CK .NE. N) THEN
       T = CK + N + 3
       GO TO 500
      ELSE
       GO TO 510
      ENDIF

500   DO 20 I = 1, C
       DO 10 J = T, C
        A(I, J-1) = A(I,J)
10     CONTINUE
20    CONTINUE
```

```
      DO 40 J = 1, C-1
       DO 30 I = T, C
        A(I-1, J) = A(I,J)
30     CONTINUE
40    CONTINUE

      DO 50 I = T, C
       B(I-1) = B(I)
50    CONTINUE

510   IF (F .EQ. 1) THEN
       DO 70 I = 1, Z
        DO 60 J = 3, Z
         A(I, J-1) = A(I,J)
60      CONTINUE
70     CONTINUE

       DO 90 J = 1, Z-1
        DO 80 I = 3, Z
         A(I-1, J) = A(I,J)
80      CONTINUE
90     CONTINUE

       DO 100 I = 3, Z
        B(I-1) = B(I)
100    CONTINUE

       Z = Z - 1
      ENDIF


      DO 130 I = 1, Z
       DO 120 J = I+1, Z

        AL(J,I) = A(J,I) / A(I,I)
         DO 110 K = I, Z

          A(J,K) = A(J,K) - AL(J,I) * A(I,K)
110      CONTINUE
120     CONTINUE
130   CONTINUE

      DO 140 I = 1, Z
       AL(I,I) = 1.
140   CONTINUE

      COEFY(1) = B(1) / AL(1,1)
      DO 160 I = 2, Z
       XR = 0.
       DO 150 J = 1, I-1
        XR = AL(I,J) * COEFY(J) + XR
150    CONTINUE
        COEFY(I) = (B(I) - XR) / AL(I,I)

160   CONTINUE

      COEFX(Z) = COEFY(Z) / A(Z,Z)
```

```
      DO 180 I = Z-1, 1, -1
       XR = 0.
       DO 170 J = Z, I+1, -1
        XR = A(I,J) * COEFX(J) + XR
170   CONTINUE
        COEFX(I) = (COEFY(I) - XR) / A(I,I)

180   CONTINUE

      IF (F .EQ. 1) THEN
       DO 190 I = Z, 2, -1
        COEFX(I+1) = COEFX(I)
190   CONTINUE

       COEFX(2) = 0.
       Z = Z + 1
      ENDIF

      T = CK + N + 2
      IF (Z .EQ. C-1) THEN
       DO 200 I = Z, T-1, -1
        COEFX(I+1) = COEFX(I)
200   CONTINUE
      ENDIF

      COEFX(T) = 0.

      RETURN
      END
```

SUBROUTINE FOR CALCULATING RADIATION PATTERN
IN THE FORWARD DIRECTION

```
      SUBROUTINE PATTERNT(DELTA_U, BETA, X, FLAG, COEF)

      PARAMETER(PI = 3.14159265358979, N = 150)
      REAL*8 THETA, ANG, U, PRAD
      COMPLEX*16 TRANS(N), RR, COEF
      INTEGER*4 X, FLAG
      COMPLEX*16 BNC(N)

      COMMON /SET13/ BNC
      COMMON /SET11/ TRANS

      WRITE(7,2) 'THE ', X, 'TIME''S TRANSMITTED RADIATION PATTERN'
2      FORMAT(3X, A4, I3, A36)

      DO 10 I = 1, FLAG
       U = DELTA_U * I
       THETA = DASIN(U) * 180 / PI
       RR = COEF * TRANS(I)
       PRAD = PI * (CDABS(BNC(I)) ** 2) * (CDABS(RR) ** 2) / BETA
       WRITE(7,1) 'ANG = ', THETA, 'RADIATION PATTERN = ', PRAD
1     FORMAT(7X, A6, F6.2, 5X, A21, D10.4)
10    CONTINUE
       RETURN
       END
```

SUBROUTINE FOR CALCULATING RADIATION PATTERN
IN THE BACKWARD DIRECTION

```
      SUBROUTINE PATTERNR(DELTA_U, BETA, X, FLAG, COEF)

      PARAMETER(PI = 3.14159265358979, N=150)
      REAL*8 THETA, ANG, U, PRAD
      COMPLEX*16 REF(N), RR, COEF
      INTEGER*4 X, FLAG
      COMPLEX*16 BNC(N)

      COMMON /SET13/ BNC
      COMMON /SET12/ REF

      WRITE(7,2) 'THE ', X, 'TIME''S REFLECTED RADIATION PATTERN'
2      FORMAT(3X, A4, I3, A36)

      DO 10 I = FLAG, 1, -1
       U = DELTA_U * I
       THETA = 180. - DASIN(U) * 180. / PI
       RR = COEF * REF(I)
       PRAD = PI * (CDABS(BNC(I)) **2) * (CDABS(RR) ** 2) / BETA
       WRITE(7,1) 'ANG = ', THETA, 'RADIATION PATTERN = ', PRAD
1     FORMAT(7X, A6, F6.2, 5X, A21, D10.4)
10   CONTINUE

      RETURN
      END
```

REFERENCE

1 Levin, B. J. and Kietzer, J. E. "Hybrid Millimeter-Wave Integrated Circuits" Tech. Rept. ECOM-74-0577-F, Contract DAAB07-74-C-0577, performed for the U.S. Army Electronic Command, Fort Monmouth, N.J. by ITT Research Institute, Chicago, Ill., October 1975.

2 Lo, Y. T. and Lee, S. W., *Antenna Handbood*, Van Nostrand Rddnhold Co., N.Y., Chapter 17, 1988.

3 Jacobs, H. and Chrepta, M. M., "Electronic Phase Shifter Millimeter-Wave Semiconductor Dielectric Integrated Circuits," IEEE Trans. Microwave Theory and Tech., Vol. MTT-22, No. 4, April 1974.

4 Andersen, J. Bach, *Metallic and Dielectric Antennas*, Copenhagen:Polyteknisk Forlay, 1971.

5 James, J. R. "Engineering Approach to the Design of Tapered Dielectric-rod and Horn Antennas," Radio and Elelctronic Engineer, Vol. 42, No. 6, June 1972.

6 Tien, P. K., Smolinsky, G., and Martin, R. J., "Radiation Fields of a Tapered Film and a Novel Film-to-Fiber Coupler." IEEE Trans. Microwave Theory and Tech., Vol. MTT-23, No. 1, Jan. 1973.

7 Bahar, E., "Propagation of Radio Waves over a Non-Uniform Layered Medium," Radio Science, Vol. 5, July 1970.

8 Shevchenko, V. V., *Continuous Transitions in Open Waveguides*, Golem Press, 1971.

9 Marcuse, D., *Theory of Dielectric Optical Waveguides*, Academic Press, N.Y., 1974.

10 Marcuse, D., "Radiation Losses of Tapered Dielectric Slab Waveguides," Bell System Tech. J., Vol. 49, No. 2, pp. 273-290, Feb. 1970.

11 Marcuse, D., *Light Transmission Optics*, 2nd Edition, Van Nostrand Reinhold, 1982.

12 Suchoski, P. G., Jr. and V. Ramaswamy, "Exact Numerical Technique for the Analysis of Step Discontinuities and Tapers in Optical Dielectric Waveguides," J. Opt. Soc. Am. A/Vol. 3, No. 2, pp. 194-203, Feb. 1986.

13 Rozzi, T.E., "Rigorous Analysis of the Step Discontinuity in a Planar Dielectric Waveguide," IEEE Trans. Microwave Theory and Tech., Vol. MTT-26, No. 10, pp. 738-746, Oct. 1978.

Reference (continued)

14 Ramaswamy, V. and Suchoski, P.G. Jr., "Power Loss at a Step Discontinuity in an Asymmetrical Dielectric Slab Waveguide," J. Opt. Soc. Am. A/Vol. 1, No. 7, pp. 754-759, July 1984.

15 Hirayama, K. and Koshiba, M., "Analysis of Discontinuities in an Open Dielectric Slab Waveguide by Combination of Finite and Boundary Elements," IEEE Trans. Microwave Theory and Tech., Vol. MTT-37, NO. 4, pp. 761-768, April 1989.

16 Press, W. H., Flannery, B. P., Teukolsky, S. A. and Vetterling, W. T., *Numerical Recipes - The Art of Scientific Computing*, Cambridge University Press, N.Y., 1986.

17 Ittipiboon, A., "Scattering of Surface Waves at a Slab Waveguide Siscontinuity," Proc. Inst. Elec. Eng., Vol. 126, No. 9, pp. 798-804, Sept. 1979.

18 Rozzi, T. E. and in't Veld, G. H., "Variational Treatment of the Diffraction at Facet of d.h. Lasers and of Dielectric Millimeter Wave Antennas," IEEE Trans. Microwave Theory and Tech., Vol. MTT-28, No. 2, pp. 61-73, Feb. 1980.

19 Gelin, P., Petenzi, M. and Citerne, J., "New Rigorous Analysis of the Step Discontinuity in a Slab Dielectric Waveguide," Elec. Letters, Vol. 15, No. 12, pp. 355-356, June 1979.

20 Gelin, P., Toutain, S. and Citerne, J., "Scattering of Surface Waves on Transverse Discontinuities in Planar Dielectric Waveguides," Radio Sci., Vol. 16, No. 6, pp. 1161-1165, Nov. - Dec. 1981.

21 Hosono, T., Hinata, T. and Inove, A., "Numerical Analysis of the Discontinuities in Slab Dielectric Waveguides," Radio Sci,. Vol. 17, No. 1, pp. 75-83, Jan.-Feb. 1982.

22 Uchida, K. and Aoki, K., "Scattering of Surface Waves on Transverse Discontinuities in Symmetrical Three-Layer Dielectric Waveguides," IEEE Trans. Microwave Theory and Tech., Vol. MTT- 32, No. 1, pp. 11-19, Jan. 1984.

23 Nichimura, E., Morita, N. and Kumagai, N., "An Integral Equation Approach to Electromagnetic Scattering from Arbitrary Shaped Junctions Between Multilayered Dielectric Planar Waveguide," J. of Lightwave Tech., Vol. LT-3, No. 4, pp. 887-894, Aug. 1985.

24 Mahdjoubi, K. and Terret, C., "An Analysis of Piecewise Homogenious Dielectric Rod Antenna," IEEE Trans. on Antennas and Propagation, Vol. AP-34, No. 4, April 1986.

Reference (continued)

25 Capsalis, C. N., Fikioris, J. G. and Uzumoglu, N. K., "Scattering from an Abruptly Terminated Dielectric-Slab Waveguide," J. Light. Tech. Vol. LT-3, No. 2, pp. 408-415, April 1985.

26 Hirayama, K. and Koshiba, K., "Numerical Analysis of Arbitrarily Shaped Discontinuities Between Planar Dielectric Waveguides with Different Thicknesses," IEEE Trans. Microwave Theory and Tech., Vol. MTT- 38, No. 3, pp. 260-264, March 1990.

27 Morita, N., "A Rigorous Analytical Solution to Abrupt Dielectric Waveguide Discontinuities," IEEE Trans. Microwave Theory and Tech., Vol. MTT- 39, No. 8, pp. 1272-1278, Aug. 1991.

28 Suchoski, P. G. Jr., "Analysis of Step Discontinuities and Tapers in Optical, Dielectric Waveguides," M.S. Thesis, University of Florida, 1985.

29 Felsen, L. B. and Marcuvitz, N., *Radiation and scattering of waves* Prentice-Hall, Inc., Englewood Cliffs, N.J., 1973.